الجمهورية الجزائرية الديمقراطية الشعبية

République Algérienne Démocratique et Populaire

Ministère de L'Enseignement Supérieur et de la Recherche Scientifique

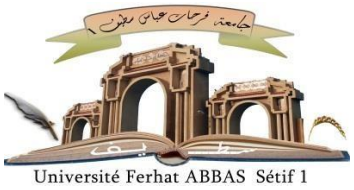

UNIVERSITÉ FERHAT ABBAS - SETIF1 FACULTÉ DE TECHNOLOGIE

THÈSE

Présentée au Département d'Electrotechnique

Pour l'obtention du diplôme de

DOCTORAT

Domaine: Sciences et Technologie

Filière: Automatique Option:Automatique et systèmes

Par

TABBI Ibtissam

THÈME

Contribution au diagnostic des défauts des systèmes non-linéaires de type Takagi-Sugeno

Soutenue le27/02/2025 devant le Jury:

BADOUD Abdessalam	Professeur	Univ. Sétif 1 Ferhat Abbas	Président
BELKHIAT Djamel E.C.	Professeur	Univ.Sétif 1 Ferhat Abbas	Directeur de thèse
JABRI Dalel	M.C.A.	Univ. Sétif 1 Ferhat Abbas	Co-Directrice
BEHIH Khalissa	M.C.A.	Univ. Sétif 1 Ferhat Abbas	Examinatrice
AGGOUN Lakhder	M.C.A.	Univ. Sétif 1 Ferhat Abbas	Examinateur
IDIR Abdelhakim	Professeur	Univ. de M'sila, Mohamed Boudiaf	Examinateur

Dedication:

I dedicate this thesis:

To my dear parents, whose unwavering love, sacrifices, and encouragement have been the foundation of all my efforts, your support has been my strength, and I am forever grateful.

To my sisters and brother, who stood by me through every step of this journey, sharing both the challenges and the joy, thank you for your presence, your care, and your faith in me.

To my professors, who generously shared their knowledge and guided me with patience and wisdom, your impact has been invaluable.

And to everyone who supported me in any way, with a kind word, a helping hand, or sincere prayers.

Acknowledgments

I would like to express my deepest gratitude to my esteemed supervisors, **Prof. Djamel E.C Belkhiat and Dalel Jabri**, for their invaluable academic support throughout my doctoral journey. Their generous investment of time, insightful guidance, and unwavering encouragement were instrumental in making my research experience both substantial and efficient

I am also deeply grateful for the thoughtful feedback and constructive criticism provided by the distinguished Jury Committee, **Prof. IDIR Abdelhakim**, **Prof. BADOUD Abdessalem**, **Dr. DEHIH Khalissa** and **Dr. AGGOUN Lakhdar**. Presenting my research to such a respected panel of experts was a privilege, and I appreciate your unwavering support throughout the process. Your dedication, guidance, and valuable contributions have significantly enriched my work.

Finally, my heartfelt thanks go out to my dear family and friends. Your constant words of wisdom, laughter, and unwavering support have been a source of immense strength and inspiration. I am truly blessed to have such a wonderful and supportive circle around me. Your presence has not only propelled me towards achieving my academic goals, but has also helped me grow as a person. Thank you for always being there for me, through thick and thin.

Ibtissam TABBI
March 20, 2025

Abstract

This thesis tackles the challenge of estimating sensor faults in a specific class of nonlinear systems. These systems operate continuously over time and can switch between different modes. We model them using Takagi-Sugeno (T-S) models, which can handle nonlinearities in the system's behavior. Additionally, the model accounts for external disturbances that are limited in size. This approach avoids the issue of having unmeasured premise variables, which can complicate estimation tasks. The core contribution of this research lies in proposing robust observers. These observers operate asynchronously with the system's switching mechanism and can simultaneously estimate state and sensor faults. The design of these observers is formulated using Linear Matrix Inequalities (LMIs), which are mathematical conditions that simplify analysis. Our approach offers several advantages compared to previous studies. First, the LMI conditions are independent of a specific dwell time, making them more flexible. Second, by applying relaxation techniques and specific constraints, we achieve less conservative results compared to prior work, especially when dealing with the unmeasured nonlinearities in the system. Furthermore, this thesis includes an optimization procedure to estimate the region within which the estimation error is guaranteed to remain. The effectiveness of the proposed design is demonstrated through several simulation examples. One example showcases the reduction in conservatism achieved by our approach. Another example illustrates the performance of the observers even when the system's switching mechanism doesn't perfectly match the observer's assumptions.

Keywords: Takagi-Sugeno fuzzy systems, switched systems, observer design, fault diagnosis, fault estimation, Lyapunov fuction, Linear Matrix Inequalities (LMIs).

Résumé

Cette thèse aborde le problème d'estimation des défauts de capteur pour une classe de systèmes à commutation non linéaires en temps continu. Ces systèmes sont modélisés par des modèles de Takagi-Sugeno (T-S) avec des parties conséquentes non linéaires et soumis à des perturbations bornées. Cette approche de modélisation permet d'éviter le problème des variables de prémisse non mesurées (UPVs). La contribution principale de cette étude consiste à proposer des observateurs à commutation asynchrones robustes pour estimer simultanément les défauts de capteur et l'état du système sous une commutation dépendante de l'état. Basée sur une fonction de Lyapunov multiple candidate, la conception de l'observateur proposé est formulée en termes d'inégalités matricielles linéaires (LMI). Ces conditions sont indépendantes du temps de séjour et moins conservatrices par rapport à des études antérieures similaires, grâce à des techniques de relaxation courantes et à des contraintes quadratiques incrémentielles appliquées aux parties conséquentes non linéaires non mesurées. Une autre contribution consiste à effectuer l'estimation du domaine d'attraction de l'erreur d'estimation à l'aide d'une procédure d'optimisation. Afin d'illustrer l'efficacité de l'approche de conception proposée, plusieurs exemples de simulation sont considérés. Le premier exemple concerne la réduction du conservatisme apporté par notre proposition par rapport aux études précédentes, tandis que le second vise à montrer, à travers un exemple illustratif, les performances des observateurs T-S à commutation proposés sous des lois de commutation inadaptées.

Mots-clés : Systèmes flous de type Takagi-Sugeno, systèmes à commutations, synthèse d'observateurs, diagnostic des défauts, estimation des défauts, fonction de Lyapunov, Inégalité Matricielles Linéaires (IML).

الملخص

تتناول هذه الأطروحة تحدي تقدير أخطاء المستشعرات في فئة معينة من الأنظمة غير الخطية. تعمل هذه الأنظمة بشكل مستمر عبر الزمن ويمكنها التبديل بين أنماط تشغيل مختلفة. نقوم بنمذجتها باستخدام نماذج تاكاغيسوجينو القادرة على التعامل مع اللاخطية في سلوك النظام. بالإضافة إلى ذلك، يأخذ النموذج بعين الاعتبار الاضطرابات الخارجية المحدودة الحجم. تساعد هذه الطريقة على تجنب مشكلة وجود متغيرات تأسيسية غير مقاسة والتي يمكن أن تعقد مهمة التقدير. تكمن المساهمة الأساسية في هذا البحث في اقتراح مراقبين قويين. تعمل هذه المراقبات بشكل غير متزامن مع آلية تبديل النظام ويمكنها تقدير أخطاء الحالة والمستشعر بشكل متزامن (رغم التركيز على أخطاء المستشعرات في النص، من المهم الإشارة إلى أن المراقبين يقيمون كلا الخطأين). يتم صياغة تصميم هذه المراقبين باستخدام مصفوفات خطية غير مساواتية، وهي شروط رياضية تعمل على تبسيط عملية التحليل. تقدم طريقتنا العديد من المزايا مقارنة بالدراسات السابقة. أولاً، لا تعتمد شروط بيس على وقت إقامة محدد، مما يجعلها أكثر مرونة. ثانياً، من خلال تطبيق تقنيات الاسترخاء والقيود المحددة، نحقق نتائج أقل تحفظًا مقارنة بالأعمال السابقة، خاصة عند التعامل مع اللاخطية غير المقاسة في النظام. علاوة على ذلك، تتضمن هذه الأطروحة إجراء تحسين لتقدير المنطقة التي يضمن بقاء خطأ التقدير ضمنها. يتم إثبات فعالية نهج التصميم المقترح من خلال العديد من أمثلة المحاكاة. يوضح أحد الأمثلة تقليل التحفظ الذي يحققه نهجنا مقارنة بالدراسات السابقة، بينما يوضح مثال آخر أداء المراقبين المقترحين حتى عندما لا تتطابق آلية تبديل النظام تمامًا مع افتراضات المراقب.

الكلمات المفتاحية: أنظمة ضبابية من نوع تاكاجيسوجينو، أنظمة التحويلات، تصميم المراقبين، تشخيص العيوب، تقدير العيوب، دالة ليابونوف، متباينات مصفوفية خطية.

Contents

List of Figures

List of Tables

Chapter 1

General introduction

1.1 Introduction

Switched systems constitute a fundamental class within the realm of hybrid dynamical systems. Their inherent strength lies in the ability to effectively model systems exhibiting switching phenomena. This ubiquitous phenomenon manifests as transitions between distinct operational modes, a characteristic observed across diverse engineering domains. For instance, switched systems find application in power electronics, where they describe the transitions between various power conversion modes. Similarly, air traffic control systems leverage switched systems to model the movement of aircraft between different flight sectors. Robotics, with its diverse gaits, and chemical processes, with their multi-stage reactions, further exemplify the applicability of switched systems. The core concept underlying switched systems lies in the synergistic combination of continuous dynamic subsystems and discrete events. These continuous subsystems represent the ongoing behavior within each operational mode, while the discrete events orchestrate the switching between them. This elegant framework offers a powerful and versatile tool for the analysis and design of complex systems exhibiting switching behavior.

Many real-world systems exhibit complex, nonlinear behavior that can be challenging to capture with traditional linear models. **Takagi-Sugeno (T-S) fuzzy models** offer a powerful approach to tackle this problem by representing a nonlinear system as a collection of interconnected linear models. A T-S fuzzy model decomposes the nonlinear system into multiple operating regions. Each region is described by a set of fuzzy rules that link input conditions to linear system dynamics. The overall system behavior is then obtained by blending the outputs of these individual linear models based on the degree of fulfillment (activation level) of the corresponding fuzzy rules.T-S models provide an intuitive and human-readable representation of the nonlinear system. The fuzzy rules explicitly capture the relationship between operating conditions and system behavior. The framework can accommodate a wide range of nonlinearity by adjusting the number and complexity of fuzzy rules. This allows for a tailored model that closely

reflects the specific characteristics of the system.

Within the domain of automatic control systems, **fault diagnosis** constitutes an indispensable facet for guaranteeing robust and reliable performance. Automatic control systems depend on intricate interplay between sensors and actuators to gather information and exert influence on the physical world. When malfunctions, such as sensor drift or actuator degradation, occur, they disrupt this delicate equilibrium, potentially leading to subpar performance or even safety risks. Fault diagnosis techniques act as a vital safeguard, enabling the prompt and precise identification of these anomalies. Through meticulous analysis of sensor data and system behavior, these techniques pinpoint the nature and location of the fault. This early detection empowers the implementation of corrective measures, such as targeted maintenance or control system reconfiguration. The ramifications extend beyond safeguarding the system itself and its environment; by minimizing downtime and ensuring continued optimal operation, fault diagnosis techniques ultimately contribute to enhanced system efficiency and cost-effectiveness.

Sensors are crucial devices used to detect and measure physical quantities such as temperature, motion speed, and pressure. They are integral to control systems, ensuring accuracy, stability, and reliability of control strategies. However, sensors, often deployed in harsh environments like industrial settings and aerospace, are prone to various issues like fouling, bias, drift, and damage. When sensor faults occur, they can compromise system performance and, in severe cases, lead to accidents if not promptly diagnosed. Estimating the magnitude and shape of faults is a challenging task and critical for initiating fault accommodation procedures, which are also essential for adapting control laws and maintaining system performance and reliability.

State observer is a mathematical model used to estimate the internal states of a dynamic system based on available input and output measurements. In many practical applications, not all system states can be directly measured due to physical constraints or sensor limitations. The operating principle of a state observer relies on reconstructing these unmeasured states by using a mathematical representation of the system, typically in the form of differential or difference equations. By comparing the estimated output with the actual system output, the observer adjusts its internal states through a correction mechanism, often incorporating feedback to minimize estimation errors. In the context of fault diagnosis, state observers play a crucial role in detecting, isolating, and estimating faults by analyzing discrepancies between expected and actual system behavior. Specifically, they can be designed to track deviations caused by faults in sensors, actuators, or system components, thereby enabling fault estimation and enhancing the system's reliability, safety, and performance.

The **primary objective** of this dissertation is to develop an effective approach for sensor fault estimation for a class of switched nonlinear systems. To achieve this, we propose the design of a switched robust observer capable of accurately estimat-

ing sensor faults while ensuring system reliability and performance. Additionally, we aim to mitigate the impact of fast-varying and even unbounded sensor faults, making the proposed approach highly adaptable to challenging fault scenarios. **Another key objective** of this thsesis is to eliminate the need for prior knowledge of the exact bounds or derivatives of sensor faults, thereby enhancing the practical applicability of the method. This is particularly crucial for real-world switched systems, where faults often exhibit unpredictable dynamics and are inherently difficult to characterize with precision.

In the following section, we present a literature review on fault estimation **to position our contributions** within the existing body of research.

1.2 Literature review

Broadly speaking, there are two categories of fault estimation methods, namely estimator-based fault estimation (Kamal and Aitouche, 2020, Li et al., 2020, Zhu et al., 2015, Chen and Liu, 2017) and observer-based fault estimation (Yang et al., 2015, Sun et al., 2020, Haouari et al., 2015, Li and Yang, 2019, Zhu et al., 2021). For example, the design of a fault estimator has been performed in (Kamal and Aitouche, 2020, Li et al., 2020). The main idea consists to use the output injection concept for fault estimation. The proposal seems complicated due to introducing of a first-order filter in the system model in order to eliminate noise. An extended Kalman filter-based fault estimation for satellite attitude control systems has been proposed in (Chen and Liu, 2017). The authors did not give any rigorous convergence analysis of the estimation error. In addition, this approach requires some knowledge on the noise disturbance signals.

Furthermore, fault estimation is predominantly achieved through observer-based techniques, crucial for determining fault characteristics (Habibi et al., 2023, Aouaouda et al., 2016, Zhang and Zhu, 2018, Yang and Wilde, 1988,Zhang et al., 2018, Mu et al., 2021). In nonlinear systems, a successful approach involves constructing an augmented fuzzy T-S descriptor observer, as proposed in (Aouaouda et al., 2016) for electric vehicle induction motor drives, exhibiting satisfactory performance. (Du and Cocquempot, 2017) investigates the H_∞ performance of such observers for discrete-time dynamic systems, particularly addressing sensor fault estimation, albeit with a slight matrix rank precondition (Zhang and Zhu, 2018).

Another avenue explores the Unknown Input Observer (UIO) principle (Yang and Wilde, 1988), treating fault signals as system unknowns. For instance, (Zhang et al., 2018) designs a full-order UIO for fault estimation in discrete-time T-S fuzzy systems amidst disturbances, while (Mu et al., 2021) delves into fuzzy T-S UIO design for estimating state and fault vectors in a class of nonlinear systems, under the assumption of

constant faults. It's crucial to note that most UIO methods rely on matrix rank preconditions, termed Observer Matching Conditions (OMC), aimed at decoupling unknown inputs. However, satisfying OMC can be challenging for many practical systems.

Sliding Mode Observers (SMO) have seen widespread use in addressing fault estimation (Yang et al., 2015, Sun et al., 2020, Haouari et al., 2015, Li and Yang, 2019, Zhu et al., 2021). In (Yang et al., 2015), SMO design for a category of nonlinear systems was outlined, relying on fulfilling challenging conditions such as the OMCs and the minimum phase condition. Similarly, in (Haouari et al., 2015), a high-order SMO was developed for a set of T-S fuzzy models. However, despite yielding satisfactory simulation results, this method is limited by its assumption of a piecewise constant sensor fault vector. More recently, in (Li and Yang, 2019), the design of an SMO for a subset of T-S descriptor systems was addressed, aiming to bypass the need for a norm-bounded condition on the derivative of faults. Nonetheless, this approach necessitates prior knowledge of fault bounds.

Additionally, Adaptive Observer (AO) is another type of observer extensively utilized for fault estimation (Fu et al., 2018, Chen et al., 2019, Fu et al., 2020, Han et al., 2022). For example, (Zhang et al., 2009) introduced a fast adaptive fault estimation observer, enhancing both the speed and accuracy of fault estimation. However, the design approach is rather conservative due to its reliance on the strict positive real assumption. In (Liu et al., 2018), a modified AO was proposed to concurrently estimate states and faults, under the assumption of a known fault model and fulfillment of the persistent excitation condition, along with known bounds of external disturbances. Similarly, (Han et al., 2022) developed an adaptive dynamic proportional-integral observer-based fault estimation method for a subset of nonlinear systems. This observer leverages both the output and its derivative to reconstruct process faults, particularly advantageous for time-varying process faults. Nevertheless, certain matrix rank preconditions are necessary when the nonlinear component is considered unknown.

Another intriguing approach involves leveraging robust H_∞ estimation performance to mitigate the impact of disturbances and alleviate the conservatism associated with matrix rank preconditions aimed at unknown input decoupling. Several investigations have explored robust H_∞ fuzzy T-S observers in this regard (Han et al., 2016, Chen et al., 2021). Typically, such observers do not impose constraints on fault signals; instead, they require only boundedness of external disturbances.

In the realm of switched nonlinear systems, observers exhibit distinctive characteristics, being either synchronous or asynchronous with the system's switching behavior. Synchronous observers align their mode switches precisely with those of the system, ensuring simultaneous transitions between modes. However, practical implementation often poses challenges as obtaining real-time system switching signals for the observer can be impractical (Sun et al., 2020, Chen et al., 2023, Sun et al., 2020,

Zhang et al., 2018). Asynchronous observers, on the other hand, feature non-aligned switching instants with the system, arising from delays in detecting active modes or mismatches in switching laws (Pettersson, 2005, Ren et al., 2018, Xiang et al., 2012, Hong et al., 2018,Chekakta et al., 2021,Chekakta et al., 2022). In the context of fault estimation, limited studies have explored switched nonlinear systems (Sun et al., 2020, Chen et al., 2023, Sun et al., 2020, Zhang et al., 2018). For instance, (Sun et al., 2020) investigated a descriptor SMO for switched T-S fuzzy stochastic systems, introducing dwell-time dependent conditions ensuring estimation error convergence, under known premise variables. However, this approach entails conservatism due to stringent detectability conditions (Zhang and Zhu, 2018), and requires prior knowledge of fault bounds, posing challenges for practical implementation. Similarly, fault estimation in switched fuzzy stochastic systems has been addressed in various scenarios (Han et al., 2019, Han et al., 2018, Priyanka et al., 2022, Sun et al., 2023, Yu et al., 2023), each imposing its own constraints and assumptions.

Furthermore, (Zhang et al., 2018) tackled sensor fault estimation for switched fuzzy systems using an UIO, employing mode-dependent average dwell time techniques and piecewise Lyapunov functions. However, this study only considered synchronous switching between the system and the observer, assuming measurable premise variables and verifying OMCs to decouple unknown inputs from estimation errors. Similarly, fault estimation issues for diverse systems, including those with an unknown smooth nonlinear function or continuous-time nonlinear Markovian jump systems, have been addressed in literature, relying on the verification of detectability conditions and OMCs (Fu et al., 2018, Chen et al., 2019, Fu et al., 2020, Yan et al., 2022,Chen et al., 2023).

In a recent study (Han et al., 2022), sensor fault estimation for switched fuzzy systems with UPVs was investigated using an AO. The Lipschitz condition was employed to address the UPVs issue. Convergence analysis of estimation error was formulated using a common Lyapunov matrix for different switching subsystems, under arbitrary switching sequences and synchronous switching modes. However, the design's main limitation lies in the conservatism of the proposed conditions based on LMIs, which rely on the availability of a common Lyapunov matrix. Additionally, certain matrix rank preconditions, impacting the practicality of the method, were assumed to be met. A comparison study between this approach and previous work (Zhang et al., 2018) will be presented in Section (5.4), with a critical analysis of the results obtained.

In a related field, (Han et al., 2023) delved into the development of a reduced-order observer, aiming to concurrently estimate system states and fault signals. The objective was to integrate this observer into a fault-tolerant control strategy. This innovative approach sidesteps common assumptions regarding fault bounds and their derivatives, thus extending its applicability to a broad spectrum of systems characterized by fast time-varying and unbounded faults. The formulation of sufficient conditions for the

existence and design of the switched fuzzy observer involved utilizing a common Lyapunov function across all subsystems. These conditions were expressed in terms of LMIs, under both arbitrary switching sequences and synchronous switching modes.

In a recent study (Liu and Wang, 2021), an intriguing fault estimation methodology utilizing a robust H_∞ observer with measurable premise variables was introduced for a subset of nonlinear discrete-time switched T-S fuzzy systems. Leveraging average dwell time techniques and a common Lyapunov function, conditions ensuring the convergence of estimation errors were formulated in terms of LMIs. Despite the somewhat conservative nature of the proposed design method, attributed to the use of a common Lyapunov matrix, it is noteworthy that this approach obviates the need for verifying detectability conditions or strong OMCs. Similarly, (Ladel et al., 2021) tackled the issue of system state and fault estimation for a subset of switched T-S fuzzy systems under constrained switching sequences. Sufficient conditions, ensuring favorable performance in terms of fault estimation and H_∞ disturbance attenuation, were formulated as LMI conditions. These conditions assumed that premise variables were measurable and synchronous switching modes were employed.

1.3 Contributions of the thesis

A critical examination of the aforementioned bibliography (section 1.2) highlights several noteworthy limitations inherent to existing design approaches. These limitations provide a springboard for the present study. We now delineate the core contributions our research endeavors to make (Tabbi et al., **?** :

- Most observer-based fault estimation methods rely on OMCs and/or detectability conditions, which are often overly strict for many physical systems (Sun et al., 2020, Zhang and Zhu, 2018, Zhang et al., 2018, Chen et al., 2019, Fu et al., 2020, Yan et al., 2022, Chen et al., 2023). Among these methods, robust observers are a notable exception as they are less conservative by employing H_∞ disturbance attenuation instead of unknown input decoupling (Liu and Wang, 2021, Ladel et al., 2021). Building on this insight, our work introduces a novel observer design approach based on H_∞ disturbance attenuation for a class of switched nonlinear systems. This approach circumvents the limitations of OMCs and detectability conditions or any stringent matrix rank preconditions. Furthermore, it does not necessitate knowledge of sensor fault bounds or their derivatives, making it more practical for switched systems with with fast time-varying and unbounded faults.

- By employing the sector nonlinearity approach to a system bounded within a specific sector and containing non-linear elements dependent on unmeasured state variables, we typically derive an equivalent T-S fuzzy multi-models with

UPVs. However, the challenge of UPVs in designing fault estimation observers for switched nonlinear systems remains largely unexplored, except for certain studies (Han et al., 2022, Fu et al., 2018). Our contribution aims to tackle this challenge by addressing the UPVs issue. Rather than relying on the Lipschitz condition-based approach, we propose an alternative method. This method involves separating the measured and unmeasured nonlinearities of the switched system, then applying T-S modeling techniques only to the measured nonlinearities. This results in T-S multi-models with nonlinear consequent parts (N-TS), where the membership functions depend solely on measured premise variables. One significant advantage of T-S modeling with nonlinear consequent parts is the potential reduction in the number of vertices involved in the conditions based on LMIs, compared to classical T-S modeling methods. This reduction can lead to less conservative estimates and lower computational complexity.

- As previously mentioned, the majority of the methods outlined have been conducted under constrained switching sequences, as reported in references (Sun et al., 2020, Chen et al., 2023, Sun et al., 2020, Zhang et al., 2018), with exceptions noted in studies by (Han et al., 2022, Han et al., 2019). Dwell-time dependent conditions have been utilized to address the development of observer-based fault estimation, where the switched systems are are forced to dwell in each mode during at least a minimum time. While these conditions suit systems with controlled switching sequences, many physical systems follow uncontrolled switched sequences, such as those governed by state-dependent laws (Pettersson, 2005, Xiang et al., 2012). Furthermore, almost all studies in the literature review focused on the straightforward case of synchronous switched observers. Our third contribution involves establishing dwell-time free conditions for designing asynchronous switched observers-based fault estimation. Unlike most prior works, the designed switched observers can handle unknown, arbitrary, or uncontrolled switching sequences, and address the initialization problem where the observer's switching mode may be asynchronous with that of the system.

- When the Takagi-Sugeno (T-S) fuzzy model holds true locally within a confined region of the state space, and if the state vector ventures beyond the model's validity domain, ensuring convergence of the estimation error becomes uncertain, posing a significant limitation for T-S model-based observers. Therefore, it becomes pertinent to include the estimation of the domain of attraction of the estimation error dynamics in the observer design approach. To the best of our knowledge, previous studies on switched observers-based sensor fault estimation have not addressed this issue. Consequently, our fourth contribution involves proposing an optimization procedure focused on expanding Lyapunov level sets

to estimate the attraction domain.

- The final contribution aims to alleviate the conservatism inherent in the suggested LMI conditions. By employing quadratic constraints methods to address the nonlinear consequent parts and employing standard relaxation techniques (Peaucelle et al., 2000, Tuan et al., 2001), notable enhancements in terms of feasibility domains are achieved and contrasted with previous studies (Han et al., 2022, Zhang et al., 2018).

1.4 Structure of the thesis

This dissertation is structured into five distinct chapters.

The **first Chapter** provides a general introduction, a summary of the contributions made and an overview of the thesis structure.

The **second chapter** lays the groundwork for the subsequent chapters by establishing a solid foundation in the core concepts of switched system modeling. It meticulously defines the essential terminology and key notions relevant to this field. Notably, the chapter presents two distinct classifications of switched systems, each utilizing a different categorization criterion.

Building upon the foundation laid in the first chapter, the **third chapter** delves into a comprehensive analysis of Takagi-Sugeno (T-S) fuzzy multi-model systems. It explores the core principles governing these systems and examines various methods for their derivation, with a specific emphasis on the sector nonlinearity approach.

The **the fourth chapter** tackles the intricacies of fault diagnosis specifically tailored for nonlinear systems. The chapter meticulously defines key fault diagnosis terms at the outset. This establishes a solid foundation upon which we can delve deeper into the complexities of fault diagnosis for nonlinear systems, effectively navigating this intricate landscape.

The **fifth chapter** confronts the challenge of robust sensor fault estimation in switched nonlinear systems, particularly those plagued by fast-time varying and unbounded faults. These faults present a significant threat due to their rapid fluctuations and potential to severely disrupt system behavior. To conquer this challenge, we introduce a groundbreaking approach utilizing asynchronous switched observers. These observers boast remarkable resilience: they can function effectively even when faced with uncontrolled, arbitrary, or unknown switching sequences between system modes. Additionally, they gracefully handle situations where the system and observer lack perfect initial synchronization, allowing for different starting modes. This adaptability makes them ideally suited for real-world scenarios where perfect synchronization is often unrealistic.

This dissertation culminates in a comprehensive conclusion that encapsulates the overarching findings and delineates promising avenues for future research.

Chapter 2

Preliminary notions on switched systems

2.1 Introduction

This chapter serves as an introductory foundation to the fundamental concepts that will underpin the subsequent chapters of this thesis. It meticulously delves into the precise definitions of terminology and specific notions germane to the modeling of switched systems. Two distinct categorizations of switched systems are presented, each employing a unique classification criterion.

The first categorization utilizes the switching mechanism as the basis for differentiation, introducing the concepts of state-dependent switched systems and time-dependent switched systems. The second categorization distinguishes switched systems based on whether the switching is controlled or autonomous.

Subsequently, the chapter embarks on an in-depth exploration of concepts pertaining to the stability analysis of switched systems, drawing upon the rich foundations of Lyapunov theory. The intricate concepts of common Lyapunov functions and multiple Lyapunov functions are meticulously examined. Additionally, the chapter delves into the nuanced concepts of stability under arbitrary switching and constrained switching, providing a comprehensive understanding of these critical aspects.

The concluding section of the chapter is dedicated to elucidating the fundamental notions that underpin the synthesis of switched observers. It meticulously outlines the major challenges that arise in the context of synthesizing switched observers, encompassing both synchronous switched observers and asynchronous switched observers.

In the following, we provide a concise overview of the concept of Lyapunov stability.

2.2 Lyapunov stability analysis

Lyapunov theory provides a powerful framework for analyzing the stability of systems without explicitly solving the governing differential equations (Shevitz and Paden, 1994). It allows us to draw conclusions about the behavior of trajectories, such as their convergence or divergence from an equilibrium point, without needing to determine the exact path of the trajectory. This qualitative analysis approach offers advantages in terms of computational efficiency and applicability to a wider range of systems, especially nonlinear ones. In the following, we present some key concepts necessary for what follows (Sastry and Sastry, 1999).

Before we begin, it is important to recall the definition of a positive definite function. A function $V : \mathbb{R}^n \to \mathbb{R}$ is said positive definite if:

- $V\left(x(t)\right) \geqslant 0$ for all $x(t)$,
- $V(x(t)) = 0$ if and only if $x = 0$,
- All sublevel sets of $V(x(t))$ are bounded, which is equivalent to $V(x(t)) \to \infty$, as $x(t) \to \infty$.

Example 1 *$V\left(x(t)\right) = x(t)^T P x(t)$ with $P = P^T$ is positive definite function if and only if $P > 0$.*

2.2.1 Lyapunov global asymptotic stability theorem

Consider a continuously differentiable function, $V(x(t))$, defined on a domain $D \subset \mathbb{R}^n$. The Lyapunov global asymptotic stability theorem states that for an autonomous system described by the ordinary differential equation:

$$\dot{x}(t) = f(x(t)) \tag{2.1}$$

where $x(t) \in D$ and $f : D \to R^n$, the equilibrium point $x = 0$ is globally asymptotically stable if there exists a continuously differentiable function $V(x(t))$ satisfying the following conditions (Clarke et al., 1998):

- **Positive definiteness:** $V(x(t)) > 0$ for all $x(t) \in D$, $x(t) \neq 0$. ($V(0) = 0$ is allowed),
- **Negative definiteness of derivative:** $\dot{V}(x(t)) < 0$ for all $x(t) \in D$, $x(t) \neq 0$. ($\dot{V}(0) = 0$ is allowed).

2.2.2 Lyapunov exponential stability theorem

The Lyapunov global exponential stability theorem refines the Lyapunov global asymptotic stability theorem by providing information about the convergence rate towards the equilibrium point ($x = 0$). Let us consider a continuously differentiable function, $V(x(t))$, defined on a domain $D \subset \mathbb{R}^n$, and an autonomous system described by the ordinary differential equation (2.1). The equilibrium point $x = 0$ is said to be globally exponentially stable if there exist a continuously differentiable function $V(x(t))$ and a positive constant $\alpha > 0$ satisfying the following conditions (Hafstein, 2004):

- **Positive definiteness:** $V(x(t)) > 0$ for all $x(t) \in D$, $x(t) \neq 0$. ($V(0) = 0$ is allowed),
- **Exponential decrement of Lyapunov function derivative:** $\dot{V}(x(t)) \leqslant -\alpha V(x(t))$ for all $x(t) \in D$.

This implies that there exist a scalar $M > 0$ such that every trajectory of $\dot{x}(t) = f(x(t))$ satisfies $\|x(t)\| \leqslant Me^{-\alpha t/2} \|x(0)\|$.

2.2.3 Stability of autonomous linear systems

Consider an autonomous linear system described by the following differential equation:

$$\dot{x}(t) = Ax(t) \tag{2.2}$$

where $x(t) \in \mathbb{R}^n$ is the state vector, $A \in \mathbb{R}^{n \times n}$ is the system matrix, and t represents time. To analyze the stability of this system, we can employ a quadratic Lyapunov function of the form:

$$V(x(t)) = x(t)^T P x(t) \tag{2.3}$$

where P is a positive definite matrix ($P = P^T > 0$). The positive definiteness of P ensures that $V(x(t))$ is greater than zero for all non-zero state vectors $x(t)$.

The key lies in analyzing the derivative of the Lyapunov function along the system's trajectories. This derivative, denoted by $\dot{V}(x(t))$, provides information about how the function $V(x(t))$ changes with respect to time as the system evolves. By applying the product rule and the fact that A is constant, we can obtain the following expression for the derivative:

$$\dot{V}(x(t)) = \dot{x}(t)^T P x(t) + x(t)^T P \dot{x}(t) \tag{2.4}$$

For the system to be stable, we need the derivative to be negative definite, meaning it should be strictly less than zero for all non-zero states ($\dot{V}(x(t)) < 0$ for all $x(t) \neq 0$). To achieve this negativity, the following linear matrix inequality (LMI) must hold:

$$A^T P + PA < 0 \tag{2.5}$$

Theorem 1 *The autonomous linear system (2.2) is globally asymptotically stable, if there exists a symmetric positive matrix $P = P^T > 0$ such that the given inequality (2.5) is satisfied.*

Remark 1 *Numerous scientific computing environments and control system design software packages offer built-in LMI solvers, facilitating the solution of LMI conditions. This alleviates users from the necessity of developing intricate optimization algorithms. These solvers commonly employ interior-point methods or other highly efficient algorithms specifically tailored for handling LMIs. Notable examples encompass MATLAB's LMI toolbox (Gahinet et al., 1994) and specialized software such as YALMIP (Ravat et al., 2021).*

In the following, we briefly review some basic concepts of observer design.

2.2.4 Observer design

In control theory, a state observer, or state estimator, is a mathematical model that estimates the internal state variables of a dynamical system based on available input and output measurements. This estimate serves as a powerful tool for control design and system monitoring.

Let us consider the following linear system:

$$\begin{cases} \dot{x}(t) = Ax(t) + Bu(t) \\ y(t) = Cx(t) \end{cases} \tag{2.6}$$

where $x \in \mathbb{R}^n$ is the state vector, $u \in \mathbb{R}^q$ is the input vector, $y \in \mathbb{R}^p$ is the output vector, and $A \in \mathbb{R}^{n\times n}$, $B \in \mathbb{R}^{n\times q}$, $C \in \mathbb{R}^{p\times n}$, and $D \in \mathbb{R}^{p\times q}$ are the system matrices.

Consider the Luenberger observer (Luenberger, 1966), which is a dynamic system providing a state estimate $\hat{x}(t)$ based on the system's output. The following equation describes its behavior:

$$\begin{cases} \dot{\hat{x}}(t) = Ax(t) + Bu(t) + L(y(t) - \hat{y}(t)) \\ y(t) = C\hat{x}(t) \end{cases} \tag{2.7}$$

where $L \in \mathbb{R}^{n\times p}$ representing the observer gain to be designed.

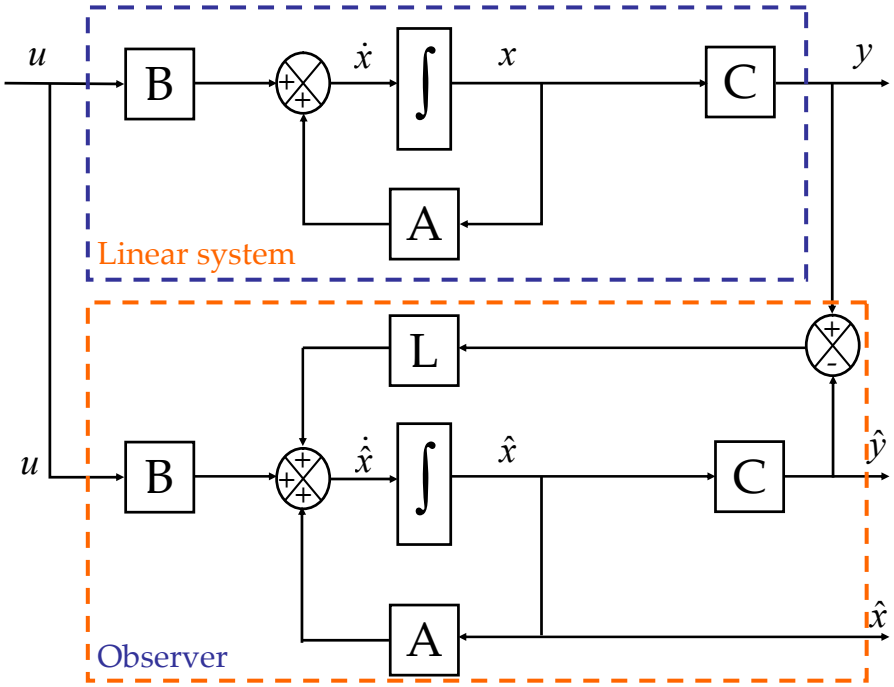

Figure 2.1: Schematic of a state observer for a linear system.

The state estimation error $e(t) \in \mathbb{R}^n$ can be defined as follows:

$$e\left(t\right) = x\left(t\right) - \hat{x}\left(t\right) \tag{2.8}$$

Thus, the state error dynamic can be written as:

$$\dot{e}\left(t\right) = \dot{x}\left(t\right) - \dot{\hat{x}}\left(t\right) \tag{2.9}$$

By introducing the dynamic of the observer (2.7), the equation (2.9) can be written as follows:

$$\dot{e}(t) = (A - LC)e(t) \tag{2.10}$$

To analyze the stability of the state error dynamic (2.10), we can employ a quadratic Lyapunov function of the form:

$$V(e(t)) = e^T(t)Pe(t) \tag{2.11}$$

Compute the derivative of the Lyapunov function along the error dynamics:

$$\dot{V}(t) = \dot{e}^T(t)Pe(t) + e^T(t)P\dot{e}(t) \tag{2.12}$$

$$= e^T(t)((A - LC)^T P + P(A - LC))e(t) \tag{2.13}$$

For the estimation error dynamics to be asymptotically stable, the time derivative of the Lyapunov function (2.13) must be strictly negative definite $\dot{V}(e(t))$. This means $\dot{V}(e(t)) < 0$ is always less than zero for any non-zero estimation error. This guarantees the estimation error converges to zero over time. To achieve this negativity, the following inequality must hold:

$$(A - LC)^T P + P(A - LC) < 0 \tag{2.14}$$

The observer design can be effectively summarized by the following theorem.

Theorem 2 *Given the linear system (2.6) and observer (2.7), the state error dynamics (2.10) achieve global asymptotic stability if a symmetric positive matrix $P = P^T > 0$ and matrix Y exist, satisfying the following LMI:*

$$A^T P - C^T Y^T + PA - YC < 0 \tag{2.15}$$

The observer gain matrix can be derived as: $L = P^{-1}Y$.

With a clear understanding of fundamental stability concepts, we now turn our attention to a detailed examination of switched systems in the coming sections.

2.3 Fundamentals of switched systems

Switched systems represent a large class of hybrid dynamical systems, which are able to describe various systems exhibiting switching phenomena. In this context, we can quote as examples, power electronics, air traffic control, robotics, chemical processes, as well as other systems in various fields. Switched systems consist of a combination of continuous dynamic subsystems and discrete events that orchestrate the switching between different subsystems (Liberzon and Morse, 1999, Zhu and Antsaklis, 2015). The mathematical representation of a switched system can be expressed as follows:

$$\dot{x}(t) = f_{\sigma_j(t)}(t, x(t), u(t)) \tag{2.16}$$

In this context, the system state $x(t)$, where $x(t) \in \mathbb{R}^n$, pertains to time $t \geqslant 0$. The input $u(t)$, where $u(t) \in \mathbb{R}^q$, and the vector fields $f_{\sigma_j(t)}$, for all $j \in Q$, describing the various modes of the system. $\sigma_j(t)$ are switching functions defined, when the l^{th} mode is activated, as:

$$\begin{cases} \sigma_j(t) = 1 \text{ when } j = l. \\ \sigma_j(t) = 0 \text{ when } j \neq l. \end{cases} \tag{2.17}$$

where obviously $\sum_{j=1}^{m} \sigma_j(t) = 1$.

With the aim of fostering a comprehensive grasp of switched system concepts among

readers, we shall delve into a simplified and pedagogically structured example of a heating system.

Example 2 (Heating system (Belkhiat, 2011)) *A practical example of an explicit switched system can be found in residential heating systems that regulate room temperature (see Figure 2.2). The key component is the thermostat. This system comprises two essential elements:*

- ***Heating unit:*** *Generates heat (e.g., furnace, boiler).*
- ***Temperature sensor:*** *Continuously monitors the room temperature.*

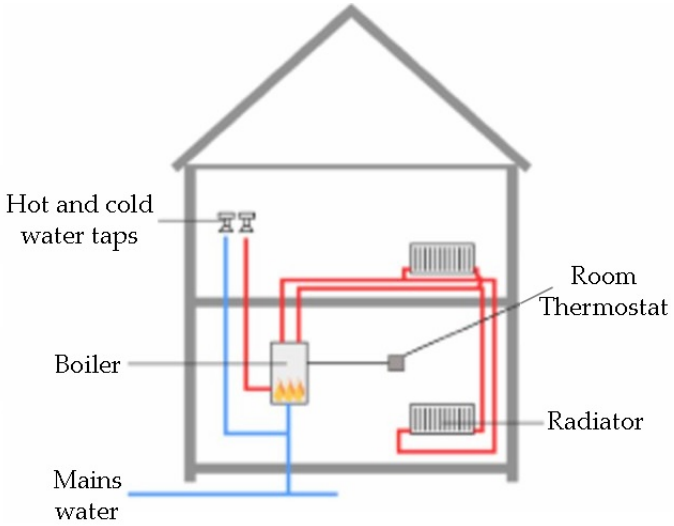

Figure 2.2: Schematic of an heating system. (Belkhiat, 2011).

The thermostat functions as a discrete controller using pre-programmed temperature thresholds:

- ***Lower threshold*** *(T_{low})**:** When the room temperature falls below T_{low} (e.g., $18°C$), the thermostat acts as a closed switch, triggering the heating unit's activation.*
- ***Upper threshold*** *(T_{high})**:** When the room temperature reaches T_{high} (e.g., $22°C$), the thermostat acts as an open switch, deactivating the heating unit.*

This switching behavior regulates the room temperature. The heating system is "ON" when the temperature is below T_{low} and "OFF" when it reaches T_{high}. The system remains in this "judgment" state until:

- ***Temperature drops below** T_{low}**:** This triggers the heating system to turn back ON.*
- ***Optional time-based switching:** Some thermostats might cycle the heating system ON and OFF even within the acceptable temperature range based on a preset timer.*

The interplay between the room temperature and the thermostat's switching behavior exemplifies an explicit switched system:

- ***Continuous evolution:** Represented by the gradual rise or fall of the room temperature.*
- ***Discrete evolution:** Characterized by the abrupt transitions between the heating system's "ON" and "OFF" states, triggered by the thermostat based on temperature thresholds.*

In the sequel, while subsystems can exhibit both linear and nonlinear dynamics, and operate autonomously ($u(t) = 0$ for all $t \geqslant 0$) or under external control, for the sake of analytical tractability and a foundational understanding, the remainder of this section will restrict its focus to autonomous switched linear systems. This choice simplifies the analysis and enhances the pedagogical value of the content.

Switched systems can be categorized according to the characteristics of their switching events. Two primary distinctions exist:

2.3.1 Switching mechanism-based categorization

This subsection outlines two common switching mechanisms:

2.3.1.1 State-dependent switching

In this case, a continuous system is divided into regions by switching surfaces (which can be finite or infinite). These regions represent different operating conditions, each governed by its own set of differential equations (Wu et al., 2013).

The system's behavior is determined by its current state. When the state trajectory crosses a switching boundary, a switch occurs. A new subsystem is activated, and the system's evolution follows a different set of differential equations (as depicted in Figure

2.3). This switching process is directly influenced by the continuous state itself (as described by Liberzon, 2003).

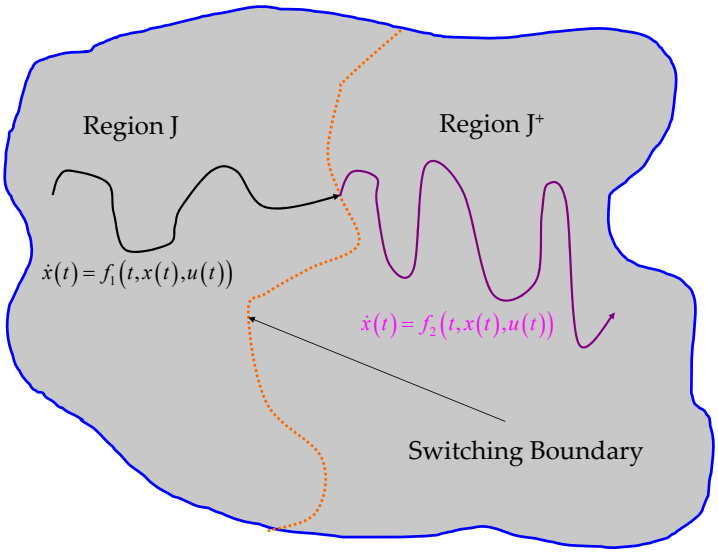

Figure 2.3: A visual representation of state-dependent switching.

A classic example is a thermostat. The internal state is the room temperature, constantly monitored by a sensor. The threshold is a specific temperature setting. When the room temperature dips below this threshold (the boundary), the thermostat "switches gears" and activates the heating system. This demonstrates how state-dependent switching allows a system to react intelligently to changes in its internal environment.

2.3.1.2 Time-dependent switching

In contrast to state-dependent switching, which relies on the system's internal state to trigger transitions, time-dependent switching utilizes a predetermined schedule. This approach is analogous to a traffic light system, where phase changes occur at set intervals irrespective of the current traffic volume. In this case, the switching signal is solely governed by time (Zhang et al., 2016).

One can conceptualize the switching signal $q(t)$ as a control mechanism dictating the system's operational mode. Between consecutive switching points, the signal maintains a constant value, signifying the currently active subsystem or mode. Figure 2.4 depicts a typical example of a time-dependent switching signal. This methodology offers a predictable and reliable means of managing system behavior, making it particularly well-suited for applications where precise timing is paramount.

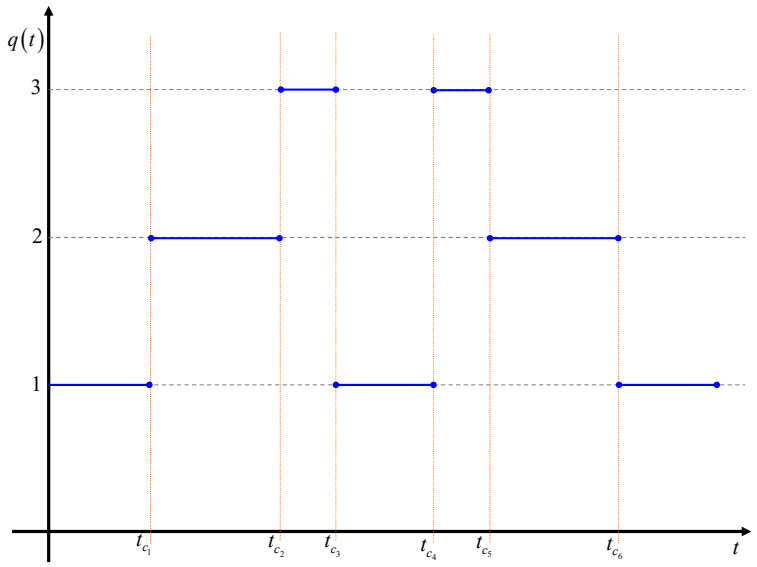

Figure 2.4: A visual representation of time-dependent switching signal.

2.3.2 Switching control-based categorization

In switched systems, the transitions between different subsystems can be triggered by various factors.This subsection outlines two common switching control.

2.3.2.1 Arbitrary (Autonomous) switching

Let explore the concept of arbitrary (autonomous) switching, wherein the switching mechanism operates independently without external influence. In this kind of systems, the switching signal responsible for transitioning between subsystems is not governed by any external input or feedback. Instead, the system autonomously determines when to switch based on its internal states or predefined rules. Consequently, the timing and sequence of switching events are often unpredictable. This unpredictability adds a layer of complexity when analyzing the behavior of the overall system, compared to situations where switching is controlled externally. Moreover, analyzing stability, performance, and reachability properties under arbitrary switching conditions can be challenging due to the inherent unpredictability (Fainshil et al., 2009).

2.3.2.2 Constrained (Controlled) switching

In contrast to autonomous switching, constrained (controlled) switching relies on an external factor to dictate the switching behavior between subsystems. This external factor can be:

- **Human operator:** A human operator actively monitors the system state and makes informed decisions on when to switch based on experience, pre-defined

protocols, or real-time analysis. For instance, manual transmission in the context of automobiles corresponds to switching being controlled by the driver.

- **Supervisory control program:** A pre-programmed control system monitors system variables and triggers switching based on predefined conditions or algorithms. This allows for automated control with more complex decision-making capabilities compared to human operators. As examples, we can mention the following cases:
  - *Flight control systems:* Autopilots in airplanes use control algorithms to switch between flight modes (e.g., takeoff, climb, cruise) based on flight parameters.
  - *Process control systems:* Industrial processes often utilize control algorithms to switch between operating modes based on process variables (e.g., temperature, pressure) to maintain desired product quality and efficiency.

In summary, constrained switching allows for optimization of system performance by strategically selecting the most suitable subsystem for the current operating conditions. In addition, predictable switching sequences simplify analysis of the overall system's behavior compared to autonomous switching (Philippe et al., 2016).

Remark 2 *The categorization of switching control in switched dynamical systems, while useful, doesn't always present a clear-cut picture. Many real-world systems exhibit characteristics of both autonomous and constrained (controlled) switching, depending on their design and operational needs. Here is how automatic gearboxes illustrate this concept: In automatic transmissions, gear changes primarily occur autonomously based on internal factors like engine speed and vehicle load. The Transmission Control Unit (TCU) acts as the internal decision-maker, utilizing pre-programmed algorithms to determine the optimal gear ratio. However, drivers can introduce an element of constrained switching through features like:*

- ***Gear shift modes:*** *Many automatics offer options like "Sport" or "Manual" modes that alter the TCU's shifting strategy to prioritize performance or driver control over pure fuel efficiency.*
- ***Paddle shifters:*** *Some automatics provide paddle shifters on the steering wheel that allow the driver to manually trigger gear changes for a more engaging driving experience. In these instances, the driver acts as an external factor influencing the switching behavior, albeit within a limited scope.*

Having laid the groundwork with a concise introduction to switched systems, the following section delves into the crucial issue of their stability analysis.

2.3.3 Stability analysis of switched systems

In this section, we review some notions related to the stability analysis of switched systems. Indeed, the stability problem of switching systems is both delicate and intriguing. To illustrate the complexity of this issue, we examine the classic example of two asymptotically stable subsystems that, when switched between each other, result in either unstable or stable overall behavior depending on the switching signal (Branicky, 1998).

Example 3 *Let us consider the autonomous linear switched system S, consisting of two subsystems, $S_1 : \dot{x}(t) = A_1 x(t)$ and $S_2 : \dot{x}(t) = A_2 x(t)$, where $A_1 = \begin{bmatrix} -0.5 & -0.4 \\ 3 & -0.5 \end{bmatrix}$ and $A_2 = \begin{bmatrix} -0.5 & -3 \\ 0.4 & -0.5 \end{bmatrix}$. Since the eigenvalues of both A_1 and A_2 have negative real parts, each individual subsystem exhibits **asymptotically stable** behavior as shown by the phase trajectories in Figure 2.5. This implies that, when left alone (without switching), any initial state of the system will eventually converge to the equilibrium point (origin) over time.*

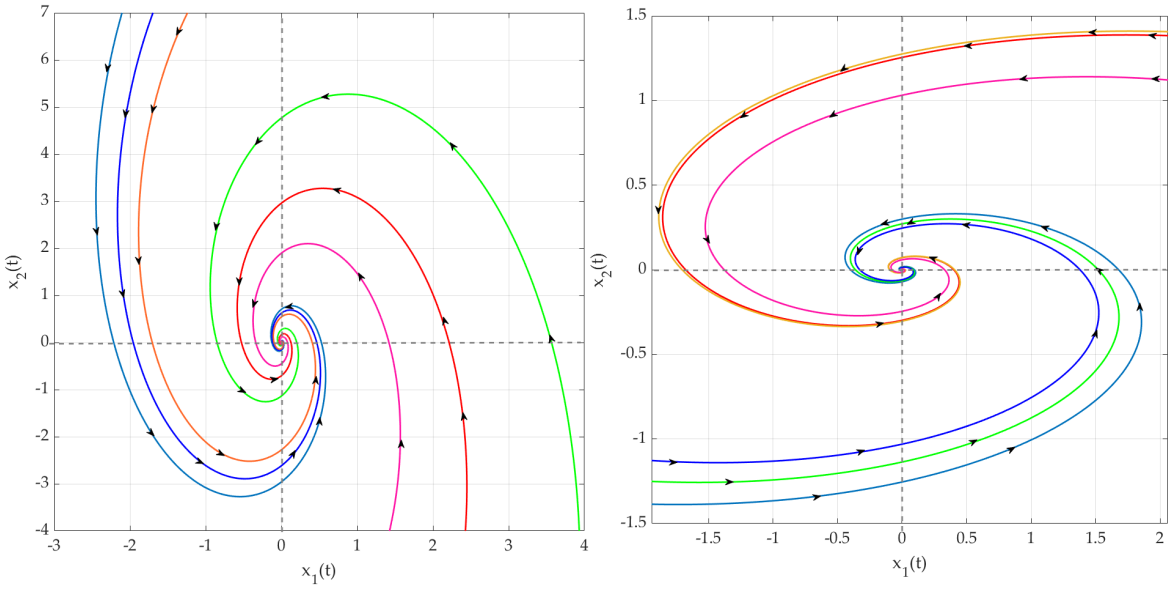

Figure 2.5: Phase trajectories for multiple initial states: subsystem 1 (Left) and subsystem 2 (Right).

Let us analyze the effects of two distinct switching laws:

$$\sigma_1(t) = \begin{cases} 1 & \text{if } x_1 x_2 \geqslant 0 \\ 2 & \text{if } x_1 x_2 < 0 \end{cases} \tag{2.18}$$

and

$$\sigma_2(t) = \begin{cases} 1 & \text{if } x_1 x_2 \leqslant 0 \\ 2 & \text{if } x_1 x_2 > 0 \end{cases} \tag{2.19}$$

As depicted in Figure 2.6, the overall stability of the switched system is contingent upon the selected switching law. Evidently, trajectories produced under the influence of switching law (2.18) exhibit an unstable behavior for the entire system, as illustrated in Figure 2.6 (left). Conversely, trajectories governed by switching law (2.19) demonstrate a stable behavior of the overall system, as depicted in Figure 2.6 (right). Similarly, other remarkable examples illustrate the case of unstable linear systems which, thanks to a particular switching law, would lead to a stable behavior (Branicky, 1998).

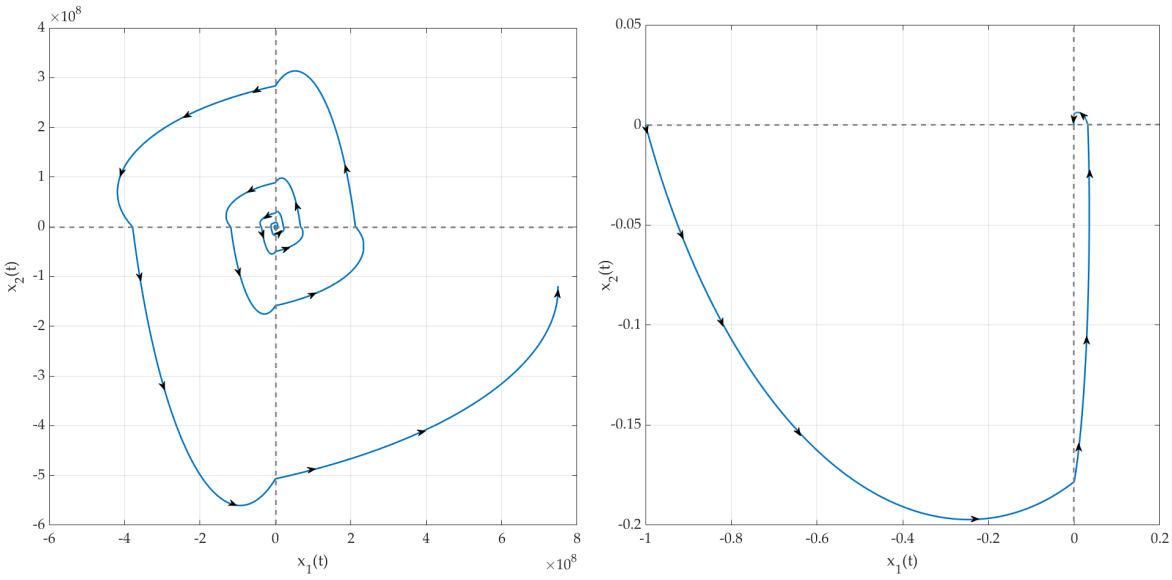

Figure 2.6: Phase trajectories for an unstable switched system (Left) and a stable switched system (Right) $(x_1(0) = -1, x_2(0) = 0)$

From the previous example, it can be observed that the asymptotic stability of each subsystem is not sufficient to guarantee the asymptotic stability of a switched system. The choice of the switching law has a significant influence on the stability of switched systems.

Motivated by these observations, our primary objective now becomes the identification of a general stability condition applicable to switched systems. This condition

should hold true irrespective of the nature of the switching signal, whether it be arbitrary or constrained. The subsequent sections will explore these two scenarios in detail: stability under arbitrary switching and stability under constrained switching.

2.3.3.1 Stability under arbitrary switching

This section explores the stability of switched systems when no constraints are imposed on the switching law. In other words, switching occurs arbitrarily and without any dwell-time restrictions (Liberzon, 2003). This implies that the overall system can be viewed as a dynamical system whose dynamics change over time due to the switching behavior. Consequently, stability analysis must consider all possible switching sequences.

Early investigations into the Lyapunov stability of switched systems adopted a methodology akin to that employed for linear systems (Liberzon, 2005). This approach hinges on the construction of a common quadratic Lyapunov function candidate applicable to all subsystems within the switched system. This strategy offers a significant advantage: it guarantees the asymptotic stability of the entire interconnected system, irrespective of the specific switching law governing the transitions between subsystems.

In essence, the existence of a common Lyapunov function that satisfies specific properties for each subsystem constitutes a sufficient condition for establishing the system's stability. To delve deeper into this concept, let us consider a linear switched system governed by the following state equation in open-loop mode:

$$\dot{x}\left(t\right)=\sum_{j=1}^{m}\sigma_{j}(t)A_{j}x\left(t\right) \tag{2.20}$$

where $x(t)\in\mathbb{R}^{n}$ is the state vector, $A_{j}\in\mathbb{R}^{n\times n}$ are constant coefficient matrices representing the dynamics of each mode, for $j\in Q=1,2,...,m$ represent the j^{th} subsystem, where m denotes the total number of subsystems. $\sigma_{j}(t)$ are switching functions defined above (5.2).

Let us consider a quadratic Lyapunov candidate function (common to all subsystems) described by:

$$V\left(x\left(t\right),t\right)=x^{T}\left(t\right)Px\left(t\right) \tag{2.21}$$

The switched linear system (2.20) is globally asymptotically stable if there exist matrices $P=P^{T}>0$ and satisfy $\forall x(t)\neq 0$:

$$\dot{V}(x(t)) = \dot{x}^T(t) Px(t) + x^T(t) P\dot{x}(t) < 0 \tag{2.22}$$

$$= x^T(t) \left(\sum_{j=1}^{m} \sigma_j(t) \left(A_j^T P + P A_j \right) \right) x(t) < 0 \tag{2.23}$$

The inequality (2.23) is satisfied for all $x(t) \neq 0$ if the following set of LMI hold, for $j = 1, ..., m$:

$$A_j^T P + P A_j < 0 \tag{2.24}$$

The stability of the switched linear system (2.20) can be effectively analyzed using the following theorem.

Theorem 3 *The switched linear system (2.20) is globally asymptotically stable, if there exists a symmetric positive matrix $P = P^T > 0$ such that the given inequalities (2.24) are satisfied for $j = 1, ..., m$.*

Remark 3 *It's important to note that finding a common Lyapunov function is a sufficient condition to guarantee the stability of switched systems (Branicky, 1998). However, this approach tends to lead to conservative results, especially when dealing with a large number of subsystems. This is because it requires finding a single Lyapunov matrix, P, that satisfies a set of LMI constraints. Additionally, it can be analytically shown that there exist stable switched systems for which no common quadratic Lyapunov function exists (Dayawansa and Martin, 1999).*

To illustrate these points, Figure 2.7 depicts the shape of a common quadratic Lyapunov function in the case of a linear switched system with two modes. In this scenario, the Lyapunov function decreases continuously regardless of the system's operating modes, including at the switching instants t_{c_i}, meaning $V\left(x(t_{c_i})^-\right) = V\left(x(t_{c_i})^+\right)$. In the context of switched systems, a prevailing challenge lies in mitigating conservatism during stability analysis. To address this, the employment of a multiple quadratic Lyapunov function (MQLF) approach offers a promising avenue (Lin and Antsaklis, 2009). The MQLF approach leverages a collection of local Lyapunov functions $V_j(x(t))$, each associated with a specific subsystem. These local functions are then combined to construct a "global Lyapunov function" $V(x(t)) = \sum_{j=1}^{m} \sigma_j(t) V_j(x(t))$, encompassing the entire system's state. However, due to the inherent switching behavior between subsystems, the global Lyapunov function might exhibit discontinuities at these switching instances. Consequently, it transforms into a pseudo-Lyapunov function, necessitating the introduction of supplementary conditions at switching instants for stability anal-

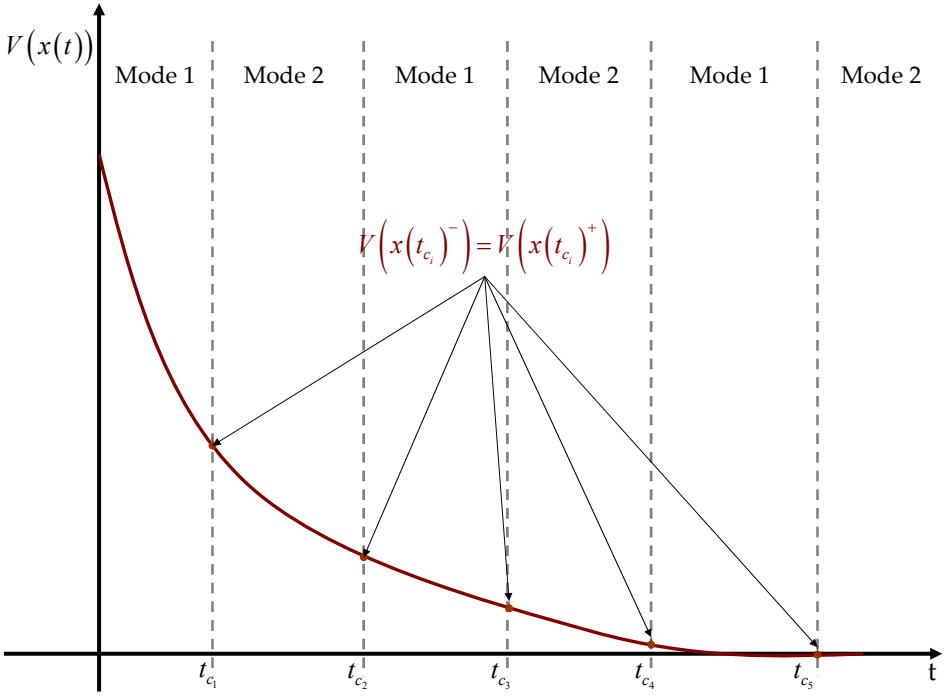

Figure 2.7: Trajectory of the common quadratic Lyapunov function.

ysis (DeCarlo et al., 2000). Fortunately, for stability analysis purposes, continuity of the global Lyapunov function is not an absolute requirement. This opens the door to exploring various possibilities for defining these additional conditions:

- A first alternative requires that the level of each local Lyapunov function V_j decreases when they are activated. Stability theorems developed in this context are based on the decrease of the Lyapunov function V_j at successive activations t_{c_l} and t_{c_k} of the same subsystem according to the equation (2.25) (, stabilityswitched00). Figure 2.8 illustrates the behavior of a global Lyapunov function for the case of a two-mode linear switched system.

$$V_j\left(x\left(t_{c_l}\right)\right) - V_j\left(x\left(t_{c_k}\right)\right) \leqslant -\gamma \left\|x\left(t_{c_k}\right)\right\|^2 \tag{2.25}$$

- Another alternative was proposed in (Jabri, 2011, Belkhiat, 2011). Let us consider two local Lyapunov functions, $V_{j^+}(x(t))$ and $V_j(x(t))$, associated with two successor modes: j^+ is the successor mode of j. Let us also assume that there exists a scalar $\mu_{j^+,\hat{j}} \leqslant 1$. The global Lyapunov function decreases at the switching instant t_{c_i} if the two Lyapunov functions $V_j(x(t))$ and $V_{j^+}(x(t))$ satisfy the condition 2.26.

$$V_{j^+}\left(x\left(t_{c_i}\right)\right) \leqslant \mu_{j^+,j} V_j\left(x\left(t_{c_i}\right)\right) \tag{2.26}$$

Figure 2.9 illustrates the behavior of a global Lyapunov function for the case of a two-mode linear switched system.

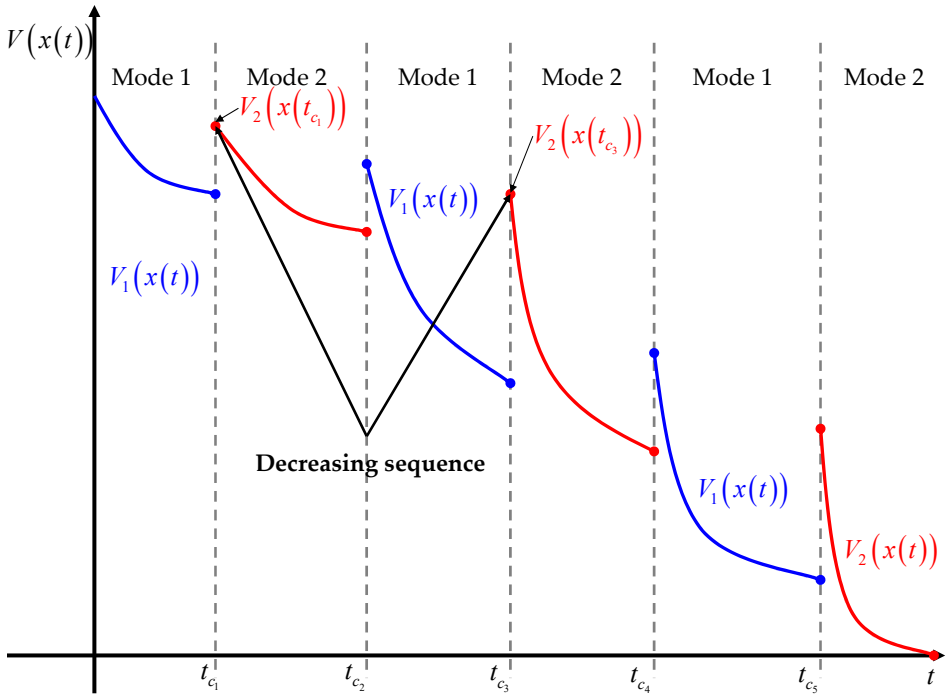

Figure 2.8: Trajectory of the multiple quadratic Lyapunov function (First method) (DeCarlo et al., 2000).

Remark 4 *While this chapter provides specific conditions for multiple Lyapunov functions, it is well-documented that alternative conditions exist in the literature. The degree of restrictiveness in these conditions varies. We will provide a more comprehensive discussion in the contribution chapter of the thesis.*

2.3.3.2 Stability under constrained switching

Another established method for guaranteeing the stability of switched systems involves imposing restrictions on the switching sequence. This constrained switching can be implemented during the design of the switching law or when enforcing a time-based switching strategy. Intuitively, if all individual subsystems are stable and the switching occurs slowly enough to allow transient effects from each switch to dissipate, then the overall switched system remains stable. Control theory for switched systems utilizes various dwell time concepts to quantify the "slowness" of switching. The dwell time $\tau_d > 0$ satisfies this inequality $t_{c_l} - t_{c_l}^+ \geqslant \tau_d$ with t_{c_l} and $t_{c_l}^+$ are consecutive

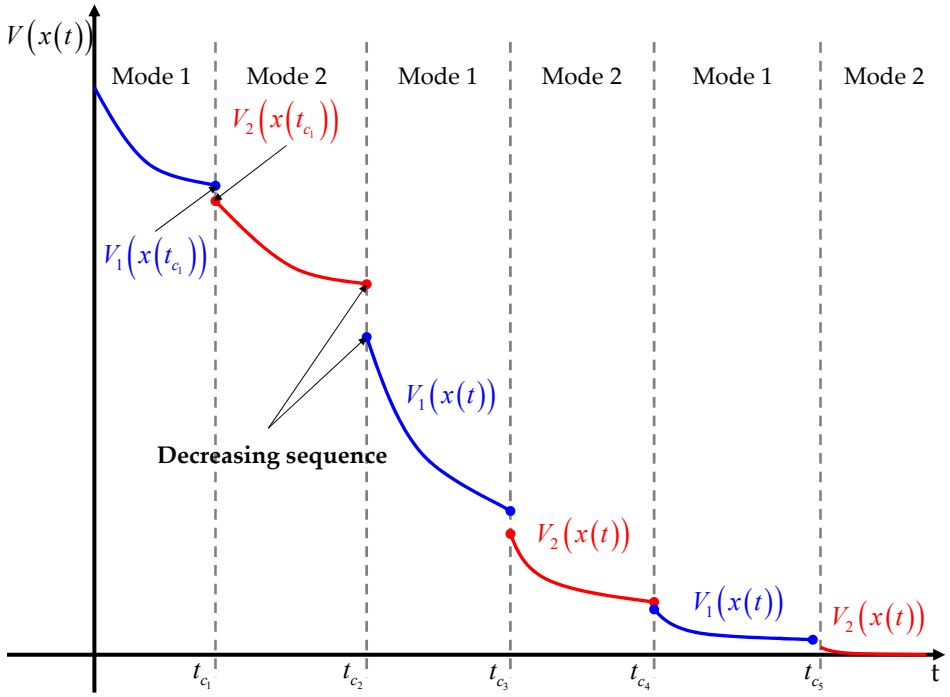

Figure 2.9: Trajectory of the multiple quadratic Lyapunov function (Second method)(Belkhiat, 2011).

switching times. In this subsection, we focus on two key metrics: minimum dwell time (MDT) and average dwell time (ADT) (Allerhand and Shaked, 2010).

- **Minimum Dwell Time (τ_{MDT}):** This refers to the shortest allowable time interval between consecutive switchings. A switching sequence that satisfies the MDT constraint ensures stability, but it can be overly restrictive in practice.
- **Average Dwell Time (τ_{ADT}):** This concept captures the average time spent in each system mode over a longer switching period. A switching sequence with an ADT exceeding a specific threshold guarantees stability, offering more flexibility compared to MDT.

The choice between these dwell time concepts depends on the specific system and desired level of control over the switching behavior. While MDT offers a more robust guarantee of stability, it may lead to unnecessary limitations on switching frequency. Conversely, ADT allows for more frequent switching while still ensuring stability on average, but requires careful design of the switching law to avoid excessively rapid switching.

Given the critical role of stability analysis, the following section explores the design of switched observer.

2.3.4 Challenges in observer design for switched systems

A switched observer departs from conventional observers by employing a collection of mode-specific observers. Each observer within this collection is meticulously tailored to excel at estimating the state of the system within a particular operating mode. By leveraging the unique dynamics associated with each mode, switched observers can generate accurate state estimates even amidst the system's switching phenomena (Figure 2.10, Chen and Mehrdad, 2004). A critical aspect of switched observer design and application is their synchronization with the system's switching dynamics. Two primary categories emerge:

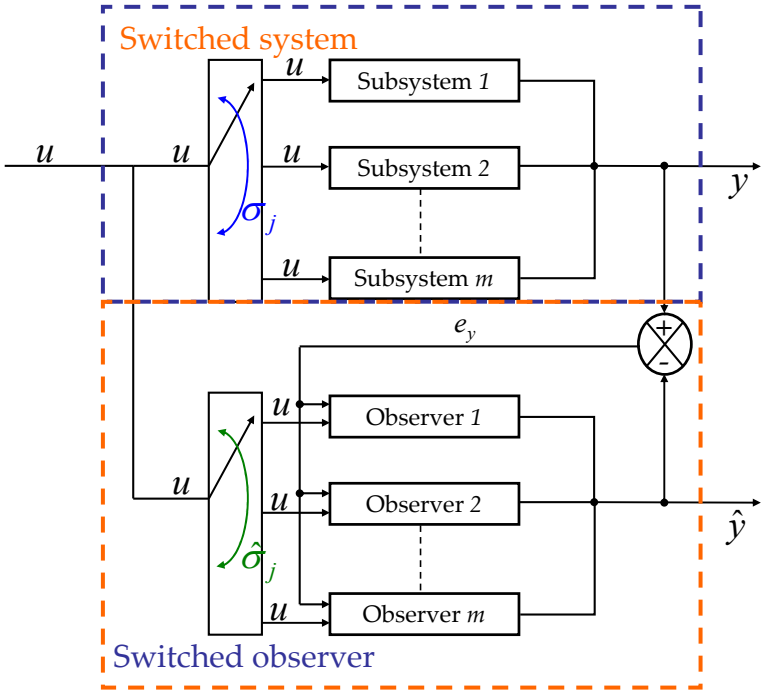

Figure 2.10: Schematic of a state observer for switched systems.

- **Synchronous observers:** These observers exhibit perfect concordance with the system's switching behavior. The active mode of the observer aligns precisely with the system's mode at every instant. However, this ideal scenario often necessitates unrealistic assumptions. Real-time access to the system's switching signals, without measurement limitations or delays, can be quite challenging to achieve in practice (Yang et al., 2015).

- **Asynchronous observers:** This represents a more pragmatic scenario where the observer's switching behavior deviates from that of the system (Han et al., 2019, Huang et al., 2020). The observer's switching signals may exhibit lags or discrepancies compared to the system's. This asynchronicity can manifest due to:

- *Detection delays:* In multi-mode systems, identifying the active mode can incur time delays, causing the observer's switching to lag behind the system's.
- *Mismatched switching laws:* When switching is governed by the system's state, inconsistencies between the observer's internal switching logic and the system's actual switching rules can lead to asynchronicity.

let us consider a switched linear systems described as follows:

$$\begin{cases} \dot{x}(t) = \sum_{j=1}^{m} \sigma_j(t) \left(A_j x(t) + B_j u(t)\right) \\ y(t) = Cx(t) \end{cases} \tag{2.27}$$

where $x(t) \in \mathbb{R}^n$, $u(t) \in \mathbb{R}^q$ and $y(t) \in \mathbb{R}^p$ are respectively the state vector (non-measurable or partially measurable), the input vector and the output vector. For all $j \in Q$, A_j, B_j and C_j are known matrices of appropriate dimensions. All state-output pairs (A_j, C_j) are assumed observable. $\sigma_j(t)$ are switching functions of the switched systems defined by 5.2.

Consider the switched observers given by:

$$\begin{cases} \dot{\hat{x}}(t) = \sum_{j=1}^{m} \hat{\sigma}_j(t) \left(A_j \hat{x}(t) + B_j u(t) + L_j \left(y(t) - \hat{y}(t)\right)\right) \\ \hat{y}(t) = C\hat{x}(t) \end{cases} \tag{2.28}$$

where $\hat{x}(t) \in \mathbb{R}^n$ and $\hat{y}(t) \in \mathbb{R}^p$ are the estimated state and output vectors, respectively, and L_j are the gain matrices to be determined. $\hat{\sigma}_j(t)$ are switching functions associated with the switched observer.

Let us assume that state-dependent switching between different subsystems occurs according to a switching signal defined by linear hyperplanes:

$$G_{j,j^+} = \left\{ x \in \mathbb{R}^n \middle| \, g_{j,j^+}(x) = a^1_{j,j^+} x_1 + a^2_{j,j^+} x_2 + \ldots + a^n_{j,j^+} x_n = 0 \right\} \tag{2.29}$$

With: $(j, j^+) \in I_g$ and $\left(a^1_{j,j^+}, a^2_{j,j^+}, \ldots, a^n_{j,j^+}\right) \in \mathbb{R}^n$. We define I_g as the set of tuples gathering the different possible transitions, between two modes, that can occur in a switched systems.

As mentioned below, two cases regarding the evolution of the switched observer are possible.

2.3.4.1 Synchronous observers

In this scenario, we assume perfect mode synchronization between the switched observers and the underlying switched system. This implies that the active mode for

both the observer (denoted by $\hat{\sigma}_j(t)$) and the system itself (denoted by $\sigma_j(t)$) are identical at every instant in time (i.e., $\hat{\sigma}_j(t) = \sigma_j(t)$). Under this assumption of perfect synchronization, the estimation error between the system's true state, $x(t)$, and the state reconstructed by the observer, $\hat{x}(t)$, can be expressed as:

$$e\left(t\right) = x\left(t\right) - \hat{x}\left(t\right) \tag{2.30}$$

Thus, the state error dynamic can be written as:

$$\dot{e}\left(t\right) = \sum_{j=1}^{m} \sigma_j\left(t\right)(A_j - L_j C)e\left(t\right) \tag{2.31}$$

Indeed, under the aforementioned assumption of perfect synchronization, the design of the switched observers L_j consists to analyzing the stability of the estimation error dynamics (2.31). Two main approaches can be considered for this purpose as indicted in sections 2.3.3.1 and 2.3.3.2: stability under arbitrary switching and stability under constrained switching.

For the state error dynamics (Eq. (2.31)), a common quadratic Lyapunov function facilitates stability analysis under arbitrary switching. This function offers a unified framework for all subsystems within the switched system, simplifying the analysis.

$$V(e(t)) = e^T(t)Pe(t) \tag{2.32}$$

Compute the derivative of the Lyapunov function along the error dynamics:

$$\dot{V}(t) = \dot{e}^T(t)Pe(t) + e^T(t)P\dot{e}(t) \tag{2.33}$$

$$= e^T(t)((A_j - L_j C)^T P + P(A_j - L_j C))e(t) \tag{2.34}$$

For the estimation error dynamics to be asymptotically stable, the time derivative of the Lyapunov function (2.34) must be strictly negative definite. This means $\dot{V}(e(t))$ is always less than zero for any non-zero estimation error ($\dot{V}(e(t)) < 0$). This guarantees the estimation error converges to zero over time. To achieve this negativity, the following inequalities must hold, for $j = 1, ..., m$:

$$(A_j - L_j C)^T P + P(A_j - L_j C) < 0 \tag{2.35}$$

The following theorem provides a foundation for switched observer design.

Theorem 4 *Given the switched linear system (2.27) and the switched observer (2.28), the state error dynamics (2.31) achieve global asymptotic stability, if a symmetric positive matrix $P = P^T > 0$ and matrices Y_j exist, satisfying the following LMIs, for $j = 1, ..., m$:*

$$A_j^T P - C^T Y_j^T + P A_j - Y_j C < 0 \tag{2.36}$$

The observer gain matrix can be derived as: $L_j = P^{-1} Y_j$.

Remark 5 *The utilization of a single Lyapunov function in Theorem 4 leads to conservative conditions. This can be mitigated by employing separate Lyapunov functions for each subsystem (multiple quadratic Lyapunov function (MQLF)). However, to guarantee a decrease in the global Lyapunov function at each switching instant, additional conditions are necessary.*

2.3.4.2 Asynchronous observers

In the case of asynchronous observers, a key distinction lies in the divergence between the respective modes of the switched observers and the switched systems (i.e., $\hat{\sigma}_j(t) \neq \sigma_j(t)$). Thus, the state error dynamic can be written as:

$$\dot{e}(t) = \bar{A}_{\hat{\sigma}_j} e(t) + \Delta\bar{A}_{\sigma_j,\hat{\sigma}_j} x(t) + \Delta\bar{B}_{\sigma_j,\hat{\sigma}_j} u(t) \tag{2.37}$$

with: $\bar{A}_{\hat{\sigma}_j} = \sum_{j=1}^{m} \hat{\sigma}_j(t)(A_j - L_j C)$, $\Delta\bar{A}_{\sigma_j,\hat{\sigma}_j} = \sum_{j=1}^{m} \sigma_j(t) A_j - \sum_{j=1}^{m} \hat{\sigma}_j(t) A_j$ and $\Delta\bar{B}_{\sigma_j,\hat{\sigma}_j} = \sum_{j=1}^{m} \sigma_j(t) B_j - \sum_{j=1}^{m} \hat{\sigma}_j(t) B_j$.

Analyzing the estimation error dynamics reveals its dependence on both the state vector $x(t)$ and the input vector $u(t)$. Consequently, studying the stability of the estimation error in the context of asynchronous observers becomes significantly more challenging compared to the initial case.

Remark 6 *Building upon the principles of conventional observers, switched observer design employs LMI conditions to ensure the asymptotic stability (convergence) of the state estimation error. While this chapter presents the fundamentals of switched observer design, a deeper dive into asynchronous observers, including advanced techniques for handling the challenges of asynchronicity, is provided in the contribution chapter.*

2.4 Conclusion

In conclusion, this chapter has established a firm foundation for the analysis and design of switched systems. We commenced by providing a comprehensive overview of this class of systems, introducing fundamental modeling concepts and illustrating them through well-chosen examples. Subsequently, we delved deeper into the subject by exploring two distinct categorization schemes. The first categorization differentiated switched systems based on their switching mechanism, classifying them as state-dependent or time-dependent. The second focused on the nature of switching control, distinguishing between autonomous and controlled switching.

Following the establishment of these categories, the chapter addressed the critical issue of stability analysis in switched systems. We presented two primary approaches: stability under arbitrary switching and stability under constrained switching. Finally, the chapter explored the design of observers for switched systems, introducing two categories of observers based on their synchronous or asynchronous switching behavior relative to the system itself.

A critical examination of the provided bibliography has led us to the following key findings:

- The analysis of stability and observer design presents a significant challenge under arbitrary switching conditions. This stems from the inherent unpredictability of both the timing and sequence of switching events. As opposed to scenarios with externally controlled switching, the lack of control over these events introduces a substantial layer of complexity in analyzing the overall system's behavior.

- While the existence of a common Lyapunov function guarantees the stability of switched systems, this method often yields conservative stability results, especially for systems with a high number of subsystems. To mitigate this conservatism, the multiple quadratic Lyapunov function approach offers a promising avenue for analysis. However, due to the inherent switching behavior between subsystems, additional stability conditions must be introduced at switching instants.

- In contrast to synchronous observers, asynchronous observers present a more realistic scenario where the observer's switching behavior deviates from the system's due to inherent detection delays and potentially mismatched switching laws. This asynchronicity, manifested as lags or discrepancies in the observer's switching signals compared to the system's, introduces significant challenges in observer design.

The analysis and control of switched systems are often hampered by their inherent nonlinearities, rendering traditional linear control techniques less effective. To address

this challenge, the next chapter introduces Takagi-Sugeno (T-S) models as a powerful modeling approach. These models represent the nonlinear dynamics of each subsystem within the switched system using a set of linear rules defined in a compact region of the overall state space. By leveraging T-S models, we can overcome the limitations of linear control and pave the way for the design of more effective control strategies for switched systems.

Chapter 3

Preliminary notions on Takagi-Sugeno fuzzy modeling

3.1 Introduction

THIS chapter presents a comprehensive investigation of Takagi-Sugeno (T-S) fuzzy multi-model systems. It delves into the fundamental concepts underlying these systems and explores various methodologies for their derivation, with a particular focus on the sector nonlinearity approach.

Moreover, this chapter analyzes the stability of T-S fuzzy multi-model systems by employing the robust theoretical framework of Lyapunov function theory. A critical challenge addressed in this chapter is state observer design for T-S systems. The intricate issue of unmeasurable premise variables, which are known to significantly influence observer design, is meticulously examined along with its impact on observer design methodologies.

Finally, the chapter explores a specialized class of T-S systems, namely switched T-S fuzzy systems. It provides a detailed exposition of their structural characteristics and showcases their application through a switched tunnel diode circuit. This section concludes by highlighting challenges associated with observer design in the context of switched T-S fuzzy systems.

3.2 Fundamentals of Takagi-Sugeno fuzzy modeling

Takagi-Sugeno (T-S) models have been extensively studied since their introduction in 1985 (Takagi and Sugeno, 1985). They belong to the class of convex polytopic systems and allow to extend some concepts of linear systems control to the case of nonlinear systems. Originally based on fuzzy formalism, the most recent methods for obtaining T-S models, such as nonlinear sector decomposition (Taniguchi et al., 2001), allow to exactly represent a nonlinear system on a compact space of its state variables. As

a result, a T-S model can be written as a collection of linear dynamics (polytopes) interpolated by a set of nonlinear functions (satisfying convex sum properties). Many research works are interested in this class of systems. For example, they deal with the stability and stabilization of standard T-S systems (Takagi and Sugeno, 1985, Yoneyama et al., 2001, Guerra and Vermeiren, 2004), the stabilization of T-S descriptor systems (Yoneyama, 2020, Taniguchi et al., 2000), or with diagnosis and observation (Ichalal et al., 2014, Rodríguez et al., 2024).

In this section, we present the structure of T-S multi-models, as well as the most common methods for their derivation.

3.2.1 Takagi-Sugeno multi-model approach

A T-S multi-model consists of a set of linear models connected by an interpolation structure represented by nonlinear membership functions. In 1985, based on fuzzy formalism, Takagi and Sugeno, 1985 proposed a modeling approach for nonlinear systems based on a set of fuzzy "If ... Then" rules whose conclusions represent a set of linear dynamics. Thus, if we denote r as the number of fuzzy rules describing a T-S model, the i^{th} rule R^i is given by:

$$\begin{aligned} &R^i : IF\ z_1\, is\, F_1^i\left(z_1\left(t\right)\right)\ \ AND\, z_2\, is\, F_2^i\left(z_2\left(t\right)\right) \ldots z_p\, is\, F_p^i\left(z_p\left(t\right)\right) \\ &THEN\ \begin{cases} \dot{x}_i\left(t\right) = A_i x\left(t\right) + B_i u\left(t\right) \\ y_i\left(t\right) = C_i x\left(t\right) \end{cases} \end{aligned} \tag{3.1}$$

where, for $j = 1, ..., p$, $F_j^i\left(z_j\left(t\right)\right)$ are fuzzy subsets realizing an exact partition of the universe of discourse (sometimes called the reference set), $z_j\left(t\right)$ are the premise variables dependent on the inputs and/or the state of the system. $x\left(t\right) \in \mathbb{R}^\eta$ is the state vector of the system, $u\left(t\right) \in \mathbb{R}^\vartheta$ is the input vector and $y\left(t\right) \in \mathbb{R}^q$ is the output vector, A_i, B_i and C_i are the matrices describing the dynamics of the system.

For each fuzzy rule R^i, a weight function $w_i\left(z_j\left(t\right)\right)$ can be attributed, determining the contribution of each of the linear dynamics composing the multi-model in its entirety. This weight function depends on the degree of membership of the premise variables $z_j\left(t\right)$ to the fuzzy subsets $F_j^i\left(z_j\left(t\right)\right)$ and the choice of the operator AND, such as:

$$w_i\left(z\left(t\right)\right) = \prod_{j=1}^{p} F_j^i\left(z_j\left(t\right)\right) \text{ for } i = 1, ..., r \tag{3.2}$$

Let us consider:

$$h_i\left(z\left(t\right)\right) = \frac{w_i\left(z\left(t\right)\right)}{\sum\limits_{i=1}^{r} w_i\left(z\left(t\right)\right)} \tag{3.3}$$

The activation function $h_i\left(z\left(t\right)\right)$ of the i^{th} fuzzy model rule satisfies the following

convex sum properties: $0 < h_i(z(t)) < 1$ and $\sum_{i=1}^{r} h_i(z(t)) = 1$. These properties ensure that the overall output of the T-S multi-model is a convex combination of the local models. This is important because it guarantees that the multi-model will be smooth and continuous.

Thus, after defuzzification, the state representation of a T-S multi-model can be written in the form:

$$\begin{cases} \dot{x}(t) = \sum_{i=1}^{r} h_i(z(t)) (A_i x(t) + B_i u(t)) \\ y(t) = \sum_{i=1}^{r} h_i(z(t)) C_i x(t) \end{cases} \tag{3.4}$$

A schematic of the structure of a T-S multi-model system is given in Figure 3.1.

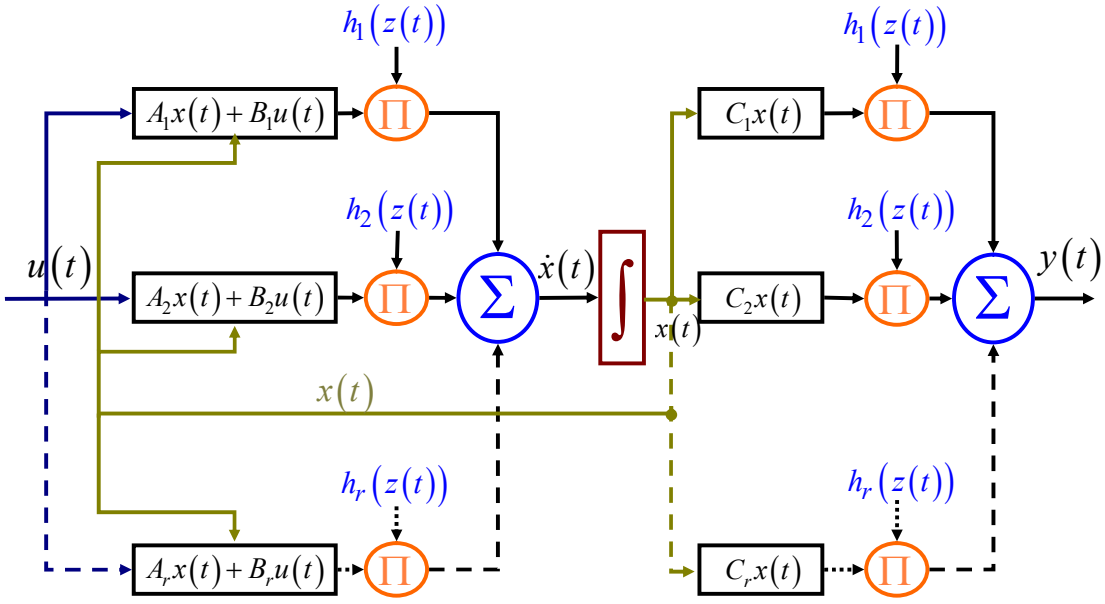

Figure 3.1: Schematic of the structure of a T-S multi-models (Jabri, 2011).

3.2.2 Derivation of Takagi-Sugeno multi-models

Several established techniques exist in the literature for constructing T-S multi-models. Some techniques are particularly valuable when a non-linear knowledge model of the controlled system is readily available, such as:

- **Linearization-based approach:** This method involves linearizing the non-linear model at various operating points. The resulting linear models are then aggregated using fuzzy membership functions (e.g., triangular, trapezoidal) as described by Ma et al., 1998. This approach offers a computationally efficient way to obtain a T-S model. However, the resulting model may be an approximation of the original non-linear system as the chosen membership functions might not accurately capture the non-linear interpolation mechanisms between the subsystems.

- **Convex polytopic transformation approach:** This more rigorous approach utilizes convex polytopic transformations to generate a T-S multi-model that exactly represents the non-linear model within a compact state space. Among the various convex polytopic transformations, "sector nonlinearity approach" (Taniguchi et al., 2001, Morère, 2001) is a commonly used method for obtaining T-S models. This approach offers a more accurate representation of the non-linear system but may require more complex computations compared to the linearization-based approach.

T-S model identification becomes a suitable alternative when a control system lacks a readily available analytical model. The methodology outlined by Gasso et al., 2000 offers a valuable framework for this purpose. This data-driven approach leverages input-output measurements acquired from the real system. By analyzing these measurements around pre-defined operating points, both the local models and the activation functions are identified, thereby constructing the T-S model representation of the system.

This dissertation predominantly employs the Sector Nonlinearity Approach (SNA) for analysis. SNA capitalizes on the well-established mathematical principle that any nonlinear function can be guaranteed to have finite upper and lower bounds within its defined domain. A systematic methodology for SNA is subsequently established based on the following lemma.

Lemma 1 (Morère, 2001) *If* $\forall x \in [-b, a]$, $a, b \in \mathbb{R}^+$, *the function* $f(x(t)) : \mathbb{R} \to \mathbb{R}$ *is bounded on* $[-b, a]$, *there always exist two functions* $w_1(x(t))$ *et* $w_2(x(t))$ *as well as two scalars* α *and* β *such that :*

$$f(x(t)) = \alpha \times w_1(x(t)) + \beta \times w_2(x(t)) \tag{3.5}$$

with $\alpha = \max(f(x(t)))$, $\beta = \min(f(x(t)))$, $w_1(x(t)) = \frac{f(x(t))-\beta}{\alpha-\beta}$ *and* $w_2(x(t)) = \frac{\alpha-f(x(t))}{\alpha-\beta}$.

To elucidate the methodology of obtaining T-S multi-models through nonlinear sector decomposition, we consider two representative examples.

Example 4 (Jabri, 2011) *Consider a nonlinear autonomous system given by the following equation:*

$$\dot{x}(t) = x(t)\cos(x(t)) \tag{3.6}$$

The nonlinear term $f(x(t)) = \cos(x(t))$ *is continuous and bounded by* $\begin{bmatrix} -1 & 1 \end{bmatrix}$. *According to Lemma 1, we can write :*

$$\cos(x(t)) = \underbrace{\frac{\cos(x(t))+1}{2}}_{h_1(x(t))} \times 1 + \underbrace{\frac{1-\cos(x(t))}{2}}_{h_2(x(t))} \times (-1) \tag{3.7}$$

The nonlinear system (3.6) can be rewritten as a T-S multi-model given by:

$$\dot{x}(t) = \sum_{i=1}^{2} h_i(x(t))\, a_i x(t) \tag{3.8}$$

where $a_1 = 1$ *and* $a_2 = -1$.

Example 5 (Coupled inverted pendulums (Jabri et al., 2020)) *Let us consider the modelling problem of balancing two interconnected inverted pendulums coupled by a spring. Figure 3.2 depicts a schematic representation of this system, modeled as two nonlinear interconnected subsystems.*

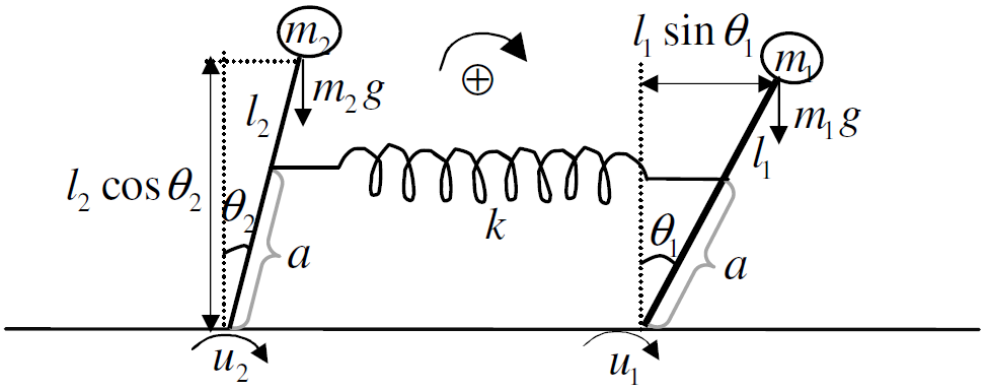

Figure 3.2: Schematic of two nonlinear interconnected subsystems (Jabri et al., 2020).

Equations (3.9)-(3.10) describes the system's dynamics. DC motors provide independent torque actuation for each pendulum's position control.

$$J_1\ddot{\theta}_1 = m_1 g l_1 \sin\theta_1 - ka^2(\theta_2 - \theta_1) - d_1\dot{\theta}_1 + u_1 + w_1 \tag{3.9}$$

$$J_2\ddot{\theta}_2 = m_2 g l_2 \sin\theta_2 + ka^2(\theta_2 - \theta_1) - d_2\dot{\theta}_2 + u_2 + w_2 \tag{3.10}$$

where S_i denote the i^{th} subsystem, g the acceleration of gravity, k = the spring constant, l_i the i^{th} pole length, a the distance between the pendulum hinges, L the natural length of the connecting spring, J_i the i^{th} moment of inertia, m_i the i^{th} pendulum end masses, θ_i the i^{th} angular position (rad) with $\theta_i \in \left[-\frac{\pi}{3}, \frac{\pi}{3}\right]$, $\dot{\theta}_i$ the i^{th} angular velocity (rad/s), d_1 the i^{th} friction constant, u_i the i^{th} torque input applied by the i^{th} DC motor (N.m), w_i the i^{th} disturbances (N.m). The table 3.1 lists the parameter values for the coupled inverted pendulums.

Table 3.1: Parameters of the coupled inverted pendulums.

Parameter	Value	Designation
m_1	$0.25\,kg$	Mass of pendulum 1
m_2	$0.2\,kg$	Mass of pendulum 2
J_1	$2\,kgm^2$	Inertia of pendulum 1
J_2	$2.5\,kgm^2$	Inertia of pendulum 2
$l_1 = l_2$	$1\,m$	Length of the pendulums
a	$0.2\,m$	Distance from pendulum to spring hinges
d_1	$3.5\,Nms/rad$	Joint friction coefficient of pendulum 1
d_2	$4.5\,Nms/rad$	Joint friction coefficient of pendulum 2
k	$8\,Nm^{-1}$	Spring stiffness coefficient
g	$9.81\,ms^{-2}$	Acceleration of the gravity
L	$1.2\,m$	Natural length of the connecting spring

To facilitate in-depth analysis, we propose a modeling approach that decomposes the system (3.9)-(3.10) into a set of two interconnected T-S fuzzy subsystems, described as follows.

$$\begin{cases} \dot{x}_i(t) = \sum\limits_{j_i=1}^{\nu_i} h_{j_i}(z_i(t)) \left(A_{j_i}x_i(t) + B_{j_i}u_i(t) \right. \\ \qquad\qquad \left. + B_{j_i}^{w}w_i(t) + \sum\limits_{\substack{\alpha=1 \\ \alpha\neq i}}^{n} h_{j_i}(z_i(t))F_{j_i}^{\alpha}x_\alpha(t)\right) \\ y_i(t) = \sum\limits_{j_i=1}^{\nu_i} h_{j_i}(z_i(t))\, C_{j_i}x_i(t) \end{cases} \tag{3.11}$$

where $x_i(t) \in \mathbb{R}^{\eta_i}$, $y_i(t) \in \mathbb{R}^{\rho_i}$, $u_i(t) \in \mathbb{R}^{\upsilon_i}$ are respectively the i^{th} state, measurement (output) and input vectors. $w_i(t) \in \mathbb{R}^{\mu_i}$ is a time-varying L_2-norm-bounded external disturbance associated to the i^{th} subsystem (assumed to be uncontrolled). ν_i is the number of vertices of the i^{th} T-S subsystem and, for $j_i = 1, ..., \nu_i$, $A_{j_i} \in \mathbb{R}^{\eta_i \times \eta_i}$, $B_{j_i} \in \mathbb{R}^{\eta_i \times \upsilon_i}$, $B_{j_i}^{wi} \in \mathbb{R}^{\eta_i \times \mu_i}$ and $C_{j_i} \in \mathbb{R}^{\rho_i \times \eta_i}$ are constant matrices. The matrices $F_{j_i}^{\alpha} \in \mathbb{R}^{\eta_i \times \eta_\alpha}$ express the interconnection between the i^{th} subsystem and the α^{th} subsystem with $\alpha = 1, \ldots, n$ and $\alpha \neq i$. $z_i(t)$ are the premise variables of the i^{th} TS subsystem. Finally, $h_{j_i}(z(t)) \geq 0$ are the fuzzy membership functions of the i^{th} TS subsystem, which satisfy the convex sum proprieties $\sum_{j_i=1}^{\nu_i} h_{j_i}(z_{j_i}(t)) = 1$.

For the purposes of this investigation, we consider the state vector $x_i = \begin{bmatrix} x_{1_i} \\ x_{2_i} \end{bmatrix} = \begin{bmatrix} \theta_i \\ \dot{\theta}_i \end{bmatrix}$. Hence, the equations (3.9)-(3.10) can be written as following, for $i, \alpha = 1, 2$ and $\alpha \neq i$

$$S_i : \begin{cases} \dot{x}_{1_i} = x_{2_i} \\ \dot{x}_{2_i} = \frac{m_i g l_i \left(\sin x_{1_i}/x_{1_i}\right) - k a_i^2}{J_i} x_{1_i} - \frac{d_i}{J_i}x_{2_i} + \frac{1}{J_i}u_i + \frac{1}{J_i}w_i - \frac{k a_i^2}{J_i}x_{1_i} \\ y_i = x_{1_i} \end{cases} \tag{3.12}$$

Note that, each subsystem contains one nonlinear bounded term:

$$\frac{m_i g l_i \left(\sin x_{1_i}/x_{1_i}\right) - k a_i^2}{J_i}$$

(such $\sin\theta_i/\theta_i \in [-0.217, 1]$*) Using the sector nonlinearity approach (Taniguchi et al., 2001, Morère, 2001) to deal with the nonlinear terms, the whole system can be represented as two interconnected T-S subsystem with:*

$$A_{1_1} = \begin{bmatrix} 0 & 1 \\ -1.97 & -1.75 \end{bmatrix}, A_{2_1} = \begin{bmatrix} 0 & 1 \\ 9.97 & -1.75 \end{bmatrix},$$

$$A_{1_2} = \begin{bmatrix} 0 & 1 \\ -2.00 & -1.80 \end{bmatrix}, A_{2_2} = \begin{bmatrix} 0 & 1 \\ 9.94 & -1.80 \end{bmatrix},$$

$$B_{j_1} = B_{j_1}^w = \begin{bmatrix} 0 \\ 0.50 \end{bmatrix}, B_{j_2} = B_{j_2}^w = \begin{bmatrix} 0 \\ 0.40 \end{bmatrix},$$

$$C_{j_i} = \begin{bmatrix} 1 & 0 \end{bmatrix}, F_{1_1}^2 = F_{2_1}^2 = \begin{bmatrix} 0 & 0 \\ -0.16 & 0 \end{bmatrix},$$

$$F_{1_2}^1 = F_{2_2}^1 = \begin{bmatrix} 0 & 0 \\ -0.13 & 0 \end{bmatrix},$$

$$h_{1_i} = [9.81\left(1 - \left(\sin\left(x_{1_i}\right)/x_{1_i}\right)\right)]/11.94, h_{1_i} = 1 - h_{2_i}.$$

For simulation purpose, let us consider that the coupled inverted pendulums is governed by a controller designed according to approach presented in (Jabri et al., 2020). The results are shown in Figures 3.3 and 3.4. Figure 3.3 exhibits the state vector trajectories while Figure 3.4 shows the evolution of activation functions, for each pendulum. We can observe that the sum of the activation functions for each pendulum is always one 1.

Remark 7 *The number of fuzzy rules in a T-S model constructed via a convex polytopic transformation exhibits a direct dependence on the number of nonlinear terms* n_l *extracted from the system's underlying nonlinear representation. This implies that a more complex system with* n_l *nonlinearities will necessitate a T-S model with a correspondingly larger number of fuzzy rules* (2^{n_l}) *to accurately capture its behavior.*

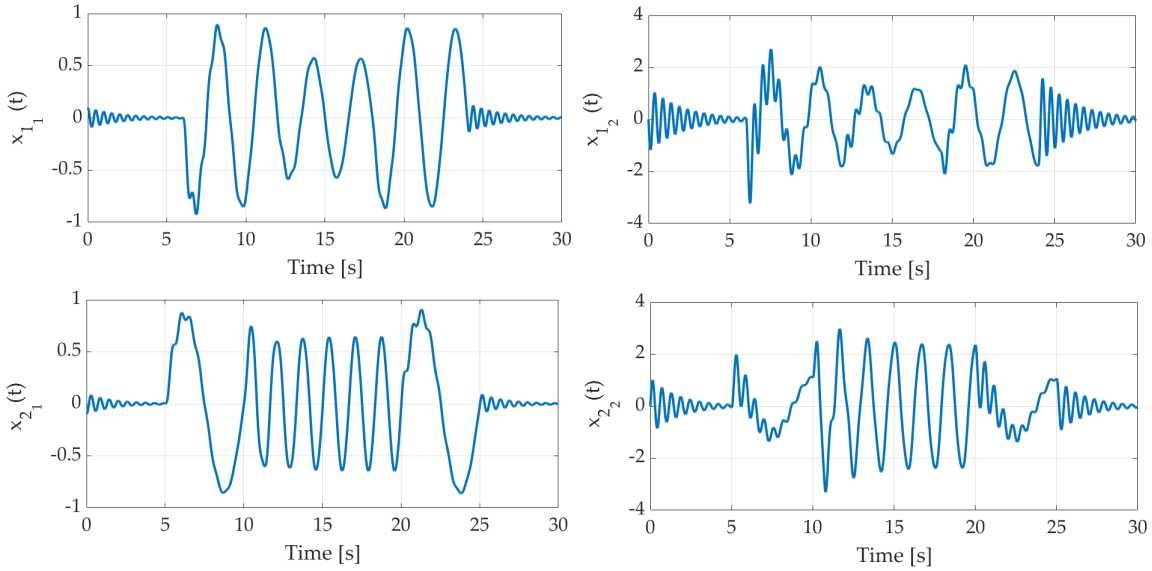

Figure 3.3: State vector trajectories (Jabri et al., 2020).

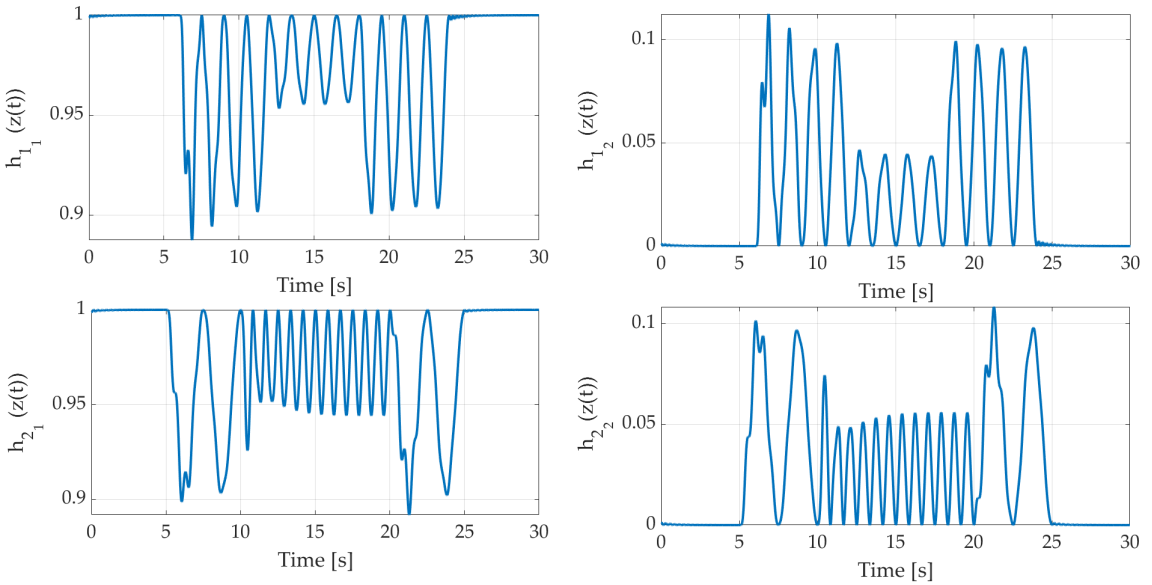

Figure 3.4: Activation functions trajectories (Jabri et al., 2020).

Remark 8 *It's noteworthy that applying the sector nonlinearity approach (Taniguchi et al., 2001) can yield an exact T-S model from a nonlinear system. However, this exact model's validity is strictly confined to a domain of validity $\mathcal{D}_x$, defined as follows:*

$$\mathcal{D}_x = \{x(t) \in \mathbb{R}^{n_x} : \mathcal{L}x(t) \leq \mathcal{Q}, \zeta \in \mathcal{I}_\zeta\} \tag{3.13}$$

where $\mathcal{L} \in \mathbb{R}^{2\zeta \times n_x}$ is a given matrix, $\mathcal{Q} \in \mathbb{R}^{2\zeta}$ is a given vector, and ζ is the number of state variable bounds.

A nonlinear sector is considered local if the the domain of validity $\mathcal{D}_x$ is a subset of the real numbers $\mathbb{R}$. A common example is when $\mathcal{D}_x$ is a closed interval between negative d and positive d, where d is a positive number ($\mathcal{D}_x = [-d, d]$ with $d > 0$). Otherwise, if $\mathcal{D}_x$ is equal to the entire set of real numbers ($\mathcal{D}_x = \mathbb{R}$), the nonlinear sector is considered global (Taniguchi et al., 2001).

3.2.3 Quadratic Lyapunov stability analysis of T-S fuzzy systems

As we have seen above, T-S systems are composed of linear models interconnected by nonlinear functions. This particular structure allows us to extend certain concepts related to linear systems to the case of nonlinear systems, including stability analysis and stabilization. In order to better understand the contributions presented in the following chapters, some basic concepts are presented below.

This section establishes fundamental stability conditions for T-S fuzzy autonomous systems by employing Lyapunov theory.

Consider the following T-S multi-model:

$$\dot{x}(t) = \sum_{i=1}^{r} h_i(z(t)) A_i x(t) \tag{3.14}$$

and the following quadratic Lyapunov function candidate:

$$V(x(t)) = x^T(t) P x(t) \tag{3.15}$$

note that for $x(0) = 0$, the value of the function $V(x(t))$ evaluated at the initial state is equal to zero ($V(x(0)) = 0$). The function (3.15) is said to be a Lyapunov function and the system (3.6) is stable if there exists a matrix P such that, $\forall x\,(t) \neq 0$:

$$V\,(x\,(t)) = x^T\,(t)\,P x\,(t) > 0 \tag{3.16}$$

and

$$\dot{V}\,(x\,(t)) < 0 \tag{3.17}$$

It is evident that the inequality (3.16) is satisfied if and only if P is a symmetric positive definite matrix $P = P^T > 0$. Furthermore, by substituting (3.6) in (3.17), The derivative of the Lyapunov function (3.17) can be written as follows:

$$\dot{V}\,(x\,(t)) = \dot{x}^T\,(t)\,P x\,(t) + x^T\,(t)\,P \dot{x}\,(t) < 0 \tag{3.18}$$

$$\dot{V}\,(x\,(t)) = x^T\,(t) \left(\sum_{i=1}^{r} h_i\,(z\,(t)) \left(A_i^T P + P A_i \right) \right) x\,(t) < 0 \tag{3.19}$$

The inequality (3.19) holds $\forall x(t) \neq 0$ if:

$$\sum_{i=1}^{r} h_i(z(t)) \left(A_i^T P + P A_i\right) < 0 \tag{3.20}$$

Assuming the membership functions $h_i(z(t))$ satisfy the convex sum properties and in particular $h_i(z(t)) > 0$, the inequality (3.20) is satisfied if all the terms of the sum are negative. Therefore, the stability conditions, based on the quadratic Lyapunov candidate function, are expressed as a Linear Matrix Inequality (LMI) problem (Boyd et al., 1994) in the following theorem.

Theorem 5 (Tanaka and Sugeno, 1992) *The autonomous T-S fuzzy system is asymptotically stable if there exists a matrix $P = P^T > 0$, such that the following LMIs are satisfied for all $i = 1, ..., r$:*

$$A_i^T P + P A_i < 0 \tag{3.21}$$

Remark 9 *The established stability conditions (3.21) for fuzzy T-S systems, as presented in the theorem (5), provide sufficient conditions to ensure stability. However, these conditions might exhibit a degree of conservatism, potentially excluding some truly stable systems from satisfying the LMI constraints. This highlights the need for further research to refine these conditions and achieve a more accurate characterization of system stability.*

Remark 10 *To reduce conservatism in T-S stability analysis, particularly when the T-S model originates from a nonlinear knowledge model, non-quadratic Lyapunov candidate functions offer a valuable alternative. This approach has been explored by various researchers (Jadbabaie, 1999, Tanaka and Sugeno, 1992, Liu et al., 2024). Notably, some methods utilize a Lyapunov candidate function (3.22) that mirrors the fuzzy interconnection structure (membership functions) of the T-S system under study (Tanaka and Sugeno, 1992, Taniguchi et al., 2001). This can lead to less conservative stability conditions.*

$$V(x(t)) = x^T(t) \left(\sum_{i=1}^{r} h_i(z(t)) P_i\right)^{-1} x(t) \tag{3.22}$$

The figure 3.5 visually demonstrates how non-quadratic approaches expand the feasible region in the LMI space compared to quadratic approaches, leading to less conservative stability conditions for T-S fuzzy systems.

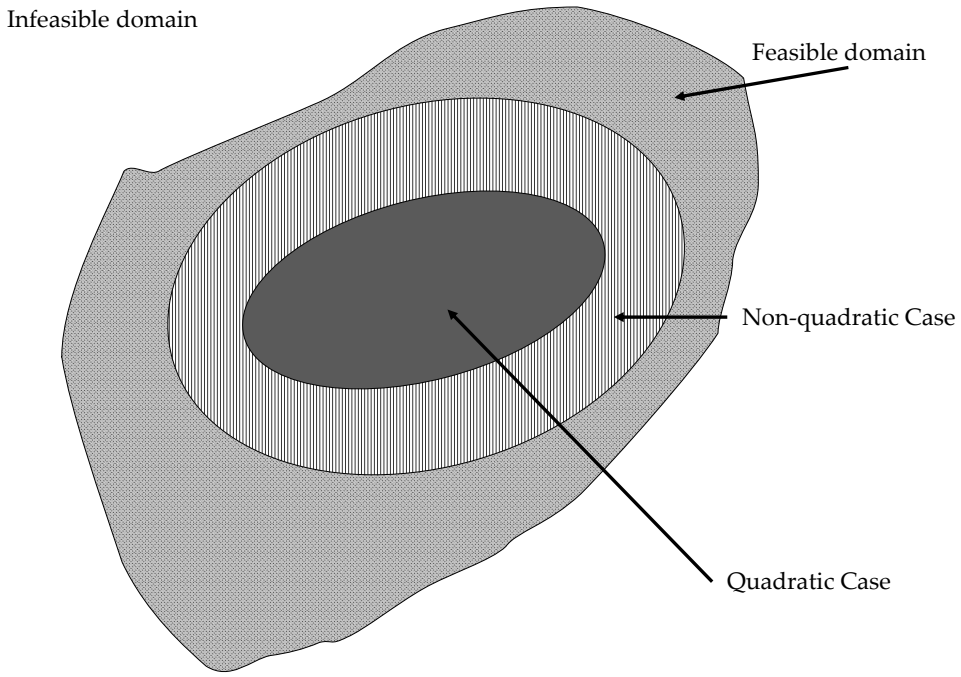

Figure 3.5: Comparison of feasibility domains in quadratic and non-quadratic approaches Jabri, 2011.

3.2.4 Challenges in observer design for T-S fuzzy systems

This section explores the design of observers for T-S fuzzy systems, examining two fundamental scenarios distinguished by the measurability of premise variables.

- **Measured Premise Variables (MPV):** When all premise variables are directly measurable, both the system and its observer share the same activation functions. This advantageous feature allows for factoring these functions during the analysis of state estimation error dynamics (Guelton, 2003, Lendek et al., 2011, Belkhiat et al.).

- **Unmeasured Premise Variables (UPV):** In a more realistic setting, premise variables may not be directly measurable. The broader applicability of T-S models with unmeasured premise variables lies in the fact that most practical applications involve system dynamics whose state variables are not fully accessible. Moreover, the sector nonlinearity approach often results in T-S models with unmeasured premise variables (Ichalal et al., 2012, Garbouj et al., 2019, Chekakta et al., 2021, Chekakta et al., 2021). The lack of measurability for these variables introduces complexity, preventing a simplified representation of the state estimation error dynamics.

Let's analyze a T-S fuzzy multi-models system described as follows:

$$\begin{cases} \dot{x}\left(t\right) = \sum_{i=1}^{r} h_i\left(z\left(t\right)\right)\left(A_i x\left(t\right) + B_i u\left(t\right)\right) \\ y\left(t\right) = \sum_{i=1}^{r} h_i\left(z\left(t\right)\right)\left(C_i x\left(t\right) + D_i u(t)\right) \end{cases} \tag{3.23}$$

An observer with this structure will be designed to estimate the system's states:

$$\begin{cases} \dot{\hat{x}}(t) = \sum_{i=1}^{r} h_i(\hat{z}(t))(A_i\hat{x}(t) + B_i u(t) + L_i(y(t) - \hat{y}(t))) \\ \hat{y}(t) = \sum_{i=1}^{r} h_i(\hat{z}(t))(C_i\hat{x}(t) + D_i u(t)) \end{cases} \tag{3.24}$$

$\hat{x}(t) \in \mathbb{R}^n$, $\hat{y}(t) \in \mathbb{R}^p$, and $\hat{z}(t) \in \mathbb{R}^\eta$ represent the estimated state, output, and premise variable vectors, respectively, while L_i are the gain matrices to be determined. The activation function $h_i(\hat{z}(t))$ of the i^{th} fuzzy model rule adheres to the following convex sum properties: $0 < h_i(\hat{z}(t)) < 1$ and $\sum_{i=1}^{r} h_i(\hat{z}(t)) = 1$.

In the sequel, We consider two cases depending on the availability of the premise variables $z(t)$ for the observer design.

3.2.4.1 Observer design for T-S fuzzy systems with MPV

In the design of state observers for T-S fuzzy systems, a prevalent assumption is the accessibility of the system's premise variables. This enables the observer to leverage the identical premise variables employed within the system model ($z(t) = \hat{z}(t)$). Consequently, when evaluating the state estimation error dynamics, factorization by the activation functions becomes feasible. More precisely, the state estimation error dynamics is written as follows:

$$\dot{e}(t) = \sum_{i=1}^{r} h_i(z(t))((A_i - L_i C)e(t)) \tag{3.25}$$

To determine the observer gains L_i, a simple stability analysis of system (3.25) is required. This analysis can be performed using a quadratic Lyapunov function of the form $(e(t)^T P e(t))$. This approach allows for the derivation of LMI conditions for observer design.

3.2.4.2 Observer design for T-S fuzzy systems with UPV

A critical assumption in T-S fuzzy multi-models is the measurability of premise variables. However, in practical applications, these variables may not be directly obtainable. When some or all elements of the premise variable vector are unmeasurable, the factorization utilized within the state estimation error dynamics becomes infea-

sible. As a consequence, the state estimation error dynamics must be expressed in a different form, as shown below:

$$\dot{e}(t) = \sum_{i=1}^{r} h_i(z(t))(A_i x(t) + B_i u(t)) - \sum_{i=1}^{r} h_i(\hat{z}(t))(A_i \hat{x}(t) + B_i u(t) + L_i(y(t) - \hat{y}(t))) \tag{3.26}$$

Analyzing the structure of the state estimation error dynamics (3.26) unveils a key limitation. Observer gain design methods for T-S systems with measurable premise variables (MPV) cannot be directly applied when the premise variables are not measurable (UPV). The UPV case presents a more substantial design challenge. We explore various techniques from the literature that address this issue in the contribution chapter to keep this chapter focused.

3.3 Switched Takagi-Seguno fuzzy systems

Many switched systems exhibit inherent nonlinearities within their dynamics. These nonlinearities can arise from factors like saturation (limits on actuator or sensor outputs), friction (varying depending on velocity), or component nonlinearities (e.g., power converters). These nonlinearities make it challenging to directly apply linear control design methods, which often rely on the assumption of constant system parameters. Fortunately, the T-S fuzzy model framework offers a powerful approach to address these complexities (Chekakta et al., 2021, Wang et al., 2024). This framework enables the representation of not only nonlinear systems but also, by extension, switched nonlinear systems. Notably, each individual nonlinear switched mode can be effectively modeled using a T-S model. These T-S models leverage smoothly weighted combinations of operating points (vertices) that are valid within a well-defined region of the state space. This key strength is attributed to the inherent polytopic convex structure of the T-S framework. This structure paves the way for extending established linear control design concepts to the nonlinear domain.

We consider a class of switched nonlinear systems represented by a collection of T-S models.

$$\begin{cases} \dot{x}(t) = \sum\limits_{j=1}^{m} \sum\limits_{i_j=1}^{r_j} \sigma_j(t) h_{i_j}(z_j(t)) \left(A_{i_j} x(t) + B_{i_j} u(t)\right) \\ y(t) = \sum\limits_{j=1}^{m} \sum\limits_{i_j=1}^{r_j} \sigma_j(t) h_{i_j}(z_j(t))(C_{i_j} x(t) + D_{i_j} u(t)) \end{cases} \tag{3.27}$$

In this context, $x(t) \in \mathbb{R}^n$, $u(t) \in \mathbb{R}^q$, and $y(t) \in \mathbb{R}^p$ represent the state vector, input vector, and output vector, respectively. The total number of switched modes is denoted by m, and within each mode j, denoted by r_j $(j = 1, \ldots, m)$, $z_j(t)$ represents the vectors of premise variables. For each $j = 1, \ldots, m$, and $\forall i = 1, \ldots, r_j$, $h_{i_j}(z_j(t)) \geq 0$ signifies

the fuzzy membership functions in each switched mode j, satisfying the convex sum property $\sum_{i_j=1}^{r_j} h_{i_j}(z_j(t)) = 1$. The matrices $A_{i_j} \in \mathbb{R}^{n\times n}$, $B_{i_j} \in \mathbb{R}^{n\times p}$, and $C \in \mathbb{R}^{v\times n}$ are associated with each T-S subsystem, while $\sigma_j(t)$ denotes the switching functions (switching law). Specifically, when the l^{th} mode is activated, $\sigma_j(t)$ is defined as:

$$\begin{cases} \sigma_j(t) = 1 \text{ when } j = l. \\ \sigma_j(t) = 0 \text{ when } j \neq l. \end{cases} \tag{3.28}$$

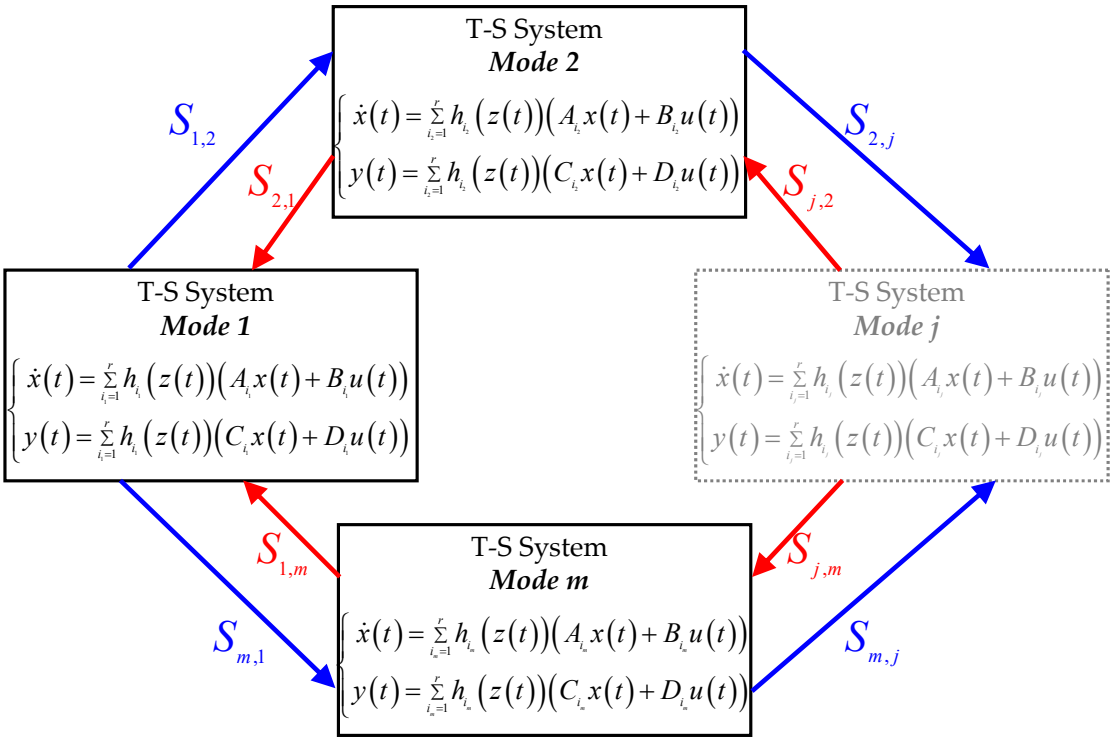

Figure 3.6: Schematic of switched Takagi-Sugeno multi-models (Jabri, 2011).

Figure 3.6 shows a diagram of a switched T-S multi-models system. The capacity of T-S multi- models to capture the nonlinearity present in switched nonlinear systems is widely acknowledged in literature. This adaptability finds practical utility, demonstrated by numerous instances where switched T-S multi-models have effectively represented real-world applications (see Figure 3.7).

- **A robotic manipulator with joint saturation:** The T-S framework can model the different dynamics of the manipulator depending on whether the joint torques are saturated or not.

- **A power converter with switching modes:** T-S models can represent the different operating modes of the converter, such as boost mode, buck mode, and bypass mode, each with its own linear dynamics.
- **A flight control system with different flight regimes:** The T-S framework can capture the varying aerodynamic characteristics of an aircraft during takeoff, cruise, and landing phases.

A robotic manipulator with joint saturation

A flight control system with different flight regimes

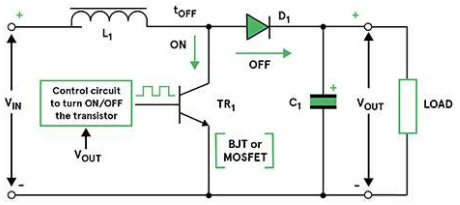

A power converter with switching modes

Figure 3.7: Real-world applications of switched T-S multi-models.

To exemplify the capability of T-S fuzzy multi-models in representing switched nonlinear systems, we will delve into a case study involving a switched tunnel diode circuit. This exploration will demonstrate the process of constructing a switched T-S fuzzy system from a real-world physical system.

Example 6 (Switched Tunnel Diode Circuit) *Let us examine the modified tunnel diode circuit system illustrated in Fig. 3.8, with its state-space representation provided by Chekakta et al., 2021:*

$$\begin{cases} \dot{x}_1(t) = \frac{0.2}{C}x_1(t) + \frac{0.01}{C}x_1^3(t) + \frac{1}{C}x_2(t) \\ \dot{x}_2(t) = -\frac{1}{L}x_1(t) - \frac{R_{\sigma(t)}}{L}x_2(t) + \frac{1}{L}u(t) \end{cases} \tag{3.29}$$

where $x_1(t) = v_D(t)$ and $x_2(t) = i_D(t)$ represent respectively the voltage and current of the tunnel diode (state variables). $\sigma(t) \in 1, 2$ indicates the switching modes, while the resistances $R_{\sigma(t)}$ switch between two distinct values ($R_1 = 1\Omega$ and $R_2 = 2\Omega$). $C = 0.1F$ denotes the circuit capacitance, and $L = 1H$ stands for the circuit inductance.

Let us assume that only $x_2(t)$ is measured such that $y(t) = Cx(t)$ with $C = \begin{bmatrix} 0 & 1 \end{bmatrix}$. Moreover, assuming $x_1(t) \in [-3, 3]$, the state dependent premise variables $z_1(t) = z_2(t) = x_1^2(t) \in [0, 9]$ and $x(t) = \begin{bmatrix} x_1(t) & x_2(t) \end{bmatrix}^T$, the switched nonlinear system (3.29) can be exactly rewritten as a switched T-S system (3.27), by applying the sector nonlinearity approach, with $m = 2$, $r_1 = r_2 = 2$, $A_{1_1} = \begin{bmatrix} 2 & 10 \\ -1 & -1 \end{bmatrix}$, $A_{2_1} = \begin{bmatrix} 2.9 & 10 \\ -1 & -1 \end{bmatrix}$, $A_{1_2} = \begin{bmatrix} 2 & 10 \\ -1 & -2 \end{bmatrix}$, $A_{2_2} = \begin{bmatrix} 2.9 & 10 \\ -1 & -2 \end{bmatrix}$, $B_{1_1} = B_{1_2} = B_{2_1} = B_{2_2} = \begin{bmatrix} 0 \\ 1 \end{bmatrix}$ and the membership functions:

$$h_{1_1}(z_1(t)) = h_{1_2}(z_2(t)) = 1 - \frac{z_1(t)}{9}$$
$$h_{2_1}(z_1(t)) = h_{2_2}(z_2(t)) = 1 - h_{1,1}(z_1(t))$$

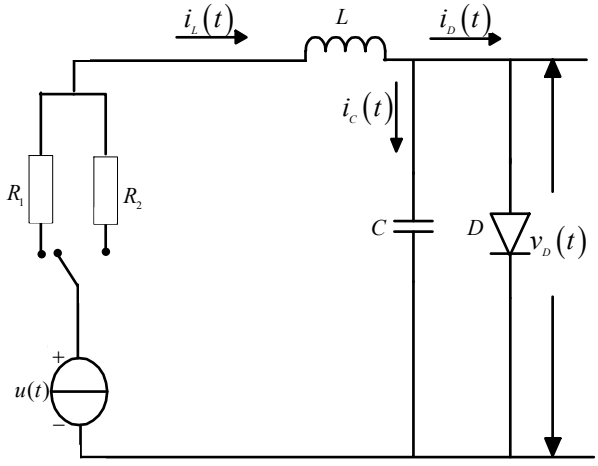

Figure 3.8: Switched Tunnel diode circuit (Chekakta et al., 2021).

By effectively representing the nonlinear behavior of switched systems using T-S multi-models, we can unlock the power of linear control design methods for a broader range of real-world applications.

3.3.1 Challenges in observer design for switched Takagi-Seguno fuzzy systems

The design of observers for switched T-S fuzzy system lies at the intersection of two complex domains: switched system theory and Takagi-Sugeno fuzzy control. This thesis delves into the fundamental challenges encountered in this domain and presents established approaches to bridge this gap. Two primary obstacles hinder the design of robust observers for switched T-S systems:

- **Unmeasurable Premise Variables:** In many physical systems, the premise variables defining the active fuzzy rule in the T-S multi-models are often not directly measurable. This lack of complete information makes it difficult for the observer to replicate the system's behavior accurately. Therefore, exploring design approaches that address the issue of unmeasurable premise variables would be valuable.
- **Asynchronicity between the observer and the switched T-S system:** In real-world applications, the switching behavior of the observer deviates from that of the system. The observer's switching signals may experience delays or discrepancies compared to those of the system. These observers exhibit discrepancies in their switching behavior compared to the switched T-S system, which poses a much greater challenge compared to the synchronous switching.

Despite these challenges, researchers have developed various observer design approaches that address the issues of unmeasurable premise variables and asynchronous switching. A more in-depth analysis of these dominant approaches will be presented in the contribution chapter. This will provide a comprehensive framework for understanding observer design in the context of switched T-S fuzzy systems. Additionally, we also present our contribution to addressing these two primary problems.

3.4 Conclusion

This chapter has provided a comprehensive foundation for understanding T-S fuzzy multi-model systems. We delved into the core concepts, explored various derivation methodologies with an emphasis on the sector nonlinearity approach, and analyzed system stability using Lyapunov function theory.

Furthermore, the chapter tackled the critical challenge of state observer design for T-S systems. We meticulously examined the impact of unmeasurable premise variables on observer design methodologies, highlighting the complexities introduced by this limitation.

Finally, we explored the intricacies of switched T-S fuzzy systems, analyzing their structural characteristics and demonstrating their application with a switched tunnel diode circuit example. This section concluded by emphasizing the specific challenges associated with observer design in the context of switched T-S systems.

Our critical examination of the provided bibliography revealed several key findings that will shape our research focus:

- Lyapunov stability analysis can be significantly enhanced by constructing a candidate function that reflects the specific fuzzy interconnection structure (membership functions) of the T-S system under investigation. This approach can lead to less conservative stability conditions compared to generic methods.

- Realistically, premise variables in T-S models may not always be directly measurable. The lack of measurability for these variables introduces complexity and hinders the development of simplified representations for state estimation error dynamics.

- Designing observers for switched T-S systems lies at the complex intersection of switched system theory and Takagi-Sugeno fuzzy control. Two primary obstacles hinder the design of robust observers for switched T-S systems: unmeasured premise variables and asynchronicity between observer and system

With this comprehensive study, the subsequent chapters will leverage this understanding of T-S fuzzy multi-model systems to delve deeper into specific areas of research, such as fault diagnosis, fault estimation and advanced observer techniques that address the challenges outlined in this conclusion .

Chapter 4

Fault Diagnosis of Nonlinear Systems

4.1 Introduction

THE present chapter specifically addresses the intricacies of fault diagnosis tailored for nonlinear systems. To navigate this intricate landscape effectively, the chapter begins by providing clear and concise definitions of key terms associated with fault diagnosis. This shared understanding serves as a vital foundation as we delve deeper into the subject matter.

The chapter then proceeds to meticulously classify faults into distinct categories. This systematic approach facilitates the identification of the fault's nature, ultimately guiding the selection of the most appropriate diagnosis methods. Following the establishment of a comprehensive fault classification system, we explore diverse methods for fault diagnosis. These methods are categorized into two primary branches: model-free and model-based approaches. Model-free methods offer flexibility by not requiring a detailed system model. Conversely, model-based methods leverage system models to potentially achieve more precise diagnoses. Each category is further subdivided into quantitative and qualitative approaches. Quantitative methods rely on the analysis of numerical data, while qualitative methods focus on non-numerical observations and reasoning.

4.2 Definitions

A significant challenge in the field of fault diagnosis is the inconsistent use of terminology. This is evident in the varying definitions assigned to the same word, such as "diagnosis." For instance:

- **In finance**: Diagnosis becomes a dynamic analysis tool used to forecast future financing needs.

- **In medicine**: It signifies the process of identifying an infection based on symptoms and causes.
- **In automation**: Diagnosis transforms into a decision support system that pinpoints faulty components and, if possible, their root causes.

This inconsistency can lead to miscommunication and confusion between researchers and practitioners. To address the ambiguities arising from inconsistent terminology in fault diagnosis, the SAFEPROCESS technical committee of the International Federation of Automatic Control (IFAC) has undertaken the task of standardizing key definitions. In this context, it is crucial to revisit the terminology employed in this report, which is based on the work of the SAFEPROCESS technical committee (Zwingelstein, 1995, Isermann and Balle, 1997, Isermann and Phalle, 2000).

- **Fault:** It is an inadmissible deviation in at least one characteristic property, variable, or behavior of a system from its acceptable standard (usual) behavior. It does not necessarily lead to a system malfunction but indicates a potential future failure.
- **Failure:** It is the realized impairment or cessation of a device's ability to perform one or more of its intended functions. It can be a consequence of a fault.
- **Breakdown:** It is the manifestation of a failure that disrupts the normal operation of a process. In other words, it is a state of non-functionality or malfunction, either hardware or software, where a unit is unable to perform a required function due to a failure. A breakdown can be considered either permanent or intermittent:
  - *Permanent breakdown:* It is a malfunction of a component that needs to be replaced or repaired. It can be caused by a gradual change in the characteristics of a component, such as aging, or a sudden change such as hardware failure.
  - *Intermittent breakdown:* This may allow the process to return to its normal operating mode. These breakdowns very often lead to permanent breakdowns due to a progressive degradation of the system's performance.
- **Degradation:** It is a decline in the performance of one or more functions of a device.
- **Prognostics:** It is forecasting the evolution of faults and their consequences.
- **Operating mode:** This term is used to describe the different operational states of a process. There are three main operating modes: normal, degraded, and failed:

  - *Normal operating mode:* The system is functioning correctly and meeting its intended performance requirements.
  - *Degraded operating mode:* The system is experiencing some level of performance degradation or malfunction, but it is still able to operate to some extent.
  - *Failed operating mode:* The system has ceased to function or has experienced a critical failure and is no longer able to meet any of its intended requirements.

- **Monitoring:** It is the process of observing and evaluating the state of a system or process to detect and identify anomalies or deviations from normal behavior.
- **Diagnosis:** It is the process of identifying the type, extent, location, and time of occurrence of a fault using logical reasoning based on the symptoms and observations of the system.
- **Fault detection:** It is the process of determining whether a system is operating normally or if a fault has occurred.
- **Fault localization:** It is the process of identifying the specific cause or location of a fault within a system, building upon the anomalies detected during the fault detection phase.
- **Fault identification and estimation:** This phase involves determining the magnitude and probable evolution over time of the detected fault.
- **Residual:** It is the indicator of the presence or absence of a fault. It is the difference between the observed system behavior and the expected behavior based on a reference model.
- **Fault tolerance:** It is the ability of a system to continue fulfilling its intended mission(s), or if necessary, to achieve new objectives to avoid catastrophic trajectories, even in the presence of one or more faults. It is based on two main approaches: configuration and accommodation.
  - *Reconfiguration:* It is the process of dynamically modifying the system's control strategy or hardware configuration to maintain acceptable performance despite faults, utilizing the remaining non-faulty components.
  - *Accommodation:* It is the ability of the system to adapt to faults without compromising its overall objectives or structure. It involves correcting or mitigating the effects of a fault through recovery procedures or error compensation.

4.2.1 Classification of Faults

A fault is defined as an unacceptable deviation between the actual value of a system characteristic and its nominal value. As shown in Figure 4.1, three types of faults are distinguished: actuator fault, sensor fault, and process fault (or component fault) (Methnani, 2012).

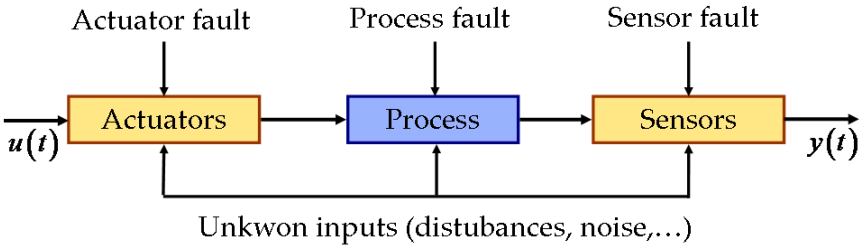

Figure 4.1: Classes of faults in physical systems.

- **Actuator faults:** Generally modeled as additive or multiplicative signals to the input signals. They act at the level of the operating part and thus deteriorate the input signal of the system.
- **Component or process faults:** Generally modeled as additional or multiplicative dynamics with a state matrix. They are identified by modifying the system's characteristics.
- **Sensor faults:** Generally modeled as additive or multiplicative signals to the output signals. They provide an inaccurate representation of the system's physical state.

Another classification of faults based on their time-varying behavior can be considered (Schwarte and Isermann, 2002).

- **Abrupt fault:** It is characterized by a sudden and discontinuous change in the behavior of a system variable. This type of fault is typically caused by a catastrophic failure of a system component, such as a sudden breakdown, disconnection, or complete or partial stoppage. The fault's temporal behavior can be represented mathematically as:

$$f(t) = \begin{cases} \delta & t \geqslant t_f \\ 0 & t < t_f \end{cases} \tag{4.1}$$

  $f(t)$ represents the fault behavior at time t, t_f represents the instant of fault occurrence and δ represents a constant threshold.

- **Intermittent fault:** It is a special type of abrupt fault characterized by the random return of the affected signal to its normal value. This type of fault is often associated with loose connections, damaged wires, or faulty components that intermittently lose or regain their functionality. The mathematical representation of an intermittent fault can be expressed as:

$$f(t) = \begin{cases} \delta & t_{f_1} \leqslant t \leqslant t_{f_2} \\ 0 & otherwise \end{cases} \tag{4.2}$$

  $f(t)$ represents the fault behavior at time t, $t_{f_2} - t_{f_1}$ represent the random time intervals during which the fault is active and δ represents a constant threshold.

- **Gradual fault:** It is characterized by a slow and continuous change in the behavior of a system variable. This type of fault is often caused by wear and tear, degradation of components, or gradual changes in system parameters. The mathematical representation of a gradual fault can be expressed as:

$$f(t) = \begin{cases} \delta\left(1 - e^{-\alpha(t)}\right) & t \geqslant t_f \\ 0 & t < t_f \end{cases} \tag{4.3}$$

  where α and δ are positive constants. This type of fault is very difficult to detect because its temporal evolution has the same signature as a slow parametric change representing a non-stationarity of the process. This type of fault is characteristic of fouling or wear of a part.

Faults can also be classified based on their effects on system performance (Figure 4.2).

- **Additive faults:** They are characterized by the addition of an extraneous signal to the system's variable at a specific point. These faults are often caused by external disturbances, sensor biases, or actuator malfunctions. Additive faults can be modeled as a summation between the normal system variable and the fault signal.

- **Multiplicative faults:** In contrast, cause a scaling or gain change in the system's variable. These faults are often associated with component failures, such as gain loss in an amplifier or loss of sensitivity in a sensor. Multiplicative faults can be modeled as a multiplication between the normal system variable and the fault factor:

Actuator and sensor faults are generally modeled as additive faults, whereas component faults are modeled as multiplicative faults. The latter induce changes in the correlation

of the system's output signal, as well as changes in the system's spectral characteristics and dynamics.

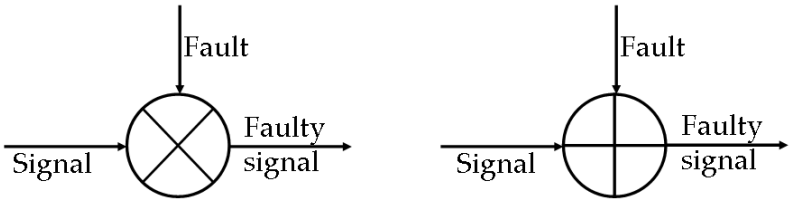

Figure 4.2: Additive and multiplicative fault.

4.3 Classification of fault diagnosis methods

In the context of automatic control, fault diagnosis methods can be broadly classified into two main categories (Figure 4.3, Ding, 2021):

- **Model-free methods:** These methods do not require a mathematical model of the system and do not rely on extensive knowledge of the physical system. They are often based on data-driven approaches and pattern recognition techniques.
- **Model-based methods:** These methods utilize a mathematical model of the system to predict its expected behavior and compare it to actual observations. Deviations between the predicted and observed behavior indicate potential faults.

4.3.1 Model-free fault diagnosis methods

In certain industrial applications, developing a mathematical model can be challenging or even impossible due to the dynamic nature of the production process or the complexity of the phenomena involved. In such cases, model-free fault diagnosis methods are employed, which do not require in-depth knowledge of the process. Two main categories of model-free approaches can be distinguished (Ding, 2021):

- **Quantitative methods (Knowledge-based Methods):** These methods utilize expert knowledge or historical data to establish relationships between system variables and potential faults. They often employ rule-based systems, statistical analysis, or machine learning techniques.
- **Qualitative methods (Data-driven methods):** These methods directly analyze sensor data or process signals to identify patterns indicative of faults. They often employ signal processing techniques, pattern recognition algorithms, and anomaly detection approaches.

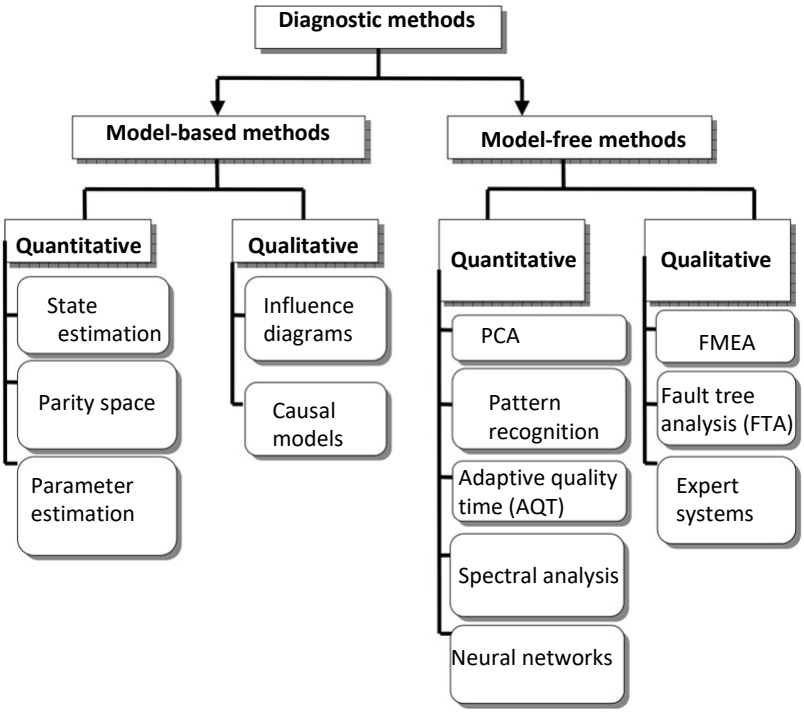

Figure 4.3: Non-exhaustive classification of fault diagnosis methods.

4.3.1.1 Quantitative methods

Quantitative methods, also known as knowledge-based methods, are used in automatic control when most of the measurements are unavailable and when it is difficult to build a model of the system. They can be used to identify the causes of failures in an industrial process. These methods involve functional and structural analyses that are based on the operator's experience and knowledge.

- *Fault tree analysis (FTA):* It is a top-down method for identifying the root causes of failures in a system (Figure 4.4). It is a graphical tool that is used to represent the various combinations of events that can lead to an undesirable event.

- *Expert systems:* They are computer systems that are designed to solve a specific problem by emulating the decision-making ability of a human expert. They are typically used in domains where the rules and heuristics for solving problems are not well-defined or are difficult to formalize.Expert systems can be used to diagnose faults in complex systems by identifying the likely causes of symptoms.

4.3.1.2 Qualitative methods

Qualitative methods in automatic control rely on processing a symbolic knowledge base and require a vast amount of historical data representing the various operational

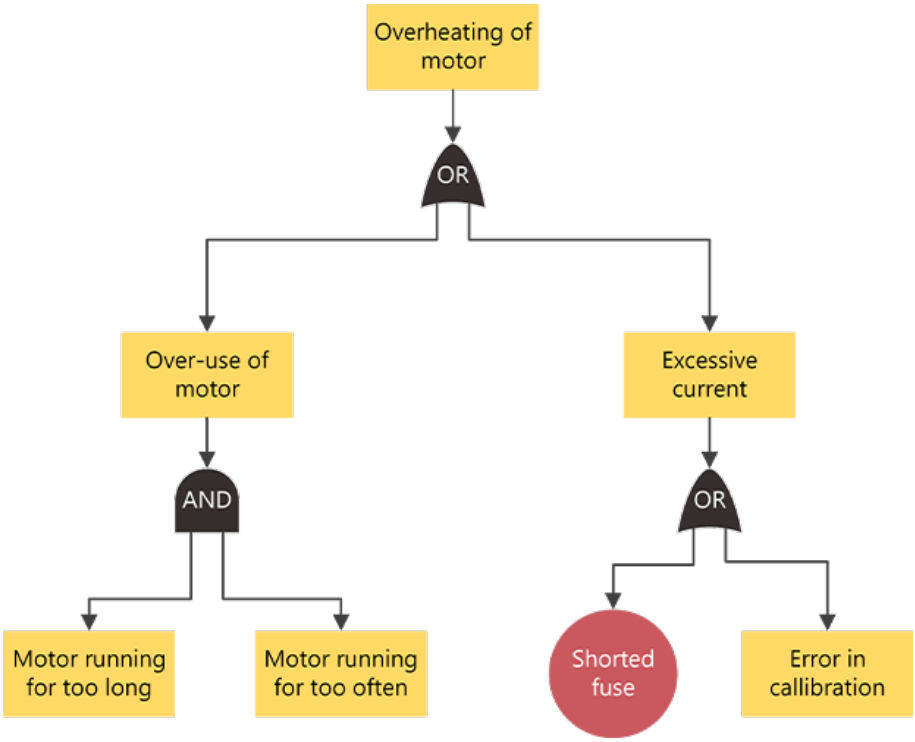

Figure 4.4: Fault tree analysis: Identifying root causes of motor overheating.

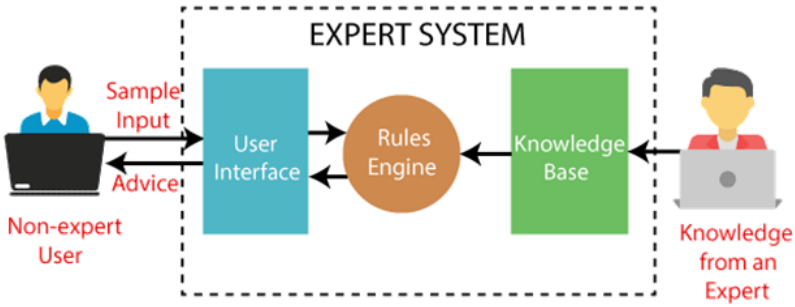

Figure 4.5: Schematic of an expert system.

modes of the system. These methods offer advantages in situations where detailed mathematical models are unavailable (Methnani, 2012):

- Qualitative methods can operate effectively when a complete or accurate mathematical model is not feasible due to system complexity or dynamic behavior.
- These methods can incorporate valuable insights from human experts and historical operational data to identify and diagnose faults.
- They can handle complex systems with numerous interacting variables by analyzing relationships between variables and their behavior under different fault conditions.

However, there are also drawbacks associated with qualitative methods:

- Their effectiveness heavily relies on the quality and completeness of the knowledge base and historical data. Biases or errors within this data can negatively impact fault diagnosis accuracy.
- Building and maintaining a comprehensive knowledge base can be a significant investment of time and effort.
- The methods are inherently susceptible to biases and errors that might exist in the expert knowledge or historical data used.

In this context, quantitative methods for fault diagnosis encompass a diverse range of techniques:

- *Principal Component Analysis (PCA):* it is a multivariate statistical technique that can be used to compress data and reduce its dimensionality. PCA can be used to detect and isolate faults in a system by monitoring the residuals of the system's output when it is projected onto the principal components. This method has been successfully used in diagnostic studies (Jolliffe, 2002).
- *Pattern recognition:* It is a branch of machine learning that deals with the classification of objects based on their similarity to reference objects. In the context of fault diagnosis, pattern recognition can be used to diagnose faults in a system by identifying patterns in sensor data that are indicative of specific faults.
- *Spectral analysis:* It is a technique that is used to study the frequency content of a signal. Spectral analysis can be used to detect faults in a system by identifying changes in the frequency content of sensor data.

4.3.2 Model-based fault diagnosis methods

Model-based methods are a type of fault diagnosis technique that uses a model of the system to identify faults. The model is used to predict the system's behavior under normal conditions, and any deviations between the predicted and actual behavior are used to identify faults. Model-based methods have a number of benefits over other fault diagnosis techniques, including:

- They can be used to diagnose faults in a wider range of systems.
- They are more sensitive to faults than other techniques.
- They can provide more information about the nature of the fault.

Similar to model-free diagnosis techniques, model-based approaches can be categorized into two main groups: quantitative and qualitative methods.

4.3.2.1 Quantitative methods

Quantitative model-based diagnosis methods rely on the mathematical relationships between system variables to identify faults. These models are developed using fundamental physical laws (mass balance, energy balance, momentum balance, etc.) or input-output relationships. According to Marcu and Frank, 1998, quantitative model-based diagnosis methods can be classified into three main groups:

- *Parity space approach:* It is a model-based fault diagnosis technique that utilizes parity equations to verify the consistency between process models and sensor measurements. It is particularly useful in identifying additive faults in linear systems. The parity space approach establishes analytical redundancy (either in the time or frequency domain) between system inputs and outputs, independent of the system's states. The parity matrix, derived from the observability matrix, eliminates the influence of states on the residuals, making it easier to detect faults.

- *Parameter estimation:* It is a fault diagnosis technique that uses real-time parameter estimation to identify faults in a system. The principle is to continuously estimate the parameters of the system using input and output measurements. The residual, which is the difference between the estimated parameter values and the reference values for normal operation, is then used to detect faults. Early applications of parameter estimation for fault diagnosis were conducted by 49. The technique has been successfully applied to fault detection in nonlinear systems.

- *State estimation:* It is a fault diagnosis technique that uses an observer to estimate the state of the system and identify faults. The observer is a mathematical model that can be used to predict the system's output based on its input and the current state of the system. The residual, which is the difference between the estimated output and the measured output, is then used to detect faults. State estimation is a powerful tool for fault diagnosis because it can provide information about the internal state of the system, which is often not directly measurable. This information can be used to identify faults that are not easily detectable by other techniques, such as sensor faults or actuator faults. Several state estimation techniques have been applied to fault diagnosis:

  - Filter-based fault Diagnosis: This method was pioneered by Beard, 1971 and later formalized by Massoumnia, 1986. The approach aims to construct detection spaces for each potential fault.

  - Observer-based fault Diagnosis: Observers are computational algorithms designed to estimate unmeasured state variables, either due to the absence of

suitable measuring devices or to replace expensive sensors in a plant. The core idea of observer-based residual generation is to compare process measurements with their estimates generated by observers. The weighted estimation error serves as a residual for fault detection and diagnosis (FDD). Ideally, this residual should be zero or near zero when no fault is present and significantly different from zero when a fault occurs. However, due to disturbances, noise, and model uncertainties, the residual may also become nonzero. Thus, the optimal scenario is for the residual to be insensitive to noise, disturbances, and model uncertainties while being sensitive to faults. To isolate and identify faults, a bank of state estimators is typically used, where each estimator is sensitive to a specific fault and insensitive to others. One of the most challenging tasks in fault diagnosis is estimating the magnitude and shape of faults to facilitate fault accommodation procedures. Observer-based fault estimation is the primary technique used for this purpose. In the context of nonlinear systems, observer-based methods have garnered significant attention. Over the past few decades, numerous results for observer design aimed at fault estimation have been presented, as detailed in Section 1.2.

4.3.2.2 Qualitative methods

The Artificial Intelligence (AI) community has proposed qualitative (or semi-qualitative) reasoning based on the establishment of cause-and-effect relationships. Indeed, diagnosis is typically a causal system since it involves making hypotheses about the faulty components that are the origin of the observed malfunction. Qualitative reasoning expresses the link between a component and the formulas describing its behavior. Among the most widely used methods, we can cite:

- *Causal Graphs (or Influence Graphs):* Causal graphs (or influence graphs) are used to identify the faulty components that can explain the observed abnormal behavior. Causal graph-based diagnosis involves searching for the source variable whose deviation is sufficient to explain all the deviations detected on other variables (Travé-Massuyès and Milne, 1997). Two main types of causal structure are proposed: the first type links causality to the equations describing the system (global analysis) while the second axis links causality to the structure of the system (local analysis).

- *Fuzzy logic:* Fuzzy logic is a mathematical theory introduced by (Zadeh, 1965) that allows for the consideration of uncertainties and the fusion of information. The idea behind the fuzzy approach is to construct a device, called a fuzzy inference system, capable of imitating the decision-making of a human operator

based on verbal rules translating their knowledge of a given process.Establishing a mathematical relationship between a fault and its symptoms can often be challenging. However, drawing upon their experience, human operators can determine the faulty element that is causing the observed symptoms. This type of knowledge can be expressed using rules of the form: IF condition THEN conclusion. Where the condition part contains the observed symptoms and the conclusion part the faulty element. Thus, the diagnostic problem is considered a classification problem. The symptom vector of the classifier, developed from the measured quantities on the system, can be seen as a shape that needs to be classified among the set of shapes corresponding to normal or abnormal operation.

4.4 Conclusion

This chapter has embarked on a comprehensive exploration of fault diagnosis within the intricate world of nonlinear systems. We established a clear foundation with fault definitions and a meticulous classification system, paving the way for effective diagnosis strategies. We then delved into the diverse approaches utilized for fault diagnosis, encompassing both model-free and model-based methods, with their quantitative and qualitative subcategories.

Building upon the knowledge gleaned in this chapter, the next chapter takes center stage. It delves into our original contribution in the realm of observer-based fault estimation for nonlinear systems. We present a novel approach to observer design that addresses the limitations discussed earlier. This novel approach aims to improve the robustness and efficiency of fault estimation, paving the way for more reliable and practical applications in complex systems.

Chapter 5

Asynchronous observer design for robust sensor fault estimation in switched nonlinear systems with fast time-varying and unbounded faults

5.1 Introduction

SWITCHED nonlinear systems are a prevalent class of models used to represent a wide range of dynamic processes in engineering and control applications. These systems exhibit complex behavior due to their ability to switch between different subsystems based on specific operating conditions. However, the presence of sensor faults can significantly degrade system performance and compromise safety. Reliable and robust sensor fault estimation techniques are therefore crucial for ensuring the reliable operation of such systems.

This chapter delves into the challenge of robust sensor fault estimation in switched nonlinear systems with a particular focus on fast time-varying and unbounded faults. These types of faults pose a significant challenge due to their rapid changes and potentially severe impact on system behavior. To address this challenge, we propose a novel approach utilizing asynchronous switched observers. These observers offer several advantages: They can function effectively even under uncontrolled, arbitrary, or unknown switching sequences among system modes. In addition, they can handle situations where the system and observer are not perfectly synchronized at the start, allowing for different initial modes. The design of these observers leverages a powerful mathematical framework and incorporates techniques for handling fast time-varying and unbounded faults. This chapter details the design process, analyzes the conver-

gence properties of the proposed observer, and demonstrates its effectiveness through rigorous simulations.

5.2 Preliminaries and Problem Statement

Let us consider the following class of switched nonlinear systems with m switching modes:

$$\begin{cases} \dot{x}(t) &= g_{\sigma_j(t)}(x(t), u(t), d(t)) \\ y(t) &= Cx(t) \end{cases} \tag{5.1}$$

where $x(t) \in \mathbb{R}^{n_x}$ is the state vector, $y(t) \in \mathbb{R}^{n_y}$ is the measured output vector, $u(t) \in \mathbb{R}^{n_u}$ is the input vector and $d(t) \in \mathbb{R}^{n_d}$ is a L_2 norm bounded disturbance vector. $g_{\sigma_j(t)}(x(t), u(t), d(t)) \in \mathbb{R}^{n_x}$ is the nonlinear vector that describes the dynamics of the considered system, $C \in \mathbb{R}^{n_y \times n_x}$ is the output matrix which is common and linear for all the switched modes. $\sigma_j(t)$ are switching functions defined, when the l^{th} mode is activated, as:

$$\begin{cases} \sigma_j(t) = 1 \text{ when } j = l. \\ \sigma_j(t) = 0 \text{ when } j \neq l. \end{cases} \tag{5.2}$$

where obviously $\sum_{j=1}^{m} \sigma_j(t) = 1$.

Remark 11 *Without loss of generality, let us consider that the switches occur according to switching sets defined by linear hyper-planes as follows:*

$$S_{jj^+} = \{x(t) \in \mathbb{R}^{n_x} : s_{jj^+} x(t) = 0\}, \qquad \left(j, j^+\right) \in \mathcal{I}_s \tag{5.3}$$

where s_{jj^+} are real vectors with appropriate dimensions, j and j^+ respectively the active mode at time t and its successor. $\mathcal{I}_s$ is the set of admissible switches.

In addition, the following assumption is considered for the purpose of transforming the switched nonlinear system (5.1) into a switched T-S fuzzy system by applying the sector nonlinearity approach using the convex polytopic transformation. (Tanaka and Wang, 2001)

Assumption 1 *$\forall j \in \{1, ..., m\}$, let us assume that the nonlinear vector-valued functions $g_{\sigma_j(t)}(x(t), u(t), d(t))$ involves p sector-bounded scalar state-dependent nonlinearities $\eta_\rho(x(t)) \in [\underline{\eta}_\rho, \bar{\eta}_\rho]$, $\rho \in \{1, \ldots, p\}$.*

Based on the Assumption 1, an exact Takagi-Sugeno model (see e.g., Takagi and Sugeno, 1985) for each mode j of the switched nonlinear system (5.1) can be achieved using the well-known sector nonlinearity approach (see e.g., Tanaka and Wang, 2001)

on each nonlinearities $\eta_\rho(x(t)) \in [\eta_\rho, \bar{\eta}_\rho]$. Nevertheless, if some state variables involved in the nonlinearities $\eta_\rho(x(t))$ are unmeasurable, the obtained Takagi-Sugeno models would be in this case with UPVs (see e.g., Ichalal et al., 2010, Moodi and Farrokhi, 2014, Moodi and Bustan, 2018, Xie et al., 2019, Chekakta et al., 2021). For the reasons previously explained in this dissertation and to overcome the UPVs problem, it would need to rewrite the considered system (5.1) as a switched Takagi-Sugeno (T-S) model with nonlinear consequent parts (see e.g., Chekakta et al., 2023)

$$\begin{cases} \dot{x}(t) = \sum_{j=1}^{m} \sum_{i_j=1}^{r_j} \sigma_j(t) h_{i_j}(Mx(t)) \Big(A_{i_j}^0 x(t) + H_{i_j}^0 \Phi(N^0 x(t)) + B_{i_j}^0 u(t) + E_{i_j}^0 d(t) \Big) \\ y(t) = Cx(t) \end{cases} \tag{5.4}$$

where $M \in \mathbb{R}^{n_m \times n_x}$ and $N^0 \in \mathbb{R}^{n_{um} \times n_x}$ are known matrices selecting respectively the measured and unmeasured state variables. $A_{i_j}^0 \in \mathbb{R}^{n_x \times n_x}, B_{i_j}^0 \in \mathbb{R}^{n_x \times n_u}, H_{i_j}^0 \in \mathbb{R}^{n_x \times n_\Phi}, E_{i_j}^0 \in \mathbb{R}^{n_x \times n_d}$ are the associated matrices to each T-S subsystems. $\forall i = 1, \ldots, r_j$, $h_{i_j}(Mx(t)) \geq 0$ are fuzzy membership functions in each switched modes j, which satisfy the convex sum property $\sum_{i_j=1}^{r_j} h_{i_j}(Mx(t)) = 1$ and depend only on measured state variables. However, the unmeasured nonlinear terms are placed in the vector valued sector-bounded nonlinear function $\Phi(N^0(x(t)) \in co\{0, Ux(t)\} \in \mathbb{R}^{n_\Phi}$, where $U \in \mathbb{R}^{n_\Phi \times n_x}$. As a reminder, the proposed N-TS modelling approach finds its application only when the considered system involves both unmeasurable and measurable state-dependent nonlinearities.

For design purpose, we consider that the following property holds.

Property 1 (Dong et al., 2009) *The vector of nonlinearities $\Phi(N^0 x(t)) \in \mathbb{R}^{n_\Phi}$ satisfies the following sector-boundedness condition:*

$$\Phi(N^0 x(t))^T \Upsilon (\Phi(N^0 x(t)) - Ux(t)) \leq 0 \tag{5.5}$$

where $\Upsilon \in \mathbb{R}^{n_\Phi \times n_\Phi}$ is any positive-definite diagonal matrix.

In order to cope with nonlinear consequent parts, let us introduce the following assumption which is a general form of the Lipschitz condition.

Assumption 2 *Let us assume that the characterisation of the nonlinear term* $\Phi(N^0x(t))$ *can be made based on a set* $\mathcal{M}$ *of symmetric matrices* $\Xi_{h_\sigma} = \text{diag}(\Xi^{11}_{h_\sigma}, \Xi^{22}_{h_\sigma})$, *with* $\Xi^{11^T}_{h_\sigma} > 0$ *and* $\Xi^{22}_{h_\sigma} = \Xi^{22^T}_{h_\sigma} < 0$. *Hence, following the work of Açıkmeşe and Corless, 2011, all* $\Xi_{h_\sigma} \in \mathcal{M}$ *satisfies the Incremental Quadratic Constraint (δQC) given by:*

$$\begin{bmatrix} q_1 - q_2 \\ \Phi(q_1,t) - \Phi(q_2,t) \end{bmatrix}^T \Xi_{h_\sigma} \begin{bmatrix} q_1 - q_2 \\ \Phi(q_1,t) - \Phi(q_2,t) \end{bmatrix} \geq 0 \tag{5.6}$$

where $q_1 = N^0x(t)$, $q_2 = N^0\hat{x}(t)$ *and* $\hat{x}(t) \in \mathbb{R}^{n_x \times n_x}$ *is the estimation of the state vector.*

Indeed, compared with the Lipschitz condition, the unknown nonlinearities $\Phi(N^0(x(t))$ satisfying incremental quadratic constraints can be characterized as a set of multiplier matrices (5.6), which may provide a significant advantage in terms of the relaxation of the conservatism of the proposed LMI-based design conditions.

Moreover, the switched N-TS model (5.4) is valid inside a domain of validity $\mathcal{D}_x$ defined as follows:

$$\mathcal{D}_x = \{x(t) \in \mathbb{R}^{n_x} : \zeta x(t) \leq \mathcal{Q}, v \in \mathcal{I}_v\} \tag{5.7}$$

where $\zeta \in \mathbb{R}^{2v \times n_x}$ is a given matrix, $\mathcal{Q} \in \mathbb{R}^{2v}$ is a given vector, and v is the number of state variable bounds.

Notations 1 *A transpose quantity in a matrix is represented by a star (∗). T^- denotes the Moore-Penrose inverse of the matrix T. In addition, convex combinations of matrices $\mathcal{K}_{(.)}$ with appropriate dimensions are denoted as:*

$$\mathcal{K}_{h_\sigma} = \sum_{j=1}^{m} \sum_{i_j=1}^{r_j} \sigma_j(t) h_{i_j}(Mx(t)) \mathcal{K}_{i_j} \; and \mathcal{K}_{h_{\hat{\sigma}}} = \sum_{\hat{j}=1}^{m} \sum_{i_{\hat{j}}=1}^{r_{\hat{j}}} \hat{\sigma}_{\hat{j}}(t) h_{i_{\hat{j}}}(Mx(t)) \mathcal{K}_{i_{\hat{j}}}$$

Furthermore, let us consider that the studied system is subject to sensor fault. Thus, the class of switched N-TS systems can be described as:

$$\begin{cases} \dot{x}(t) = A^0_{h_\sigma} x(t) + H^0_{h_\sigma} \Phi(N^0 x(t)) + B^0_{h_\sigma} u(t) + E^0_{h_\sigma} d(t) \\ y(t) = Cx(t) + F^0_s f_s(t) \end{cases} \tag{5.8}$$

where $f_s(t) \in \mathbb{R}^{n_{fs}}$ is the sensor fault vector which can be some unwanted variation of the output vector $y(t)$. For design purpose, $F^0_s \in \mathbb{R}^{n_y \times n_{fs}}$ is assumed a full column rank matrix, which is a common assumption in sensor fault estimation method (see

e.g., Han et al., 2022, Zhang et al., 2018). This assumption is needed to construct the proposed observer.

5.2.1 Observer construction

Let $\bar{x}(t) = \left[\, x^T(t)\, f_s^T(t) \,\right]^T$. Then, the extended system can be written as:

$$\begin{cases} \mathcal{G}^0 \dot{\bar{x}}\,(t) = A^1_{h_\sigma} \bar{x}\,(t) + H^1_{h_\sigma} \Phi\left(N^1\, \bar{x}\,(t)\right) + B^1_{h_\sigma} u\,(t) + F^2_s f_s\,(t) + E^1_{h_\sigma} d\,(t) \\ y\,(t) = C_1 \bar{x}\,(t) = C_0 \bar{x}\,(t) + F^0_s f_s\,(t) \end{cases} \tag{5.9}$$

with $\mathcal{G}^0 = \begin{bmatrix} I_{n_x \times n_x} & 0_{n_x \times n_{fs}} \\ 0_{n_y \times n_{fs}} & 0_{n_y \times n_{fs}} \end{bmatrix}$, $A^1_{h_\sigma} = \begin{bmatrix} A^0_{h_\sigma} & 0_{n_x \times n_{fs}} \\ 0_{n_y \times n_x} & -F^0_s \end{bmatrix}$, $H^1_{h_\sigma} = \begin{bmatrix} H^1_{h_\sigma} \\ 0_{n_y \times n_\Phi} \end{bmatrix}$, $B^1_{h_\sigma} = \begin{bmatrix} B^0_{h_\sigma} \\ 0_{n_y \times n_u} \end{bmatrix}$, $F^2_s = \begin{bmatrix} 0_{n_x \times n_y} \\ F^0_s \end{bmatrix}$, $N^1 = \begin{bmatrix} N^0 & 0_{n_\Phi \times n_{fs}} \end{bmatrix}$, $E^1_{h_\sigma} = \begin{bmatrix} E^0_{h_\sigma} \\ 0_{n_y \times n_d} \end{bmatrix}$, $C^1 = \begin{bmatrix} C & F^0_s \end{bmatrix}$, $C^0 = \begin{bmatrix} C & 0_{n_y \times n_{fs}} \end{bmatrix}$.

From the equation (5.9), the sensor fault $f_s(t)$ can be written as follows:

$$f_s\,(t) = F^1_s \left(y\,(t) - C^0 \bar{x}\,(t)\right) \tag{5.10}$$

where $F^1_s = (F^0_s)^-$ is the left inverse of F^0_s, such that $F^1_s F^0_s = \underbrace{\left(\left(F^0_s\right)^T F^0_s\right)^{-1} \left(F^0_s\right)^T}_{F^1_s} F^0_s = I_{n_{fs}}$.

Then, the equation (5.10) is introduced in the equation (5.9). This leads:

$$\mathcal{G}^0 \dot{\bar{x}}\,(t) = \left(A^1_{h_\sigma} - F^2_s F^1_s C^0\right) \bar{x}\,(t) + H^1_{h_\sigma} \Phi\left(N^1\, \bar{x}\,(t)\right) + B^1_{h_\sigma} u\,(t) + F^2_s F^1_s y\,(t) + E^1_{h_\sigma} d\,(t) \tag{5.11}$$

Adding the term $L^1_\sigma C^1 \dot{\bar{x}}\,(t)$ in the both side, the equation (5.11) become:

$$\mathcal{G}^1_\sigma \dot{\bar{x}}\,(t) = \left(A^1_{h_\sigma} - F^2_s F^1_s C^0\right) \bar{x}\,(t) + H^1_{h_\sigma} \Phi\left(N^1\, \bar{x}\,(t)\right) + B^1_{h_\sigma} u\,(t) + F^2_s F^1_s y\,(t) + E^1_{h_\sigma} d\,(t) + L^1_\sigma C^1 \dot{\bar{x}}\,(t) \tag{5.12}$$

with $\mathcal{G}^1_\sigma = \mathcal{G}^0 + L^1_\sigma C^1$ and $L^1_\sigma = \begin{bmatrix} L^{1_1}_\sigma \\ L^{1_2}_\sigma \end{bmatrix}$. We suppose that $L^{1_1}_\sigma = 0_{n_x \times n_y}$, $L^{1_2}_\sigma \in \mathbb{R}^{n_y \times n_y}$ are arbitrary nonsingular matrices. Hence, $\mathcal{G}^1_\sigma = \begin{bmatrix} I_{n_x} & 0 \\ L^{1_2}_\sigma C & L^{1_2}_\sigma F^0_s \end{bmatrix}$. Noting that the matrices $\mathcal{G}^1_\sigma$ are full column rank, because F^0_s is a full column rank matrix and $L^{1_2}_\sigma$ are arbitrary nonsingular matrices.

Let define $\mathcal{G}^2_\sigma = \begin{bmatrix} I_{n_x} & 0_{n_x \times n_y} \\ -F^1_s C & F^1_s \left(L^{1_2}_\sigma\right)^{-1} \end{bmatrix}$ is the left inverse of $\mathcal{G}^1_\sigma$, such that $\mathcal{G}^2_\sigma \mathcal{G}^1_\sigma =$

$I_{n_x+n_y}$. Thus, the equation (5.12) can be written as:

$$\dot{\bar{x}}(t) = A^2_{h_\sigma}\bar{x}(t) + H^2_{h_\sigma}\Phi\left(N^1\bar{x}(t)\right) + B^2_{h_\sigma}u(t) + F^3_{s_\sigma}y(t) + E^2_{h_\sigma}d(t) + G^2_\sigma L^1_\sigma C^1\dot{\bar{x}}(t) \quad (5.13)$$

where $A^2_{h_\sigma} = \mathcal{G}^2_\sigma\left(A^1_{h_\sigma} - F^2_s F^1_s C^0\right)$, $H^2_{h_\sigma} = \mathcal{G}^2_\sigma H^1_{h_\sigma}$, $B^2_{h_\sigma} = \mathcal{G}^2_\sigma B^1_{h_\sigma}$, $F^3_{s_\sigma} = \mathcal{G}^2_\sigma F^2_s F^1_s$ and $E^2_{h_\sigma} = \mathcal{G}^2_\sigma E^1_{h_\sigma}$.

Let us consider $S = \mathcal{G}^2_\sigma L^1_\sigma = \begin{bmatrix} 0_{n_x\times n_y} \\ F^1_s \end{bmatrix}$. Then, we can write:

$$\mathcal{G}^2_\sigma L^1_\sigma C^1\dot{\bar{x}}(t) = S\,C^1\,\dot{\bar{x}}(t) = S\,\dot{y}(t) \quad (5.14)$$

According to (5.14) and (5.13), the extended switched N-TS systems can be rewritten as:

$$\begin{cases} \dot{\bar{x}}(t) = A^2_{h_\sigma}\bar{x}(t) + H^2_{h_\sigma}\Phi\left(N^1\bar{x}(t)\right) + B^2_{h_\sigma}u(t) + F^3_{s_\sigma}y(t) + E^2_{h_\sigma}d(t) + S\,\dot{y}(t) \\ y(t) = C^1\bar{x}(t) = C^0\bar{x}(t) + F^0_s f_s(t) \end{cases} \quad (5.15)$$

Thus, the domain of validity $\mathcal{D}_{\bar{x}}$, defined in (5.7), can be reformulated as follows:

$$\mathcal{D}_{\bar{x}} = \left\{\bar{x}(t) \in \mathbb{R}^{n_x+n_{fs}} : \bar{\zeta}\bar{x}(t) \leq \mathcal{Q},\, v \in \mathcal{I}_v\right\} \quad (5.16)$$

In order to simultaneously estimate state and sensor fault vectors, the following asynchronous switched N-TS observers are proposed:

$$\begin{cases} \dot{z}(t) = A^2_{h_{\hat{\sigma}}}z(t) + H^2_{h_{\hat{\sigma}}}\Phi\left(N^1\hat{\bar{x}}(t)\right) + B^2_{h_{\hat{\sigma}}}u(t) + (F^3_{s_\sigma} + A^2_{h_{\hat{\sigma}}}S)y(t) + K_{h_{\hat{\sigma}}}\left(y(t) - \hat{y}(t)\right) \\ \hat{\bar{x}}(t) = z(t) + S\,y(t) \\ \hat{y}(t) = C^1\hat{\bar{x}}(t) \end{cases} \quad (5.17)$$

Where $z(t) \in \mathbb{R}^{n_x+n_{fs}}$ is an intermediate variable, $\hat{\bar{x}}(t) \in \mathbb{R}^{n_x+n_{fs}}$ is the estimation of $\bar{x}(t)$. $K_{h_{\hat{\sigma}}} \in \mathbb{R}^{n_x+n_{fs}\times n_y}$ are the observer gain matrices to be designed.

5.2.2 Estimation error dynamic

Let's define $\Phi_e(t) = \Phi\left(N^1\bar{x}(t)\right) - \Phi\left(N^1\hat{\bar{x}}(t)\right) \in \mathbb{R}^{n_\Phi}$ as the estimation error of the nonlinear consequent part vector. In addition, the extended state estimation error $e(t) \in \mathbb{R}^{n_x+n_{fs}}$ can be defined as follows:

$$e(t) = \bar{x}(t) - \hat{\bar{x}}(t) \quad (5.18)$$

Thus, the extended state error dynamic can be written as:

$$\dot{e}\left(t\right)=\dot{\bar{x}}\left(t\right)-\dot{\hat{\bar{x}}}\left(t\right) \tag{5.19}$$

According to (5.17) and (5.19), the equation (5.19) can be reformulated as follows:

$$\dot{e}\left(t\right)=\dot{\bar{x}}\left(t\right)-\dot{z}\left(t\right)-S\,\dot{y}\left(t\right) \tag{5.20}$$

By introducing the dynamic of the observer (5.17), the equation (5.20) can be written as follows:

$$\begin{aligned}\dot{e}\left(t\right)&=A_{h_\sigma}^2\bar{x}\left(t\right)+H_{h_\sigma}^2\Phi\left(N^1\,\bar{x}\left(t\right)\right)+B_{h_\sigma}^2u\left(t\right)+F_{s_\sigma}^3y\left(t\right)+E_{h_\sigma}^2d\left(t\right)+S\dot{y}\left(t\right)\\&\quad-A_{h_{\hat{\sigma}}}^2z\left(t\right)-H_{h_{\hat{\sigma}}}^2\Phi\left(N^1\,\hat{\bar{x}}\left(t\right)\right)-B_{h_{\hat{\sigma}}}^2u\left(t\right)-\left(F_{s_\sigma}^3+A_{h_{\hat{\sigma}}}^2S\right)y\left(t\right)-K_{h_{\hat{\sigma}}}\left(y\left(t\right)-\hat{y}\left(t\right)\right)-S\dot{y}\left(t\right)\\&=A_{h_\sigma}^2\bar{x}\left(t\right)-A_{h_{\hat{\sigma}}}^2\hat{\bar{x}}\left(t\right)+H_{h_\sigma}^2\Phi\left(N^1\,\bar{x}\left(t\right)\right)-H_{h_{\hat{\sigma}}}^2\Phi\left(N^1\,\hat{\bar{x}}\left(t\right)\right)+\left(B_{h_\sigma}^2-B_{h_{\hat{\sigma}}}^2\right)u\left(t\right)\\&\quad+E_{h_\sigma}^2d\left(t\right)-K_{h_{\hat{\sigma}}}\left(y\left(t\right)-\hat{y}\left(t\right)\right)\end{aligned} \tag{5.21}$$

Adding and subtracting $A_{h_\sigma}^2\hat{\bar{x}}\left(t\right)$ and $H_{h_\sigma}^2\Phi\left(N^1\,\hat{\bar{x}}\left(t\right)\right)$, we obtain:

$$\begin{aligned}\dot{e}\left(t\right)&=A_{h_\sigma}^2\bar{x}\left(t\right)-A_{h_\sigma}^2\hat{\bar{x}}\left(t\right)+A_{h_\sigma}^2\hat{\bar{x}}\left(t\right)-A_{h_{\hat{\sigma}}}^2\hat{\bar{x}}\left(t\right)+H_{h_\sigma}^2\Phi\left(N^1\,\bar{x}\left(t\right)\right)\\&\quad-H_{h_\sigma}^2\Phi\left(N^1\hat{\bar{x}}\left(t\right)\right)+H_{h_\sigma}^2\Phi\left(N^1\,\hat{\bar{x}}\left(t\right)\right)-H_{h_{\hat{\sigma}}}^2\Phi\left(N^1\,\hat{\bar{x}}\left(t\right)\right)+\left(B_{h_\sigma}^2-B_{h_{\hat{\sigma}}}^2\right)u\left(t\right)\\&\quad+E_{h_\sigma}^2d\left(t\right)-K_{h_{\hat{\sigma}}}C^1\left(\bar{x}\left(t\right)-\hat{\bar{x}}\left(t\right)\right)\\&=\left(A_{h_\sigma}^2-K_{h_{\hat{\sigma}}}C^1\right)e\left(t\right)+\left(A_{h_\sigma}^2-A_{h_{\hat{\sigma}}}^2\right)\hat{\bar{x}}\left(t\right)+H_{h_\sigma}^2\Phi_e\left(t\right)\\&\quad+\left(H_{h_\sigma}^2-H_{h_{\hat{\sigma}}}^2\right)\Phi\left(N^1\,\hat{\bar{x}}\left(t\right)\right)+\left(B_{h_\sigma}^2-B_{h_{\hat{\sigma}}}^2\right)u\left(t\right)\;+E_{h_\sigma}^2d\left(t\right)\end{aligned} \tag{5.22}$$

The dynamic of the estimation error can be described as:

$$\dot{e}\left(t\right)=A_{h_\sigma h_{\hat{\sigma}}}^3e\left(t\right)+H_{h_\sigma h_{\hat{\sigma}}}^3\Phi_a\left(t\right)+B_{h_\sigma h_{\hat{\sigma}}}^3\bar{d}\left(t\right) \tag{5.23}$$

where $\bar{d}\left(t\right)=\left[\begin{array}{ccc}\hat{\bar{x}}^T\left(t\right) & u^T\left(t\right) & d^T\left(t\right)\end{array}\right]^T$, $\Phi_a\left(t\right)=\left[\begin{array}{cc}\Phi_e^T\left(t\right) & \Phi^T\left(N^1\,\hat{\bar{x}}\left(t\right)\right)\end{array}\right]^T$, $A_{h_\sigma h_{\hat{\sigma}}}^3=A_{h_\sigma}^2-K_{h_{\hat{\sigma}}}C^1$, $H_{h_\sigma h_{\hat{\sigma}}}^3=\left[\begin{array}{cc}H_{h_\sigma}^2 & H_{h_\sigma}^2-H_{h_{\hat{\sigma}}}^2\end{array}\right]$ and $B_{h_\sigma h_{\hat{\sigma}}}^3=\left[\begin{array}{ccc}A_{h_\sigma}^2-A_{h_{\hat{\sigma}}}^2 & B_{h_\sigma}^2-B_{h_{\hat{\sigma}}}^2 & E_{h_\sigma}^2\end{array}\right]$.

Moreover, the domain of validity of $\mathcal{D}_{\hat{\bar{x}}}$ is similar to the one in (5.16) ((i.e. using the same nonlinear sectors). Hence, the domain of validity of the estimation error $\mathcal{D}_e$ is defined as follows:

$$\mathcal{D}_e=\left\{e(t)\in\mathbb{R}^{n_x+n_{fs}}:\,\bar{\zeta}e\left(t\right)\leq 2\mathcal{Q},\,v\in\mathcal{I}_v\right\} \tag{5.24}$$

Problem 1 *The design objective considered in this study is to determine the gain matrices K_{h_σ} of the N-TS observer-based sensor fault estimation (5.17) such that the following requirements are fulfilled, while maximizing the estimate of the attraction domain $\mathcal{D}_a \subseteq \mathcal{D}_e$ of the estimation error.*

i. *Convergence: $\forall e(t) \in \mathcal{D}_a \subseteq \mathcal{D}_e$, the estimation error $e(t)$ is convergent to the origin, i.e. $\lim_{t\to+\infty} e(t) = 0$, when $\bar{d}(t) \equiv 0$.*

ii. *Robustness: For all non-zero $\bar{d}(t) \in L_2[0,\ \infty)$, the estimation error dynamics (5.23) has a prescribed disturbance attenuation level γ, such that*

$$\frac{\|e(t)\|_{\mathcal{W}}^2}{\left\|\bar{d}(t)\right\|_{\Omega}^2} \leq \gamma^2 \tag{5.25}$$

In other words, the following H_∞ criterion is verified:

$$\int_0^\infty e^T(t)\mathcal{W}e(t)dt \leq \gamma^2 \int_0^\infty \bar{d}^T(t)\Omega\bar{d}(t)dt \tag{5.26}$$

where $\mathcal{W}$ and Ω are known positive diagonal matrices.

To conclude these preliminaries, let us recall some useful lemmas to be employed to obtain the main results developed in the next section.

Lemma 2 *(Peaucelle et al., 2000) For any matrices N, R, L, P and $\mathbf{Q}$ with appropriate dimensions, the following inequalities are equivalent.*

$$N^TP + P^TN + \mathbf{Q} < 0 \iff \exists\ R, L : \begin{bmatrix} N^TL^T + LN + \mathbf{Q} & (*) \\ P - L^T + R^TN & -R^T - R \end{bmatrix} < 0 \tag{5.27}$$

Lemma 3 *(Tuan et al., 2001) Let $i = 1, ..., r$ and $\alpha_i(.) > 0$ being scalar functions satisfying the convex sum property $\sum_{i=1}^r \alpha_i(.) = 1$. For same sized symmetric matrices $\mathcal{M}_{ik}$, the inequality $\sum_{i=1}^r \sum_{k=1}^r \alpha_i(.)\alpha_k(.)\mathcal{M}_{ik} < 0$ is verified if, $\forall (i,k) = \{1, ..., r\}^2$:*

$$\frac{1}{r-1}\mathcal{M}_{ii} + \frac{1}{2}(\mathcal{M}_{ki} + \mathcal{M}_{ik}) < 0 \quad 1 \leq i \neq k \leq r \tag{5.28}$$

5.3 Main Results

In this section, the design problem of switched fuzzy observers to simultaneously estimate the state and sensor fault vector is considered for a class of switched N-TS

systems (5.4) under arbitrary switching sequences (without dwell-time constraint). For this purpose, sufficient LMI-based conditions with incremental quadratic constraint are given to design the gain matrices K_{h_σ} of the considered observer (5.17) so that the requirements defined above in the problem statement are satisfied.

Theorem 1 *Consider the switched N-TS system (5.4) and the switched N-TS observers (5.17). $\forall(j,\hat{j}) \in \{1,...,m\}^2$, $\forall(i_j,k_j) \in \{1,...,r_j\}^2$ and $\forall q_{\hat{j}} \in \{1,...,r_{\hat{j}}\}$, if there exist a scalar $\gamma > 0$, diagonal matrices $\Upsilon_{i_j} \geq 0$ and real matrices $\Gamma_{\hat{j}}$, $P_{\hat{j}} = P_{\hat{j}}^T > 0$, $Y_{q_{\hat{j}}}$ verifying the following optimization problem:*

$$\begin{cases} \min \gamma^2, \min trace(P_{\hat{j}}) \\ s.t.\ (5.35), (5.36), (5.37) \text{ and } P_{\hat{j}} > 0 \end{cases} \tag{5.29}$$

and the state vector of switched N-TS observers is updated at the switching times according to

$$\hat{\bar{x}}^+(t) = \left(I_{n_x+n_{fs}} - \mathcal{L}_{\hat{j}}^{-1}\left(C^1\mathcal{L}_{\hat{j}}^{-1}\right)^-\right)\hat{\bar{x}}(t) + \mathcal{L}_{\hat{j}}^{-1}\left(C^1\mathcal{L}_{\hat{j}}^{-1}\right)^- y \tag{5.30}$$

$$\frac{1}{r_j - 1}\mathcal{Z}_{i_j i_j q_{\hat{j}}} + \frac{1}{2}\left(\mathcal{Z}_{i_j k_j q_{\hat{j}}} + \mathcal{Z}_{k_j i_j q_{\hat{j}}}\right) < 0,\ \forall(i_j,k_j) \in \mathcal{I}_{r_j}^2, \tag{5.31}$$

$$P_{\hat{j}^+} = P_{\hat{j}} + \Gamma_{\hat{j}}^T(C^1)^T + (C^1)^T\Gamma_{\hat{j}},\ \forall(\hat{j},\hat{j}^+) \in \mathcal{I}_m^2, \tag{5.32}$$

$$\begin{bmatrix} P_{\hat{j}} & (*) \\ \bar{\zeta}_{(v)} & 4\mathcal{Q}_{(v)}^2 \end{bmatrix} \geq 0,\ \forall v \in \mathcal{I}_v,\ \ \forall\hat{j} \in \mathcal{I}_m, \tag{5.33}$$

Thus, the requirements defined in the problem (1) are fulfilled. In addition, the intersection of Lyapunov level sets $\mathbf{L}(1)$,

$$\mathbf{L}(1) = \bigcap_{\hat{j}\in\mathcal{I}_m}\left\{e \in \mathbb{R}^{n_x+n_{fs}} : e^T(0)P_{\hat{j}}e(0) \leq 1\right\} \tag{5.34}$$

gives an estimate of the attraction domain $\mathcal{D}_a$ of the estimation error $e(t)$.
where:

$$\frac{1}{r_j-1}\mathcal{Z}_{i_j i_j q_{\hat{j}}}+\frac{1}{2}\left(\mathcal{Z}_{i_j k_j q_{\hat{j}}}+\mathcal{Z}_{k_j i_j q_{\hat{j}}}\right)<0,\ \forall(i_j,k_j)\in\mathcal{I}^2_{r_j}, \tag{5.35}$$

$$P_{\hat{j}^+}=P_{\hat{j}}+\Gamma^T_{\hat{j}}(C^1)^T+(C^1)^T\Gamma_{\hat{j}},\ \forall(\hat{j},\hat{j}^+)\in\mathcal{I}^2_m, \tag{5.36}$$

$$\begin{bmatrix} P_{\hat{j}} & (*) \\ \bar{\zeta}_{(v)} & 4\mathcal{Q}^2_{(v)} \end{bmatrix}\geq 0,\ \forall v\in\mathcal{I}_v,\ \ \forall\hat{j}\in\mathcal{I}_m, \tag{5.37}$$

$$\mathcal{Z}_{i_j k_j q_{\hat{j}}}=\begin{bmatrix} \wp_{i_j k_j q_{\hat{j}}} & (*) & (*) & (*) & (*) & (*) \\ (B^3_{i_j q_{\hat{j}}})^T P_{\hat{j}} & -\gamma^2\Omega & (*) & (*) & (*) & (*) \\ \left(H^2_{i_j}\right)^T P_{\hat{j}} & 0 & \Xi^{22}_{i_j} & (*) & (*) & (*) \\ \left(H^2_{i_j}-H^2_{q_{\hat{j}}}\right)^T P_{\hat{j}} & \Upsilon_{i_j}U\bar{\Psi} & 0 & -2\Upsilon_{i_j} & (*) & (*) \\ \Psi & 0 & 0 & 0 & -I_{n_x+n_{fs}} & (*) \\ N^1 & 0 & 0 & 0 & 0 & -\bar{\Xi}^{11}_{i_j} \end{bmatrix},$$

$$\wp_{i_j k_j q_{\hat{j}}}=\begin{bmatrix} \mathcal{H}e\left(\left(A^2_{i_j}\right)^T L^T_{k_j}-(C^1)^T Y^T_{q_{\hat{j}}}\right) & (*) \\ P_{\hat{j}}-L^T_{k_j}+R^T_{k_j}A^2_{i_j} & -R^T_{k_j}-R_{k_j} \end{bmatrix},$$

$$B^3_{i_j q_{\hat{j}}}=\begin{bmatrix} A^2_{i_j}-A^2_{q_{\hat{j}}} & B^2_{i_j}-B^2_{q_{\hat{j}}} & E^2_{i_j} \end{bmatrix},\quad \Psi=\mathcal{W}^{1/2},\quad \bar{\Psi}=\begin{bmatrix} I_{n_x+n_{fs}} & 0_{n_x+n_{fs}\times n_u} & 0_{n_x+n_{fs}\times n_d} \end{bmatrix},\quad \bar{\Xi}^{11}_{h_\sigma}=\left(\Xi^{11}_{h_\sigma}\right)^{-1},\quad \Gamma_{\hat{j}}\in\mathbb{R}^{n_y\times n_x+n_{fs}}$$ and $Y^T_{q_{\hat{j}}}=K^T_{q_{\hat{j}}}P_{\hat{j}}$.

with: $\mathcal{L}_{\hat{j}}=\Theta_{\hat{j}}\sqrt{\Lambda_{\hat{j}}}\Theta^T_{\hat{j}}$, where $\Theta_{\hat{j}}\in\mathbb{R}^{n_x+n_{fs}\times n_x+n_{fs}}$ are composed of the orthonormal eigenvectors of $P_{\hat{j}}$, and where $\Lambda_{\hat{j}}\in\mathbb{R}^{n_x+n_{fs}\times n_x+n_{fs}}$ are diagonal matrices, in which are placed the eigenvalues of $P_{\hat{j}}$.
with:

$$\mathcal{Z}_{i_j k_j q_{\hat{j}}}=\begin{bmatrix} \wp_{i_j k_j q_{\hat{j}}} & (*) & (*) & (*) & (*) & (*) \\ (B^3_{i_j q_{\hat{j}}})^T P_{\hat{j}} & -\gamma^2\Omega & (*) & (*) & (*) & (*) \\ \left(H^2_{i_j}\right)^T P_{\hat{j}} & 0 & \Xi^{22}_{i_j} & (*) & (*) & (*) \\ \left(H^2_{i_j}-H^2_{q_{\hat{j}}}\right)^T P_{\hat{j}} & \Upsilon_{i_j}U\bar{\Psi} & 0 & -2\Upsilon_{i_j} & (*) & (*) \\ \Psi & 0 & 0 & 0 & -I_{n_x+n_{fs}} & (*) \\ N^1 & 0 & 0 & 0 & 0 & -\bar{\Xi}^{11}_{i_j} \end{bmatrix},$$

$$\wp_{i_j k_j q_{\hat{j}}} = \begin{bmatrix} \mathcal{H}e\left(\left(A^2_{i_j}\right)^T L^T_{k_j} - \left(C^1\right)^T Y^T_{q_{\hat{j}}}\right) & (*) \\ P_{\hat{j}} - L^T_{k_j} + R^T_{k_j} A^2_{i_j} & -R^T_{k_j} - R_{k_j} \end{bmatrix},$$

$B^3_{i_j q_{\hat{j}}} = \begin{bmatrix} A^2_{i_j} - A^2_{q_{\hat{j}}} & B^2_{i_j} - B^2_{q_{\hat{j}}} & E^2_{i_j} \end{bmatrix}$, $\Psi = \mathcal{W}^{1/2}$, $\bar{\Psi} = \begin{bmatrix} I_{n_x+n_{fs}} & 0_{n_x+n_{fs}\times n_u} & 0_{n_x+n_{fs}\times n_d} \end{bmatrix}$, $\bar{\Xi}^{11}_{h_\sigma} = \left(\Xi^{11}_{h_\sigma}\right)^{-1}$, $\Gamma_{\hat{j}} \in \mathbb{R}^{n_y \times n_x + n_{fs}}$ and $Y^T_{q_{\hat{j}}} = K^T_{q_{\hat{j}}} P_{\hat{j}}$.

with: $\mathcal{L}_{\hat{j}} = \Theta_{\hat{j}} \sqrt{\Lambda_{\hat{j}}} \Theta^T_{\hat{j}}$, where $\Theta_{\hat{j}} \in \mathbb{R}^{n_x+n_{fs}\times n_x+n_{fs}}$ are composed of the orthonormal eigenvectors of $P_{\hat{j}}$, and where $\Lambda_{\hat{j}} \in \mathbb{R}^{n_x+n_{fs}\times n_x+n_{fs}}$ are diagonal matrices, in which are placed the eigenvalues of $P_{\hat{j}}$.

Proof. Let us consider the following multiple quadratic Lyapunov candidate function:

$$V\left(t,\, e\left(t\right)\right) = e^T\left(t\right) P_{\hat{\sigma}} e\left(t\right) \tag{5.38}$$

where $P_{\hat{\sigma}}$ are symmetric positive definite matrices $P_{\hat{\sigma}} = \left(P_{\hat{\sigma}}\right)^T > 0$. From (5.15), the time derivative of (5.38) can be formulated as:

$$\begin{aligned} \dot{V}\left(t,\, e\left(t\right)\right) &= \dot{e}^T\left(t\right) P_{\hat{\sigma}} e\left(t\right) + e^T\left(t\right) P_{\hat{\sigma}} \dot{e}\left(t\right) \\ &= \left(e^T\left(t\right)\left(A^3_{h_\sigma h_{\hat{\sigma}}}\right)^T + \Phi^T_a\left(t\right)\left(H^3_{h_\sigma h_{\hat{\sigma}}}\right)^T + \bar{d}^T\left(t\right)\left(B^3_{h_\sigma h_{\hat{\sigma}}}\right)^T\right) P_{\hat{\sigma}} e\left(t\right) \\ &+ e^T\left(t\right) P_{\hat{\sigma}}\left(A^3_{h_\sigma h_{\hat{\sigma}}} e\left(t\right) + H^3_{h_\sigma h_{\hat{\sigma}}} \Phi_a\left(t\right) + B^3_{h_\sigma h_{\hat{\sigma}}} \bar{d}\left(t\right)\right) \end{aligned} \tag{5.39}$$

Hence, both requirements **i.** and **ii.** formulated in the problem (1) are fulfilled if there exists $\gamma > 0$ such that the following inequality holds:

$$\dot{V}\left(t\right) + e^T\left(t\right) \mathcal{W} e\left(t\right) - \gamma^2\, \bar{d}^T\left(t\right) \Omega \bar{d}\left(t\right) \leq 0 \tag{5.40}$$

where $\Omega = diag\left(\varepsilon_1 I_{n_x+n_{f_s}},\ \varepsilon_2 I_{n_u},\ I_{n_d}\right)$, $\mathcal{W} = diag\left(\xi_1 I_{n_x},\ \xi_2 I_{n_{f_s}}\right)$, ε_1, ε_2, ξ_1, ξ_2 are positive scalars.

The inequality (5.40) is equivalent to:

$$\begin{bmatrix} e\left(t\right) \\ \bar{d}\left(t\right) \\ \Phi_e\left(t\right) \\ \Phi\left(N^1 \hat{\bar{x}}\left(t\right)\right) \end{bmatrix}^T \begin{bmatrix} \mathcal{H}e\left(\left(A^3_{h_\sigma h_{\hat{\sigma}}}\right)^T P_{\hat{\sigma}}\right) + \Psi^T\Psi & (*) & (*) & (*) \\ \left(B^3_{h_\sigma h_{\hat{\sigma}}}\right)^T P_{\hat{\sigma}} & -\gamma^2\Omega & 0 & 0 \\ \left(H^2_{h_\sigma}\right)^T P_{\hat{\sigma}} & 0 & 0_{n_\Phi \times n_\Phi} & 0 \\ \left(H^2_{h_\sigma} - H^2_{h_{\hat{\sigma}}}\right)^T P_{\hat{\sigma}} & 0 & 0 & 0_{n_\Phi \times n_\Phi} \end{bmatrix} \begin{bmatrix} e\left(t\right) \\ \bar{d}\left(t\right) \\ \Phi_e\left(t\right) \\ \Phi\left(N^1 \hat{\bar{x}}\left(t\right)\right) \end{bmatrix} \leq 0 \tag{5.41}$$

where $\Psi = \mathcal{W}^{1/2}$.

Based on the property (1), the vector of the nonlinear consequent part $\Phi\left(N^1 \hat{\bar{x}}\left(t\right)\right) \in$

$\mathrm{Re}^{n_\Phi \times 1}$ verifies the following sector-boundedness condition:

$$\Phi\left(N^1\,\hat{\bar{x}}\,(t)\right)^T \Upsilon_{h_\sigma}\left(\Phi\left(N^1\,\hat{\bar{x}}\,(t)\right) - U\,\hat{\bar{x}}\,(t)\right) \leq 0 \tag{5.42}$$

For design purpose, the inequality (5.42) can be developed as:

$$2\left(\Phi\left(N^1\,\hat{\bar{x}}\,(t)\right)^T \Upsilon_{h_\sigma} U\,\hat{\bar{x}}\,(t) - \Phi\left(N^1\,\hat{\bar{x}}\,(t)\right)^T \Upsilon_{h_\sigma}\Phi\left(N^1\,\hat{\bar{x}}\,(t)\right)\right) \geq 0 \tag{5.43}$$

On the other hand, the incremental quadratic constraint δQC, formulated in the assumption (2) is equivalent to:

$$\begin{bmatrix} e\,(t) \\ \Phi_e\,(t) \end{bmatrix}^T \begin{bmatrix} (N^1)^T \Xi^{11}_{h_\sigma} N^1 & 0 \\ 0 & \Xi^{22}_{h_\sigma} \end{bmatrix} \begin{bmatrix} e\,(t) \\ \Phi_e\,(t) \end{bmatrix} \geq 0 \tag{5.44}$$

where $\left(\Xi^{11}_{h_\sigma}\right)^T = \Xi^{11}_{h_\sigma} > 0$ and $\left(\Xi^{22}_{h_\sigma}\right)^T = \Xi^{22}_{h_\sigma} < 0$.

By introducing the inequalities (5.43) and (5.44), the inequality (5.41) holds, $\forall \begin{bmatrix} e^T\,(t) & \bar{d}^T\,(t) & \Phi_e^T \end{bmatrix}$ 0, if:

$$\begin{bmatrix} \mathcal{H}e\left(\left(A^3_{h_\sigma h_{\hat{\sigma}}}\right)^T P_{\hat{\sigma}}\right) + \Psi^T\Psi + (N^1)^T \Xi^{11}_{h_\sigma} N^1 & (*) & (*) & (*) \\ \left(B^3_{h_\sigma h_{\hat{\sigma}}}\right)^T P_{\hat{\sigma}} & -\gamma^2\Omega & (*) & (*) \\ \left(H^2_{h_\sigma}\right)^T P_{\hat{\sigma}} & 0 & \Xi^{22}_{h_\sigma} & (*) \\ \left(H^2_{h_\sigma} - H^2_{h_{\hat{\sigma}}}\right)^T P_{\hat{\sigma}} & \Upsilon_{h_\sigma} U\bar{\Psi} & 0 & -2\Upsilon_{h_\sigma} \end{bmatrix} \leq 0 \tag{5.45}$$

with $\bar{\Psi} = \begin{bmatrix} I_{n_x+n_{fs}} & 0_{n_x+n_{fs}\times n_u} & 0_{n_x+n_{fs}\times n_d} \end{bmatrix}$.

By applying the Schur complement, the inequality (5.45) can be formulated as follows:

$$\begin{bmatrix} \mathcal{H}e\left(\left(A^3_{h_\sigma h_{\hat{\sigma}}}\right)^T P_{\hat{\sigma}}\right) & (*) & (*) & (*) & (*) & (*) \\ \left(B^3_{h_\sigma h_{\hat{\sigma}}}\right)^T P_{\hat{\sigma}} & -\gamma^2\Omega & (*) & (*) & (*) & (*) \\ \left(H^2_{h_\sigma}\right)^T P_{\hat{\sigma}} & 0 & \Xi^{22}_{h_\sigma} & (*) & (*) & (*) \\ \left(H^2_{h_\sigma} - H^2_{h_{\hat{\sigma}}}\right)^T P_{\hat{\sigma}} & \Upsilon_{h_\sigma} U\bar{\Psi} & 0 & -2\Upsilon_{h_\sigma} & (*) & (*) \\ \Psi & 0 & 0 & 0 & -I_{n_x+n_{fs}} & (*) \\ N^1 & 0 & 0 & 0 & 0 & -\bar{\Xi}^{11}_{h_\sigma} \end{bmatrix} \leq 0 \tag{5.46}$$

where $\bar{\Xi}^{11}_{h_\sigma} = \left(\Xi^{11}_{h_\sigma}\right)^{-1}$.

Then, by applying Peaucelle lemma (lemma 2), the inequality (5.46) holds if $\exists(L_{h_\sigma}, R_{h_\sigma})$ such that:

$$\begin{bmatrix} \mathcal{H}e\left(\left(A^2_{h_\sigma}\right)^T L^T_{\hat{\sigma}} - \left(C^1\right)^T Y^T_{h_{\hat{\sigma}}}\right) & (*) & (*) & (*) & (*) & (*) & (*) \\ P_{\hat{\sigma}} - L^T_{h_\sigma} + R^T_{h_\sigma} A^2_{h_\sigma} & -R_{h_\sigma} - R^T_{h_\sigma} & (*) & (*) & (*) & (*) & (*) \\ \left(B^3_{h_\sigma h_{\hat{\sigma}}}\right)^T P_{\hat{\sigma}} & 0 & -\gamma^2\Omega & (*) & (*) & (*) & (*) \\ \left(H^2_{h_\sigma}\right)^T P_{\hat{\sigma}} & 0 & 0 & \Xi^{22}_{h_\sigma} & (*) & (*) & (*) \\ \left(H^2_{h_\sigma} - H^2_{h_{\hat{\sigma}}}\right)^T P_{\hat{\sigma}} & 0 & \Upsilon_{h_\sigma} U \bar{\Psi} & 0 & -2\Upsilon_{h_\sigma} & (*) & (*) \\ \Psi & 0 & 0 & 0 & 0 & -I_{n_x+n_{fs}} & (*) \\ N^1 & 0 & 0 & 0 & 0 & 0 & -\bar{\Xi}^{11}_{h_\sigma} \end{bmatrix} \leq 0 \tag{5.47}$$

After the application of the Tuan lemma (Lemma 3), the inequality (5.47) can be expressed as LMIs conditions (5.35) given in the theorem (1).

Furthermore, to ensure the decreasing of the Lyapunov function at the switching instants of the observer, the following inequality must be verified:

$$V\left(t^+, e^+(t)\right) \leq V\left(t, e(t)\right) \tag{5.48}$$

where $e^+(t)$ is the updated error of the switched N-TS observers in the forthcoming mode $\hat{\jmath}^+$.
Then, it can be deduced that the inequality (5.48) is fulfilled if:

$$\left(\bar{x}\left(t\right) - \hat{\bar{x}}^+\left(t\right)\right)^T P_{\hat{\jmath}^+} \left(\bar{x}\left(t\right) - \hat{\bar{x}}^+\left(t\right)\right) \leq \left(\bar{x}\left(t\right) - \hat{\bar{x}}\left(t\right)\right)^T P_{\hat{\jmath}} \left(\bar{x}\left(t\right) - \hat{\bar{x}}\left(t\right)\right) \tag{5.49}$$

Giving that $\bar{x}^+(t)$ is an arbitrary estimated state vector satisfying $y = C^1\hat{\bar{x}}^+(t)$. Since also $y = C^1\bar{x}(t)$, it can lead to $C^1\left(\bar{x}(t) - \hat{\bar{x}}^+(t)\right) = y(t) - y(t) = 0$, implying also that

$$\left(\bar{x}\left(t\right) - \hat{\bar{x}}^+\left(t\right)\right)^T \left(\Gamma^T_{\hat{\jmath}} C^1 + \left(C^1\right)^T \Gamma_{\hat{\jmath}}\right) \left(\bar{x}\left(t\right) - \hat{\bar{x}}^+\left(t\right)\right) = 0 \tag{5.50}$$

Based on the relation $P_{\hat{\jmath}^+} = P_{\hat{\jmath}} + \Gamma^T_{\hat{\jmath}}(C^1)^T + (C^1)^T\Gamma_{\hat{\jmath}}$ given in the theorem (1), the inequality (5.49) becomes:

$$\left(\bar{x}\left(t\right) - \hat{\bar{x}}^+\left(t\right)\right)^T P_{\hat{\jmath}} \left(\bar{x}\left(t\right) - \hat{\bar{x}}^+\left(t\right)\right) \leq \left(\bar{x}\left(t\right) - \hat{\bar{x}}\left(t\right)\right)^T P_{\hat{\jmath}} \left(\bar{x}\left(t\right) - \hat{\bar{x}}\left(t\right)\right) \tag{5.51}$$

The aim now is to choose $\hat{\bar{x}}^+(t) \in \hat{\bar{S}}_{\hat{\jmath},\hat{\jmath}^+}$ $(\hat{\bar{S}}_{\hat{\jmath},\hat{\jmath}^+} = \left\{\hat{\bar{x}}(t) \in \mathrm{Re}^{n_x \times n_{fs}} \middle| \hat{s}_{\hat{\jmath},\hat{\jmath}^+}\hat{\bar{x}}(t) = 0\right\})$, that the inequality (5.51) is fulfilled. In order to do so, we follow the reasoning of [80].

Since $P_{\hat{\jmath}}$ can be factorized (spectral decomposition) as $P_{\hat{\jmath}} = \mathcal{L}^T_{\hat{\jmath}}\mathcal{L}_{\hat{\jmath}}$, with $\mathcal{L}_{\hat{\jmath}} = V_{\hat{\jmath}}\sqrt{\Lambda_{\hat{\jmath}}}V^T_{\hat{\jmath}} \in \mathrm{Re}^{n_x+n_{fs}\times n_x+n_{fs}}$ [21], the inequality (5.51) is satisfied if:

$$\left\|\mathcal{L}_{\hat{\jmath}}\left(\bar{x}\left(t\right) - \hat{\bar{x}}^+\left(t\right)\right)\right\| \leq \left\|\mathcal{L}_{\hat{\jmath}}\left(\bar{x}\left(t\right) - \hat{\bar{x}}\left(t\right)\right)\right\| \tag{5.52}$$

To obtain the updated value of the estimation of the state vector $\hat{\bar{x}}^+(t)$, ling on the hyper plane $y(t) = C^1\hat{\bar{x}}^+(t)$ and minimizing the distance $\left\|\mathcal{L}_{\hat{j}}\left(\hat{\bar{x}}^+(t) - \hat{\bar{x}}(t)\right)\right\|$, we consider the following optimization problem:

$$\begin{aligned} &\min_{\hat{\bar{x}}^+} \left\|\mathcal{L}_{\hat{j}}\left(\hat{\bar{x}}^+(t) - \hat{\bar{x}}(t)\right)\right\| \\ &\text{subject to :} C^1\hat{\bar{x}}^+(t) = y(t) \end{aligned} \tag{5.53}$$

By introducing a scalar $\alpha_{\hat{j}} = \mathcal{L}_{\hat{j}}\left(\hat{\bar{x}}^+(t) - \hat{\bar{x}}(t)\right)$, we can write $\mathcal{L}_{\hat{j}}\hat{\bar{x}}^+(t) = \alpha_{\hat{j}} + \mathcal{L}_{\hat{j}}\hat{\bar{x}}(t)$. The optimization problem (5.53) can be reformulated as follows:

$$\begin{aligned} &\min_{\hat{\bar{x}}^+} \left\|\alpha_{\hat{j}}\right\| \\ &\text{Subject to } C^1\mathcal{L}_{\hat{j}}^{-1}\alpha_{\hat{j}} = y - C^1\hat{\bar{x}}(t) \end{aligned} \tag{5.54}$$

Which admits for solution the minimum least square length $y(t) - C^1\hat{\bar{x}}(t)$:

$$\alpha_{\hat{j}} = \left(C^1\mathcal{L}_{\hat{j}}^{-1}\right)^-\left(y - C^1\hat{\bar{x}}(t)\right) \tag{5.55}$$

and so:

$$\mathcal{L}_{\hat{j}}\hat{\bar{x}}^+(t) = \mathcal{L}_{\hat{j}}\hat{\bar{x}}(t) + \left(C^1\mathcal{L}_{\hat{j}}^{-1}\right)^-\left(y - C^1\hat{\bar{x}}(t)\right) \tag{5.56}$$

At last, left multiplying (5.56) by $\mathcal{L}_{\hat{j}}^{-1}$, the updated value $\hat{\bar{x}}^+(t)$ can be computed as indicated in (5.30).

To complete the proof, we still need to provide an estimate of the attraction domain $D_a \subseteq D_e$ (see the first item in the problem (1)). Hence, let us consider the Lyapunov level set $\mathbf{L}(1)$ defined, at $t = 0$, by (5.34). Applying the Schur Complement on (5.37), we obtain:

$$P_{\hat{j}} - \frac{\bar{\zeta}_{(v)}^T\bar{\zeta}_{(v)}}{4\mathcal{Q}_{(v)}^2} \geq 0,\ \forall v \in \mathcal{I}_v,\ \forall \hat{j} \in \{1,\ldots,m\}. \tag{5.57}$$

Pre and post multiplying (5.57) by $e^T(0)$ and its transpose leads:

$$e^T(0)P_{\hat{j}}e(0) - \frac{e^T(0)\bar{\zeta}_{(v)}^T\bar{\zeta}_{(v)}e(0)}{4\mathcal{Q}_{(v)}^2} \geq 0,\ \forall \hat{j} \in \{1,\ldots,m\}. \tag{5.58}$$

Therefore, for any $e(0) \in \mathbf{L}(1)$, the inequality $e^T(0)\bar{\zeta}_{(v)}^T\bar{\zeta}_{(v)}e(0) \leq 4\mathcal{Q}_{(v)}^2$ holds and, based on the definition (5.24) of the error domain D_e, one can conclude that $\mathbf{L}(1) \subseteq D_e$. At last, a simple method for enlarging $\mathbf{L}(1)$ is to minimize the trace of $P_{\hat{j}}$ with $\hat{j} \in \{1,\ldots,m\}$, as proposed in the optimization problem (5.29).

Remark 12 *It should be emphasized that by replacing the index $\hat{j}$ with j in the LMI-based conditions of Theorem 1, we can obtain the synchronous switched N-TS observers design conditions.*

In order to implement the proposed design approach, the following algorithm can be employed.

Algorithm 1

1. *Write the original switched nonlinear systems (5.1) as a switched N-TS systems (5.4) and construct the parameter matrices of the system (5.8), i.e. $A^0_{h_\sigma}$, $H^0_{h_\sigma}$, $B^0_{h_\sigma}$, $E^0_{h_\sigma}$, C and F^0_s.*
2. *Extend the switched N-TS systems (5.8) to obtain the extended switched N-TS systems and construct their parameter matrices, (5.9), i.e. $\mathcal{G}^0$, $A^1_{h_\sigma}$, $H^1_{h_\sigma}$, $B^1_{h_\sigma}$, $E^1_{h_\sigma}$, C_1, C_0 and F^1_s.*
3. *Select $L^{1_2}_\sigma \in \mathbb{R}^{n_y \times n_y}$ such that $L^{1_2}_\sigma$ are arbitrary nonsingular matrices.*
4. *Construct the parameter matrices of the switched N-TS observers, i.e. $A^2_{h_\sigma}$, $H^2_{h_\sigma}$, $B^2_{h_\sigma}$ and $F^3_{s_\sigma}$.*
5. *Solve the optimization problem (5.29). Gain matrices of the observer can be obtained as $K_{q_{\hat{j}}} = P^{-1}_{\hat{j}} Y_{q_{\hat{j}}}$.*

In the following section, the effectiveness of the proposed design approach will be illustrated over numerical simulations and some comparisons with related recent results from the literature.

5.4 Simulation Results

In this section, two simulation examples, demonstrating the effectiveness and the performances of the proposed asynchronous switched N-TS observers, are presented. The first one is an academic example dedicated to compare the conservatism of the proposed LMI-based conditions with regards to previous results by checking the feasibility field of each method. The second example aims to illustrate the effectiveness of our design methodology through an illustrative example (Zhang et al., 2015, Ren et al., 2018, Khalil, 2002).

5.4.1 Numerical example

Let us consider a switched nonlinear system with three modes ($m = 3$) defined by:

$$\text{Mode } 1 : \begin{cases} \dot{x}_1(t) = \kappa_{11}^1 x_1(t) + x_2(t) + 4\eta(x_1(t))x_2(t) + \beta_{11}^1 u(t) + \delta_{11}^1 d(t) \\ \dot{x}_2(t) = -8.5x_2(t) + \sin(x_2(t)) + 1.21u(t) + 0.5d(t) \\ \dot{x}_3(t) = 0.8x_1(t) - 12x_3(t) + u(t) + 0.1d(t) \end{cases} \tag{5.59}$$

$$\text{Mode } 2 : \begin{cases} \dot{x}_1(t) = -11x_1(t) + 2x_2(t) + 5\eta(x_1(t))x_2(t) + \kappa_{13}^2 x_3(t) + u(t) + 0.35d(t) \\ \dot{x}_2(t) = -13x_2(t) + \sin(x_2(t)) + \beta_{21}^2 u(t) + \delta_{21}^2 d(t) \\ \dot{x}_3(t) = 0.5x_1(t) + 0.1x_2(t) - 10x_3(t) + 1.2u(t) + 0.5d(t) \end{cases} \tag{5.60}$$

$$\text{Mode } 3 : \begin{cases} \dot{x}_1(t) = -12x_1(t) + 2x_2(t) + \eta(x_1(t))x_2(t) + 1.5x_3(t) + 0.95u(t) + 0.3d(t) \\ \dot{x}_2(t) = 0.5x_1(t) - 10.2x_2(t) + 0.3x_3(t) + \sin(x_2(t)) + u(t) + 0.8d(t) \\ \dot{x}_3(t) = 0.8x_1(t) + \kappa_{32}^3 x_2(t) - 9x_3(t) + \beta_{31}^3 u(t) + \delta_{31}^3 d(t) \end{cases} \tag{5.61}$$

The outputs are common and linear for all the switched modes. They are defined as:

$$\begin{cases} y_1(t) = x_1(t) + f_{s_1}(t) + \omega(t) \\ y_2(t) = c_{21}x_1(t) + c_{23}x_3(t) + f_{s_2}(t) + \omega(t) \end{cases} \tag{5.62}$$

where $\eta(x_1(t)) = x_1^2(t)$, $\kappa_{11}^1 = -20(a-b)$, $\beta_{11}^1 = 1 + \left(\frac{a}{2}\right)$, $\delta_{11}^1 = 0.25 + \left(\frac{a}{10}\right)$, $\kappa_{13}^2 = 0.5 + \left(\frac{a-b}{2}\right)$, $\beta_{21}^2 = 1.22 + \left(\frac{b}{2}\right)$ and $\delta_{21}^2 = 0.7 + \left(\frac{b}{10}\right)$, $\kappa_{32}^3 = \frac{a+b}{3}$, $\beta_{31}^3 = 1.5 + \frac{b}{2}$, $\delta_{31}^3 = 0.6 + \left(\frac{a-b}{10}\right)$, $c_{21} = \frac{a}{10}$, $c_{23} = 1 + (b/10)$.

Moreover, a and b are two scalars devoted to study the feasibility fields of the LMI-based conditions formulated in Theorem 1, then to compare their conservatism with the following related works:

- Theorem 1 in Zhang et al., 2018, which provides the design of dynamic unknown input switched TS observers to estimate the sensor fault and the system state for a class of switched T-S systems with average dwell time consideration and measured premise variables.
- The first optimization problem $\begin{cases} \min \gamma^2 \\ \text{s.t. (31) and (41)} \end{cases}$ presented in Han et al., 2022, which proposed dwell-time free conditions to design an adaptive adjustable dimension observer to estimate the sensor fault and the system state for a class of switched T-S systems with UPVs .

- The second optimization problem $\begin{cases} \min \gamma^2 \\ \text{s.t. (31), (38) and (41)} \end{cases}$ presented in Han et al., 2022. In addition to the above conditions presented in the first optimization problem, regional pole constraints are considered in the design of an adaptive adjustable dimension observer.

Follow the first step of the Algorithm (1), let us write the original switched nonlinear system (5.59)-(5.61) as a switched N-TS systems.
Noting that, the switched nonlinear systems considered in this example switches according to the following switching sequence $\mathcal{B} = (\mathcal{V}, \mathcal{E})$, where $\mathcal{V} = \{1, 2, 3\}$ is the sets of switched modes and $\mathcal{E} = \{(1,2), (2,3), (3,1)\}$ is the set of the admissible switches between modes.

Remark 13 *Two concepts can be applied in this example. The first one leads to a classical switched T-S representation of the original system (5.59)-(5.61) by considering two premise variables $\xi_1(t) = x_1^2(t)$, $\xi_2(t) = \sin(x_2(t))$, and so 4 rules in each switched modes. Since the second state variables $x_2(t)$ is unmeasured, this would make $\xi_2(t)$ unavailable, leading to T-S model with UPVs. However, the second concept consists to apply the sector nonlinearity approach only to the nonlinear terms depending on the measured state variables $\xi_1(t) = x_1^2(t)$, leading to a N-TS model containing only measured premises variables. Furthermore, the unmeasured nonlinear terms are kept as nonlinear consequent parts. In this case, the number of fuzzy rules can be reduced to 2 rules in each modes, thereby decreasing the number of vertices involved in LMI-based conditions.*

Hence, let us consider the N-TS modeling approach to address the issue of unmeasured premise variables. To achieve this, let us assume that $x(t) = \begin{bmatrix} x_1(t) & x_2(t) & x_3(t) \end{bmatrix}^T$, $y(t) = \begin{bmatrix} y_1(t) & y_2(t) \end{bmatrix}^T$ and $f_s(t) = \begin{bmatrix} f_{s_1}(t) & f_{s_2}(t) \end{bmatrix}^T$ are the augmented vector. $x_2(t) \in [-\pi/2\ \pi/2]$ is a bounded state vector which is unavailable from the measured output $y(t)$. Thus, $sin(x_2(t))$ is an unmeasured nonlinear terms that can be placed in the vector valued sector-bounded nonlinear function $\Phi(N^0 x(t)) = \sin(N^0 x(t)) \in co\{0,\ Ux(t)\}$ with $U = \begin{bmatrix} 0 & 1 & 0 \end{bmatrix}$ and $N^0 = \begin{bmatrix} 0 & 1 & 0 \end{bmatrix}$. As a consequence, the switched nonlinear system (5.59)-(5.61) can be formulated as follows:

Mode 1:

$$\dot{x}(t) = \begin{bmatrix} \kappa_{11}^1 & 1 + 4\eta(x_1(t)) & 0 \\ 0 & -8.5 & 0 \\ 0.8 & 0 & -12 \end{bmatrix} x(t) + \begin{bmatrix} 0 \\ 1 \\ 0 \end{bmatrix} \underbrace{\sin(x_2(t))}_{\Phi(N^0 x(t))} + \begin{bmatrix} \beta_{11}^1 \\ 1.21 \\ 1 \end{bmatrix} u(t) + \begin{bmatrix} \delta_{11}^1 \\ 0.5 \\ 0.1 \end{bmatrix} d(t) \quad (5.63)$$

Mode 2:

$$\dot{x}(t) = \begin{bmatrix} -11 & 2+5\eta(x_1(t)) & \kappa_{13}^2 \\ 0 & -13 & 0 \\ 0.5 & 0.1 & -10 \end{bmatrix} x(t) + \begin{bmatrix} 0 \\ 1 \\ 0 \end{bmatrix} \underbrace{\sin(x_2(t))}_{\Phi(N^0 x(t))} + \begin{bmatrix} 1 \\ \beta_{21}^2 \\ 1.2 \end{bmatrix} u(t) + \begin{bmatrix} 0.35 \\ \delta_{21}^2 \\ 0.5 \end{bmatrix} d(t) \quad (5.64)$$

Mode 3:

$$\dot{x}(t) = \begin{bmatrix} -12 & 2+\eta(x_1(t)) & 1.5 \\ 0.5 & -10.2 & 0.3 \\ 0.8 & \kappa_{32}^3 & -9 \end{bmatrix} x(t) + \begin{bmatrix} 0 \\ 1 \\ 0 \end{bmatrix} \underbrace{\sin(x_2(t))}_{\Phi(N^0 x(t))} + \begin{bmatrix} 0.95 \\ 1 \\ \beta_{31}^3 \end{bmatrix} u(t) + \begin{bmatrix} 0.3 \\ 0.8 \\ \delta_{31}^3 \end{bmatrix} d(t) \quad (5.65)$$

and the outputs are given as:

$$y(t) = \begin{bmatrix} 1 & 0 & 0 \\ c_{21} & 0 & c_{23} \end{bmatrix} x(t) + \begin{bmatrix} 1 & 0 \\ 0 & 1 \end{bmatrix} f_s(t) \quad (5.66)$$

So, let us apply the sector nonlinearity approach for $x_1^2 \in [0 \;\; 2.25]$ ($x_1(t) \in [-1.5 \;\; 1.5]$), the switched nonlinear system (5.63)-(5.65) can be rewritten as a N-TS system, according to the model (5.4), with $r_j = 2$ fuzzy rules in each of its $m = 3$ modes ($j = \{1, 2, 3\}$). The nonlinear term $\eta(x_1(t))$ can be expressed as follows:

$$\eta(x_1(t)) = h_{1_j}(x_1(t)) \times 0 + h_{2_j}(x_1(t)) \times 2.25 \quad (5.67)$$

where the membership functions are:

$$h_{1_j}(x_1(t)) = \frac{2.25 - x_1^2(t)}{2.25} \text{ and } h_{2_j}(x_1(t)) = 1 - h_{1_j}(x_1(t)) = \frac{x_1^2(t)}{2.25} \quad (5.68)$$

So, the vertices defined by the matrices:

$$A_{2_1}^0 = \begin{bmatrix} \kappa_{11}^1 & 1 & 0 \\ 0 & -8.5 & 0 \\ 0.8 & 0 & -12 \end{bmatrix}, A_{1_1}^0 = \begin{bmatrix} \kappa_{11}^1 & 10 & 0 \\ 0 & -8.5 & 0 \\ 0.8 & 0 & -12 \end{bmatrix}, A_{2_2}^0 = \begin{bmatrix} -11 & 2 & \kappa_{13}^2 \\ 0 & -13 & 0 \\ 0.5 & 0.1 & -10 \end{bmatrix},$$

$$A_{1_2}^0 = \begin{bmatrix} -11 & 13.25 & \kappa_{13}^2 \\ 0 & -13 & 0 \\ 0.5 & 0.1 & -10 \end{bmatrix}, A_{2_3}^0 = \begin{bmatrix} -12 & 2 & 1.5 \\ 0.5 & -10.2 & 0.3 \\ 0.8 & \kappa_{32}^3 & -9 \end{bmatrix}, A_{1_3}^0 = \begin{bmatrix} -12 & 4.25 & 1.5 \\ 0.5 & -10.2 & 0.3 \\ 0.8 & \kappa_{32}^3 & -9 \end{bmatrix},$$

$$B_{i_1}^0 = \begin{bmatrix} \beta_{11}^1 \\ 1.21 \\ 1 \end{bmatrix}, B_{i_2}^0 = \begin{bmatrix} 1 \\ \beta_{21}^2 \\ 1.2 \end{bmatrix}, B_{i_3}^0 = \begin{bmatrix} 0.95 \\ 1 \\ \beta_{31}^3 \end{bmatrix}, E_{i_1}^0 = \begin{bmatrix} \delta_{11}^1 \\ 0.5 \\ 0.1 \end{bmatrix}, E_{i_2}^0 = \begin{bmatrix} 0.35 \\ \delta_{21}^2 \\ 0.5 \end{bmatrix},$$

$$E_{i_3}^0 = \begin{bmatrix} 0.3 \\ 0.8 \\ \delta_{31}^3 \end{bmatrix}, C = \begin{bmatrix} 1 & 0 & 0 \\ c_{21} & 0 & c_{23} \end{bmatrix}, F_s^0 = \begin{bmatrix} 1 & 0 \\ 0 & 1 \end{bmatrix} \text{ and } H_{i_1}^0 = H_{i_2}^0 = H_{i_3}^0 = \begin{bmatrix} 0 \\ 1 \\ 0 \end{bmatrix}.$$

According to steps 2, 3 and 4 of the Algorithm (1), let us select the matrices $L_\sigma^{1_2}$

(arbitrary nonsingular matrices) as follows:

$$L_1^{1_2} = \begin{bmatrix} 0.1 & 0 \\ 0 & 0.1 \end{bmatrix}, L_2^{1_2} = \begin{bmatrix} 1 & 0 \\ 0 & 1 \end{bmatrix} \text{ and } L_3^{1_2} = \begin{bmatrix} 2 & 0 \\ 0 & 2 \end{bmatrix} \tag{5.69}$$

So, the parameter matrices of the switched N-TS observers can be constructed as:

$$A_{2_1}^2 = \begin{bmatrix} \kappa_{11}^1 & 1 & 0 & 0 & 0 \\ hy;0 & -8.5 & 0 & 0 & 0 \\ 0.8 & 0 & -12 & 0 & 0 \\ -\kappa_{11}^1 - 10 & -1 & 0 & -10 & 0 \\ -10c_{21} - 0.8c_{23} - c_{21}\kappa_{11}^1 & -c_{21} & 2c_{23} & 0 & -10 \end{bmatrix}, B_{i_1}^2 = \begin{bmatrix} \beta_{11}^1 \\ 1.21 \\ 1 \\ -\beta_{11}^1 \\ -c_{23} - c_{21}\beta_{11}^1 \end{bmatrix},$$

$$H_{i_1}^2 = H_{i_2}^2 = H_{i_3}^2 = \begin{bmatrix} 0 \\ 1 \\ 0 \\ 0 \\ 0 \end{bmatrix}, A_{1_1}^2 = \begin{bmatrix} \kappa_{11}^1 & 10 & 0 & 0 & 0 \\ 0 & -8.5 & 0 & 0 & 0 \\ 0.8 & 0 & -12 & 0 & 0 \\ -\kappa_{11}^1 - 10 & -10 & 0 & -10 & 0 \\ -10c_{21} - 0.8c_{23} - c_{21}\kappa_{11}^1 & -10c_{21} & 2c_{23} & 0 & -10 \end{bmatrix},$$

$$B_{i_2}^2 = \begin{bmatrix} 1 \\ \beta_{21}^2 \\ 1.2 \\ -1 \\ -c_{21} - 1.2c_{23} \end{bmatrix}, F_{s_1}^3 = \begin{bmatrix} 0 & 0 \\ 0 & 0 \\ 0 & 0 \\ 10 & 0 \\ 0 & 10 \end{bmatrix},$$

$$A_{2_2}^2 = \begin{bmatrix} -11 & 2 & \kappa_{13}^2 & 0 & 0 \\ 0 & -13 & 0 & 0 & 0 \\ 0.5 & 0.1 & -10 & 0 & 0 \\ 10 & -2 & -\kappa_{13}^2 & -1 & 0 \\ 10c_{21} - 0.5c_{23} & -2c_{21} - 0.1c_{23} & 9c_{23} - c_{21}\kappa_{13}^2 & 0 & -1 \end{bmatrix}, B_{i_3}^2 = \begin{bmatrix} 0.95 \\ 1 \\ \beta_{31}^3 \\ -0.95 \\ -0.95c_{21} - c_{23}\beta_{31}^3 \end{bmatrix},$$

$$F_{s_2}^3 = \begin{bmatrix} 0 & 0 \\ 0 & 0 \\ 0 & 0 \\ 1 & 0 \\ 0 & 1 \end{bmatrix}, A_{1_2}^2 = \begin{bmatrix} -11 & 13.25 & \kappa_{13}^2 & 0 & 0 \\ 0 & -13 & 0 & 0 & 0 \\ 0.5 & 0.1 & -10 & 0 & 0 \\ 10 & -13.25 & -\kappa_{13}^2 & -1 & 0 \\ 10c_{21} - 0.5c_{23} & -13.25c_{21} - 0.1c_{23} & 9c_{23} - c_{21}\kappa_{13}^2 & 0 & -1 \end{bmatrix},$$

$$A_{2_3}^2 = \begin{bmatrix} -12 & 2 & 1.5 & 0 & 0 \\ 0.5 & -10.2 & 0.3 & 0 & 0 \\ 0.8 & \kappa_{32}^3 & -9 & 0 & 0 \\ 11.5 & -2 & -1.5 & -0.5 & 0 \\ 11.5c_{21} - 0.8c_{23} & -2c_{21} - c_{23}\kappa_{32}^3 & 8.5c_{23} - 1.5c_{21} & 0 & -0.5 \end{bmatrix},$$

$$A^2_{1_3} = \begin{bmatrix} -12 & 4.25 & 1.5 & 0 & 0 \\ 0.5 & -10.2 & 0.3 & 0 & 0 \\ 0.8 & \kappa^3_{32} & -9 & 0 & 0 \\ 11.5 & -4.25 & -1.5 & -0.5 & 0 \\ 11.5c_{21} - 0.8c_{23} & -4.25c_{21} - c_{23}\kappa^3_{32} & 8.5c_{23} - 1.5c_{21} & 0 & -0.5 \end{bmatrix}, F^3_{s_3} = \begin{bmatrix} 0 & 0 \\ 0 & 0 \\ 0 & 0 \\ 0.5 & 0 \\ 0 & 0.5 \end{bmatrix}.$$

Moreover, by considering that $x_1(t) \in [-1.5\ 1.5]$ and $x_2(t) \in [-\pi/2\ \pi/2]$, the switched N-TS systems (5.4) represents exactly the switched nonlinear system (5.1) on a validity domain $\mathcal{D}_x$, which is a subset of the state space defined by the equation (5.7) with:

$$\zeta = \begin{bmatrix} 1 & 0 & 0 \\ -1 & 0 & 0 \\ 0 & 1 & 0 \\ 0 & -1 & 0 \end{bmatrix}, \quad \mathcal{Q} = \begin{bmatrix} 1.5 \\ 1.5 \\ \pi/2 \\ \pi/2 \end{bmatrix} \tag{5.70}$$

So, the validity domain $\mathcal{D}_{\bar{x}}$ of the extended switched N-TS systems is defined in (5.16) with $\bar{\zeta} = \begin{bmatrix} 1 & 0 & 0 & 0 & 0 \\ -1 & 0 & 0 & 0 & 0 \\ 0 & 1 & 0 & 0 & 0 \\ 0 & -1 & 0 & 0 & 0 \end{bmatrix}$.

It now remains to determine gain matrices K_{q_j} of the switched N-TS observers. To do so, the last step of Algorithm (1) is to solve Problem (1) defined in Theorem (1).

In what follows, our main objective is to compare the conservatism of the proposed LMI-based conditions described in Theorem (1) with respect to some previous related results (Zhang et al., 2018) and (Han et al., 2022). For several values of $a \in [-35,\ 21]$ and $b \in [-7,\ 35]$ with a step of 1 between two consecutive values of a and b, the feasibility regions, obtained by using YALMIP and SeduMi in MATLAB (Lofberg, 2004), are compared. The results of this study are shown in Fig.(5.1).

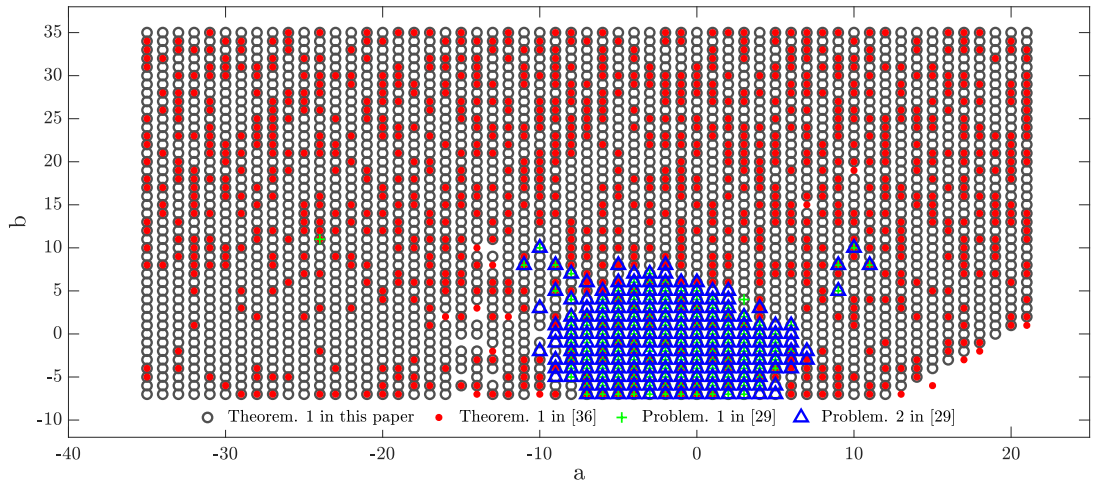

Figure 5.1: Feasibility fields obtained by Theorem (1) and the related studies.

Indeed, each LMI-based conditions considered in this study were tested 2451 times. The parameters used to perform this study are presented in Table (5.1).

Table 5.1: Parameters used in the considered studies.

Method	Parameters
Theorem. 1 in Zhang et al., 2018	$\mathcal{K}_0^1 = \begin{bmatrix} 0.1 & 0 \\ 0 & 0.1 \end{bmatrix}$, $\mathcal{K}_0^2 = \begin{bmatrix} 1 & 0 \\ 0 & 1 \end{bmatrix}$, $\mathcal{K}_0^3 = \begin{bmatrix} 2 & 0 \\ 0 & 2 \end{bmatrix}$, $\bar{T}^1 = \bar{T}^2 = \bar{T}^3 = \begin{bmatrix} 1 & 0 & 0 & 0 & 0 \\ 0 & 1 & 0 & 0 & 0 \\ 0 & 0 & 1 & 1 & 1 \end{bmatrix}$, $\nu = 3$
Problem. 1 in Han et al., 2022	$G_j^1 = \begin{bmatrix} 1 & 0 & 0 \\ 0 & 0 & 0 \\ 0 & 1 & 0 \\ 0 & 0 & 0 \\ 0 & 0 & 1 \end{bmatrix}$, $G_j^2 = \begin{bmatrix} 0 & 0 \\ 1 & 0 \\ 0 & 0 \\ 0 & 1 \\ 0 & 0 \end{bmatrix}$, $\bar{T}_j = \begin{bmatrix} 50 & 0 & 0 & 0 & 0 \\ 0 & 50 & 0 & 0 & 0 \\ 0 & 0 & 50 & 0 & 0 \end{bmatrix}$, $s = 0.0025$, $\rho = 0.04$
Problem. 2 in Han et al., 2022	same parameters as Problem. 1, $\alpha_{i_j} = 5$, $\beta_{i_j} = 50$
Theorem. 1 in this paper	$L_1^{1_2} = \begin{bmatrix} 0.1 & 0 \\ 0 & 0.1 \end{bmatrix}$, $L_2^{1_2} = \begin{bmatrix} 1 & 0 \\ 0 & 1 \end{bmatrix}$, $L_3^{1_2} = \begin{bmatrix} 2 & 0 \\ 0 & 2 \end{bmatrix}$, $\varepsilon_1 = 10$, $\varepsilon_2 = 1$, $\xi_1 = 1$, $\xi_2 = 1$

Remark 14 *It would be relevant to mention that the parameters of each considered method are selected according to the suggestions of the authors. Nevertheless, in the problems 1 and 2 in Han et al., 2022, the authors have omitted to mention the values of the parameters s and ρ. Some suggestions regarding the parameter s have been proposed in Zhang et al., 2018. This latter recommends to choose s equal to 10^{-5} to approximate correctly an equality constraint, which led to a very conservative condition and an empty feasibility field. For the purposes of comparing the conservatism of our approach, we have selected s as small as possible ($s = 0.0025$) so that the feasibility field is not empty. As regards the value of the parameter ρ, it was selected equal to 0.04 after several tests.*

Remark 15 *By looking at equations (5.21), the matrices $L_1^{1_2}$, $L_2^{1_2}$ and $L_3^{1_2}$ are of great importance for the design of the proposed observer. They could be used to set the dynamic of the estimation error. For design purpose, these matrices L_σ are preferably selected diagonal to easily adjust their eigenvalues. Their practical impact can be observed by decreasing their eigenvalues, in this case, the convergence rate of the estimation error could be increased, and vice versa when their eigenvalues are increased. In addition, the parameter matrices $\mathcal{K}_0^1$, $\mathcal{K}_0^2$ and $\mathcal{K}_0^3$ in Zhang et al., 2018 are similar to the matrices $L_1^{1_2}$, $L_2^{1_2}$ and $L_3^{1_2}$. In order to ensure a fair comparison between methods, the same values for these matrices are used as shown in Table (5.1).*

By looking at Figure (5.1) and Table (5.2), the feasibility fields achieved by Problem

1 (172 solutions, 07.02%) and Problem 2 (203 solutions, 08.28%) in Han et al., 2022 are fully included in the one provided by the proposed Theorem (1) (2451 solutions, 97.35%), which in turn includes the one obtained by Theorem 1 in Zhang et al., 2018 (984 solutions, 40.15%), except for six points.

Indeed, although the LMI conditions in Zhang et al., 2018 were developed thanks to multiple Lyapunov function, it remains that the condition proposed in this paper ($P_{j^+} < \mu P_j$) to satisfy an average dwell time constraint and to ensure the decreasing of the Lyapunov function at the switching instants of the observer is very conservative, especially when we have a looped switching sequence. Another potential source of conservatism is the matrix rank preconditions that have been formulated in Zhang et al., 2018. The matrix C is assumed of full row rank. Similarly, the matrices E_{ij}^0, F_s^0, $\begin{bmatrix} \bar{T}^j \\ C \end{bmatrix}$, CE_{ij}^0 are assumed to be of full column rank.

Furthermore, the conservatism of LMI-based conditions proposed in Han et al., 2022 lies in using a common Lyapunov function for every switching modes, especially when the switched nonlinear systems involves several subsystems with different dynamics. To this should be added the conservatism caused by the condition (41) in Han et al., 2022, which is introduced to approximate the equality constraint (32). As indicated in remark (14), several tests we carried out on the scalar s have demonstrated its effect on the conservatism of the approaches proposed in this paper. In a manner similar to that proposed in Zhang et al., 2018, the design method presented in Han et al., 2022 set out a number of assumptions, namely the matrices G_σ^1, G_σ^2, F_s^0 and CG_σ^1 are assumed to be of full column rank.

In against part, it is clear that our proposal is much less conservative because the proposed LMI-based conditions are developed thanks to multiple Lyapunov function and requires a limited number of assumptions, namely the matrix F_s^0 should be of full column rank. Likewise, the proposed approach is performed on the basis of some relaxation techniques such as, Peaucelle's lemma (Peaucelle et al., 2000), Tuan's lemma (Tuan et al., 2001) and quadratic constraints approach (Açıkmeşe and Corless, 2011) to cope with the conservatism. Indeed, our relaxed LMI conditions involve more free decision variables in order to provide a greater degree of freedom for convex optimization algorithms (solvers). However, this leads to more computational complexity. Table (5.2) compares the computational complexity of the proposed LMI conditions and the ones formulated in (Zhang et al., 2018, Han et al., 2022), and provides the number $\mathcal{N}_d$ of decision variables, the number $\mathcal{N}_c$ of conditions, and the size of the LMI rows. As can be observed in the Table (5.2), the computational complexity of our method are higher than of the Problem. 1 and Problem. 2 in Han et al., 2022, and are less than that of Theorem. 1 in Zhang et al., 2018 , especially for $\mathcal{N}_d$. Consequently, although the application of several relaxation techniques, the computational complexity of our

design approach remains reasonable due to the N-TS modeling approach that has prevented from the explosion in the number $\mathcal{N}_c$ of LMI conditions by reducing the number of vertices involved in these conditions. Moreover, the computational complexity of our proposal does not represent a great disadvantage since this computation is done off-line.

Table 5.2: Computational complexity of the different studies.

Method	Feasibility	SZ. of LMI	$\mathcal{N}_c$	$\mathcal{N}_d$
Theorem. 1 in Zhang et al., 2018	40.15%	sz.(40)=6 × 6, sz.(41)=10 × 10 and 4 × 4	75	685
Problem. 1 in Han et al., 2022	07.02%	sz.(31)=4 × 4 and sz.(41)=8 × 8	25	238
Problem. 2 in Han et al., 2022	08.28%	sz.(31)=4 × 4, sz.(38)=6 × 6 and sz.(41)=8 × 8	37	238
The. 1 in this paper	97.47%	sz.(5.35)=25 × 25, sz.(5.37)=6 × 6	88	484

For the purpose of testing the performance of the proposed design approach, let us consider the specific case of $a = 0$ and $b = 0$. Let the δQC constraints (see Assumption 5.5) be set as $\Xi_{i_j}^{11} = 0.2$, $\Xi_{i_j}^{22} = -1$. Using YALMIP and SeDuMi in Matlab (Labit et al., 2002) to solve the optimization problem (5.29) defined in Theorem 1, we obtain a minimized H_∞ performance index of $\gamma = 2.6771$ and the switched N-TS observer gain matrices given by:

$$K_{1_1} = \begin{bmatrix} 115.2 & -2.4 \\ 264.9 & -0.6 \\ -40.2 & 8.2 \\ 1463.0 & -5.8 \\ 39.6 & 7.5 \end{bmatrix}, \quad K_{1_2} = \begin{bmatrix} 115.7 & -2.4 \\ 264.7 & -0.6 \\ -40.9 & 7.3 \\ 1473.9 & -7.6 \\ 39.3 & 4.6 \end{bmatrix}, \quad K_{1_3} = \begin{bmatrix} 115.4 & -2.3 \\ 265.4 & -0.4 \\ -41.3 & 8.0 \\ 1467.1 & -8.6 \\ 38.3 & 5.2 \end{bmatrix},$$

$$K_{2_1} = \begin{bmatrix} 115.2 & -2.4 \\ 265.0 & -0.6 \\ -40.2 & 8.2 \\ 1463.2 & -5.8 \\ 39.7 & 7.5 \end{bmatrix}, \quad K_{2_2} = \begin{bmatrix} 115.5 & -2.3 \\ 265.0 & -0.6 \\ -40.9 & 7.3 \\ 1475.0 & -7.5 \\ 39.3 & 4.6 \end{bmatrix}, \quad K_{2_3} = \begin{bmatrix} 115.3 & -2.3 \\ 265.4 & -0.4 \\ -41.3 & 8.0 \\ 1467.2 & -8.6 \\ 38.3 & 5.2 \end{bmatrix}.$$

and the Lyapunov matrices are given as:

$$P_1 = \begin{bmatrix} 0.1111 & 0.0001 & 0 & 0 & 0 \\ 0.0001 & 0.1585 & 0.0031 & -0.0284 & -0.0016 \\ 0 & 0.0031 & 1.4360 & 0.0183 & 0.7346 \\ 0 & -0.0284 & 0.0183 & 0.0155 & -0.0102 \\ 0 & -0.0016 & 0.7346 & -0.0102 & 1.1177 \end{bmatrix},$$

$$P_2 = \begin{bmatrix} 0.1111 & 0.0012 & 0 & 0 & 0 \\ 0.0012 & 0.1585 & 0.0005 & -0.0282 & -0.0043 \\ 0 & 0.0005 & 1.7254 & 0.0193 & 1.0431 \\ 0 & -0.0282 & 0.0193 & 0.0154 & -0.0093 \\ 0 & -0.0043 & 1.0431 & -0.0093 & 1.4453 \end{bmatrix},$$

$$P_3 = \begin{bmatrix} 0.1111 & 0.0010 & 0 & 0 & 0 \\ 0.0010 & 0.1585 & -0.0024 & -0.0284 & -0.0072 \\ 0 & -0.0024 & 1.5930 & 0.0205 & 0.9209 \\ 0 & -0.0284 & 0.0205 & 0.0155 & -0.0080 \\ 0 & -0.0072 & 0.9209 & -0.0080 & 1.3332 \end{bmatrix}.$$

As already assumed above, the nonlinear switched systems are switching according

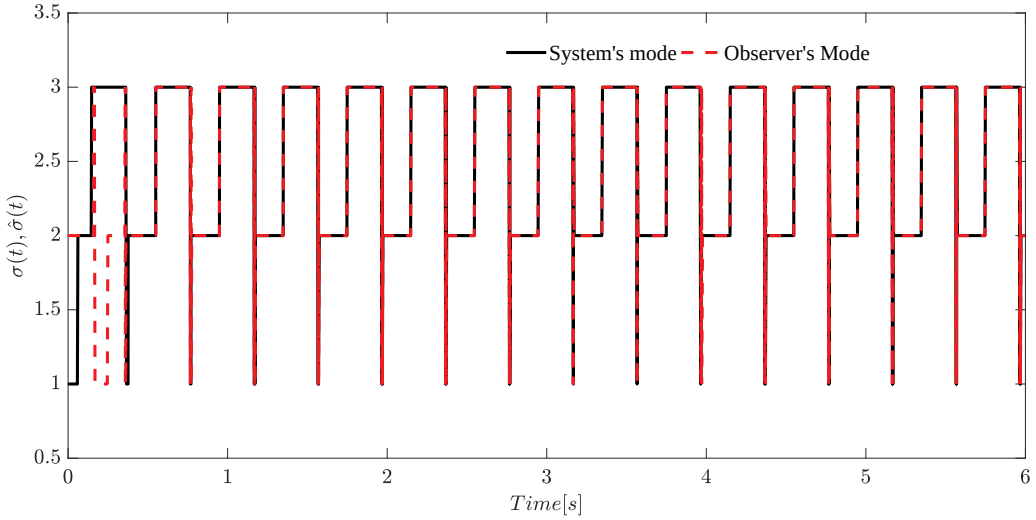

Figure 5.2: Progression of the switched modes of the nonlinear system and the designed observer (numerical example).

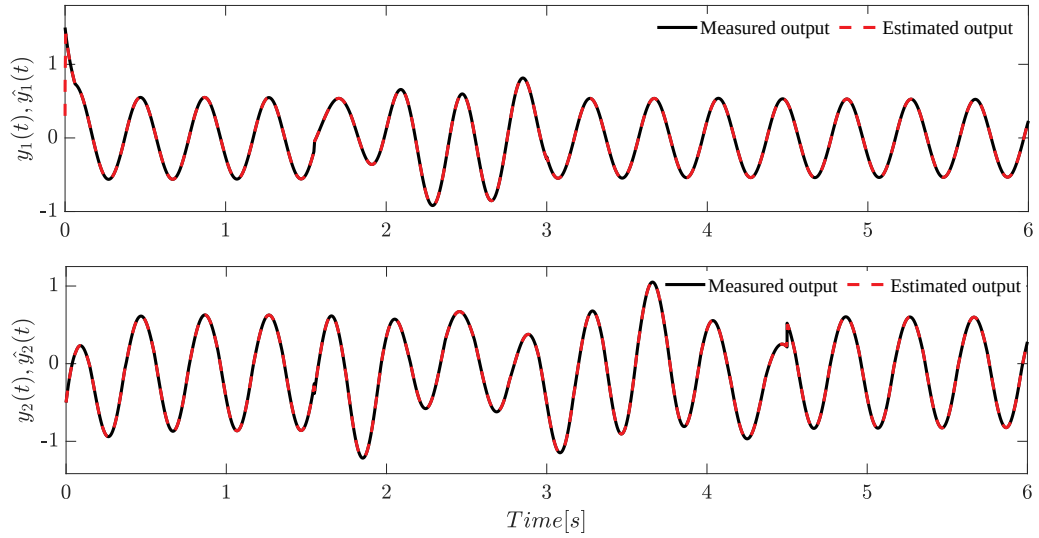

Figure 5.3: Evolution of the output estimation (numerical example).

to state-dependent hyper-planes S_{jj^+}, while the N-TS observers are switching according to the estimated hyper-planes $\hat{S}_{\hat{j}\hat{j}^+}$, depending on the estimated states. For simulation purpose, the considered hyper-planes (5.3) are given as: $S_{12} = \begin{bmatrix} -1 & 2 & -2 \end{bmatrix}$, $S_{23} = \begin{bmatrix} -1.5 & 6 & -1 \end{bmatrix}$ and $S_{31} = \begin{bmatrix} -2 & 5 & -1 \end{bmatrix}$. Moreover, given that all the aforementioned bibliography have considered the synchronous initialization between the systems and the observers, we aims in the sequel to illustrate the effectiveness of our switched observers to deal with asynchronous initialization of the switching modes. For this purpose, the switching modes of the system and the observer have been initialized as follows: ($j_{t=0} = 2$ and $\hat{j}_{t=0} = 1$) with their respective initial conditions $x(0) = \begin{bmatrix} 1.5 & 0 & -0.5 \end{bmatrix}^T$ and $z(0) = \begin{bmatrix} -1.2 & 0 & 0 & 0 & 0 \end{bmatrix}^T$.

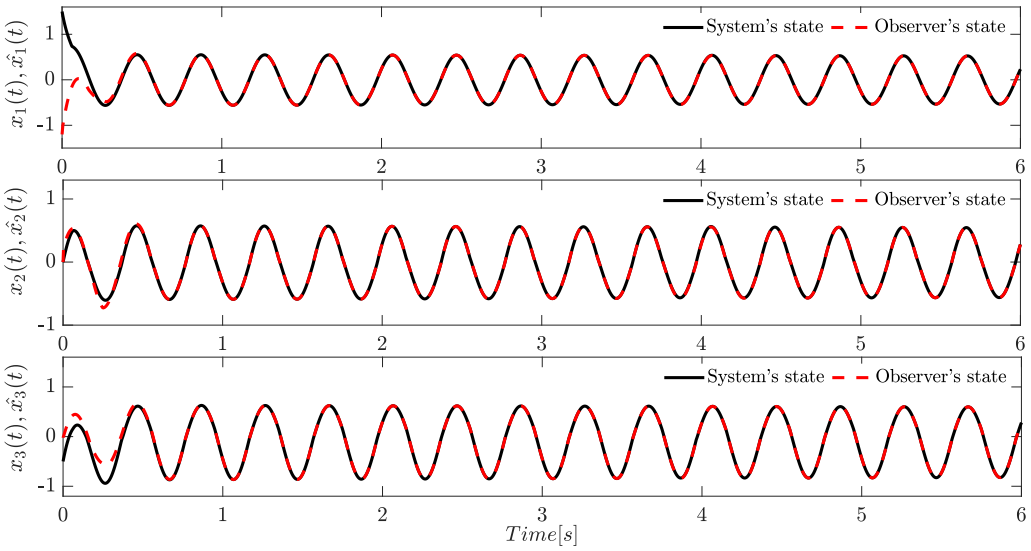

Figure 5.4: Evolution of the state vector estimation (numerical example).

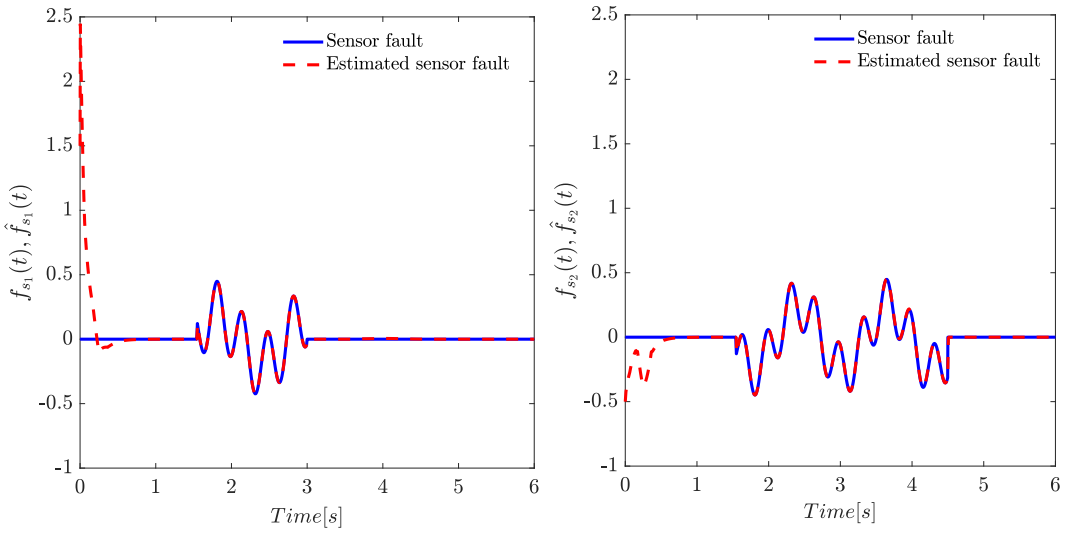

Figure 5.5: Evolution of the sensor faults estimation (numerical example).

To perform the simulation, assume that the input vector, the disturbance and the sensor faults are defined as:

$$u(t) = 10\cos(5\pi t)\, e^{-0.01t} \quad 0 \leq t \leq 6 \tag{5.71}$$

$$\begin{cases} d(t) = 0.5 & 3.6 < t \leq 4.2 \\ d(t) = 0 & \text{otherwise} \end{cases} \tag{5.72}$$

$$\begin{cases} f_{s_1}(t) = 0.2\sin(1.6\pi t - 20) + 0.25\sin(6\pi t - 20) & 1.5 < t \leq 3 \\ f_{s_1}(t) = 0 & \text{otherwise} \end{cases} \tag{5.73}$$

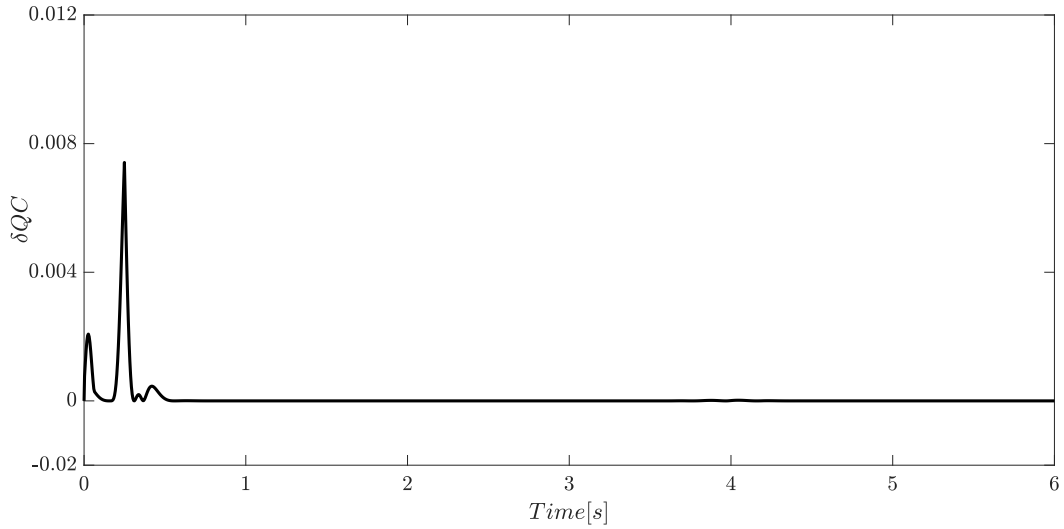

Figure 5.6: Evolution of the δQC constraint (numerical example).

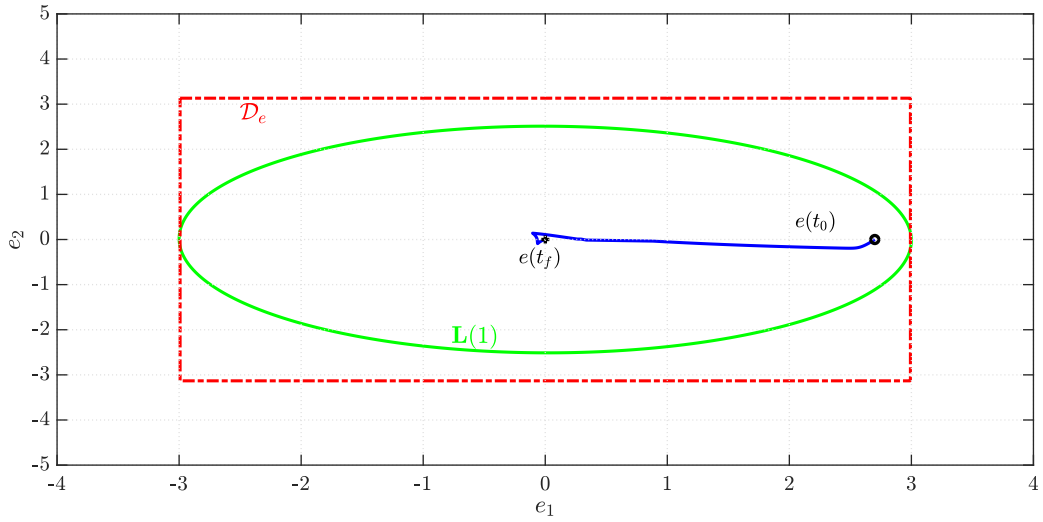

Figure 5.7: The estimate of the state error domain of attraction $\mathbf{L}(1)$ (green line), the state error domain of attraction $\mathcal{D}_e$ (red dashed-lines), state error trajectories (blue line) (numerical example).

$$\begin{cases} f_{s_2}(t) = -0.25\sin(1.6\pi t - 20) - 0.25\sin(6\pi t - 20) & 1.5 < t \leq 3 \\ f_{s_2}(t) = 0 & \text{otherwise} \end{cases} \tag{5.74}$$

As a reminder, the proposed design approach do not require any bounds concerning the sensor faults and their derivatives, which enlarges its practicability for the case of systems with fast time varying and unbounded faults.

By looking at Figure (5.2), the asynchronous switching behavior can be easily observed between the switched observers and the switched nonlinear systems. Moreover, the asynchronous switched N-TS observer is properly estimating the states vector and the sensor fault vector as illustrated in Figures (5.3)-(5.4) and 5.5. To conclude this

example, a verification post-simulation is necessary to know that the gamma-level attenuation is fulfilled. Hence, an approximation of the effective disturbance attenuation level can be calculated as:

$$\sqrt{\frac{\int_0^{t_f} e^T(t)\mathcal{W}e(t)dt}{\int_0^{t_f} \bar{d}^T(t)\Omega\bar{d}(t)dt}} = 0.0385 \tag{5.75}$$

which is lower than $\gamma = 2.6771$ obtained from Theorem (1). Once again, this confirms the effectiveness of the proposed design approach. Moreover, the evolution of the δQC function, formulated in (5.44), is positive as illustrated in Figure (5.6), which demonstrates that the δQC constraint is verified.

At last, Figure 5.7 presents the estimate $\mathbf{L}(1)$ of the state error domain of attraction $\mathcal{D}_e$. It is easy to observe that the state error trajectory remain in $\mathbf{L}(1)$.

5.4.2 Illustrative example

Consider the switched mass-spring system presented in Figure 5.8, drawn inspiration from (Zhang et al., 2015, Ren et al., 2018, Chekakta et al., 2023), where $x_1(t)$ and $x_2(t)$ denotes the position of the masses $m_1 = 6\,kg$ and $m_2 = 1\,kg$, respectively; c is the viscous friction coefficient between the masses and the horizontal surface; $u(t)$ is input vector and $d(t)$ is L_2-norm bounded exogenous disturbance input; The stiffness of the left spring k_c is constant, while the spring stiffness $k_{\sigma(t)}$ is assumed to automatically switch between two values k_1 and k_2 according to switching hyper-planes. Similar to Chekakta et al., 2023.

$$\text{For } \sigma(t) = \{1, 2\} : \begin{cases} m_1\ddot{x}_1(t) + c\dot{x}_1(t) - k_{\sigma(t)}x_2(t) + (k_c + k_{\sigma(t)})x_1(t) = u(t) + d(t) \\ m_2\ddot{x}_2(t) + c\dot{x}_2(t) - k_{\sigma(t)}x_1(t) + k_{\sigma(t)}x_2(t) = d(t) \end{cases} \tag{5.76}$$

Assume that the hardening springs in the considered system are modelled as in Khalil, 2002:

$$k_c = \kappa_c\left(1 + a_c^2x_1^2(t)\right) \text{ and } k_{\sigma(t)} = \kappa_{\sigma(t)}\left(1 + a_{\sigma(t)}^2x_2^2(t)\right), \text{ for } \sigma(t) \in \{1, 2\}. \tag{5.77}$$

where $\kappa_c = 10\,N/m$, $\kappa_1 = 10\,N/m$ and $\kappa_2 = 20\,N/m$ are the nominal springs' stiffness; $a_c = 0.4$, $a_1 = 0.1$ and $a_2 = 0.2$ are the spring's hardening coefficients.

Assuming that $x_2(t)$ is unmeasured variable, and $x_1(t) \in [-2, 2]$ and $x_2(t) \in [-1, 1]$, the switched nonlinear mass-spring system can be formulated as N-TS switched systems according to the equation(5.8) with $\sigma(t) \in \{1, 2\}$. So, the vertices defined by the matrices:

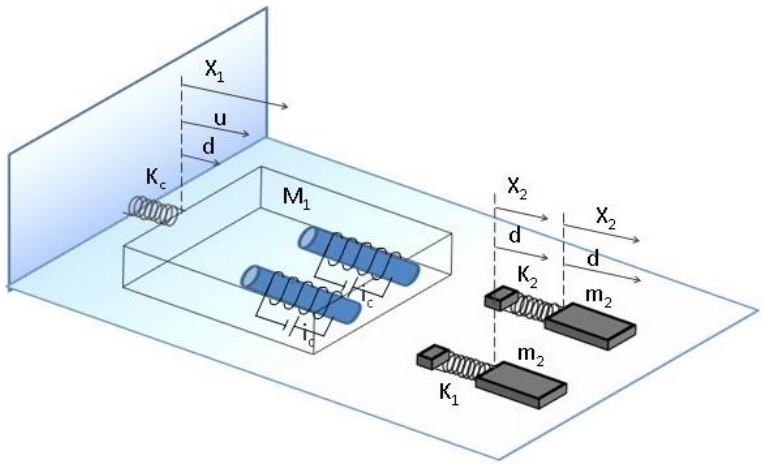

Figure 5.8: Switched mass-spring system.

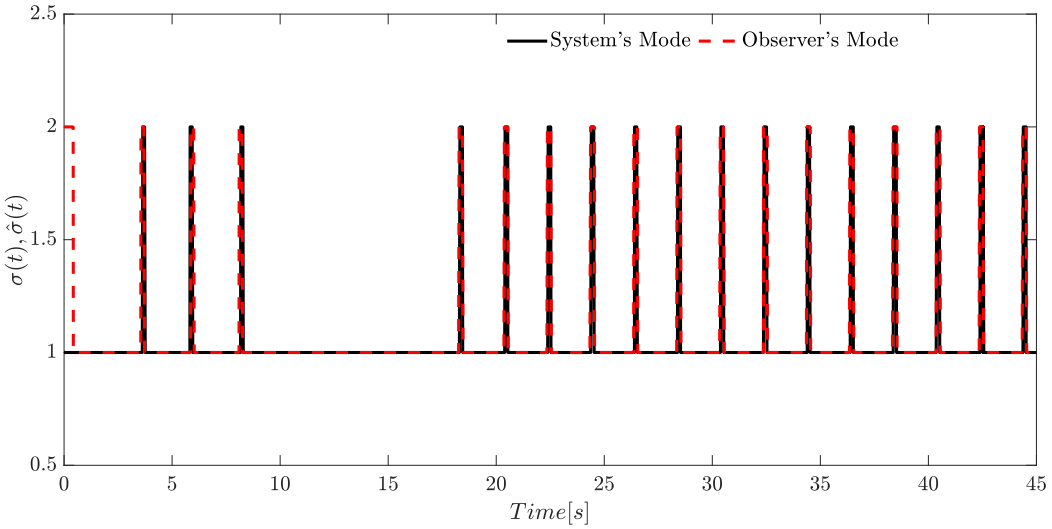

Figure 5.9: Progression of the switched modes of the nonlinear system and the designed observer (illustrative example).

$$A^0_{1_j} = \begin{bmatrix} 0 & 0 & 1 & 0 \\ 0 & 0 & 0 & 1 \\ -\frac{\kappa_c}{m_1}\left(1+4a_c^2\right)+\frac{\kappa_j}{m_1}\left(a_j^2-1\right) & \frac{\kappa_j}{m_1}\left(1-a_j^2\right) & -\frac{c}{m_1} & 0 \\ \frac{\kappa_j}{m_2}\left(1-a_j^2\right) & \frac{\kappa_j}{m_2}\left(a_j^2-1\right) & 0 & -\frac{c}{m_2} \end{bmatrix}, B^0_{1_j} = B^0_{2_j} = \begin{bmatrix} 0 \\ 0 \\ \frac{1}{m_1} \\ 0 \end{bmatrix},$$

$$E^0_{1_j} = E^0_{2_j} = \begin{bmatrix} 0 \\ 0 \\ \frac{1}{m_1} \\ \frac{1}{m_2} \end{bmatrix}, A^0_{2_j} = \begin{bmatrix} 0 & 0 & 1 & 0 \\ 0 & 0 & 0 & 1 \\ -\frac{\kappa_c}{m_1}+\frac{\kappa_j}{m_1}\left(a_j^2-1\right) & \frac{\kappa_j}{m_1}\left(1-a_j^2\right) & -\frac{c}{m_1} & 0 \\ \frac{\kappa_j}{m_2}\left(1-a_j^2\right) & \frac{\kappa_j}{m_2}\left(a_j^2-1\right) & 0 & -\frac{c}{m_2} \end{bmatrix}, H^0_{1_j} = H^0_{2_j} = \begin{bmatrix} 0 \\ 0 \\ \frac{\kappa_j}{m_1}a_j^2 \\ -\frac{\kappa_j}{m_2}a_j^2 \end{bmatrix},$$

$$C = \begin{bmatrix} 1 & 0 & 0 & 0 \\ 0 & 0 & 1 & 0 \end{bmatrix}, F^0_s = \begin{bmatrix} 1 & 0 \\ 0 & 1 \end{bmatrix}.$$

The nonlinear consequent part $\Phi(x(t)) = \bar{\Phi}(x(t)) + Ux(t) \in \text{co}\{0, 2Ux(t)\}$, where $\bar{\Phi}(x(t)) = x_2^3(t) - x_2^2(t)x_1(t) = \begin{bmatrix} -x_2^2(t) & x_2^2(t) \end{bmatrix} \begin{bmatrix} x_1(t) \\ x_2(t) \end{bmatrix} \in \text{co}\{-Ux(t), Ux(t)\}$ with

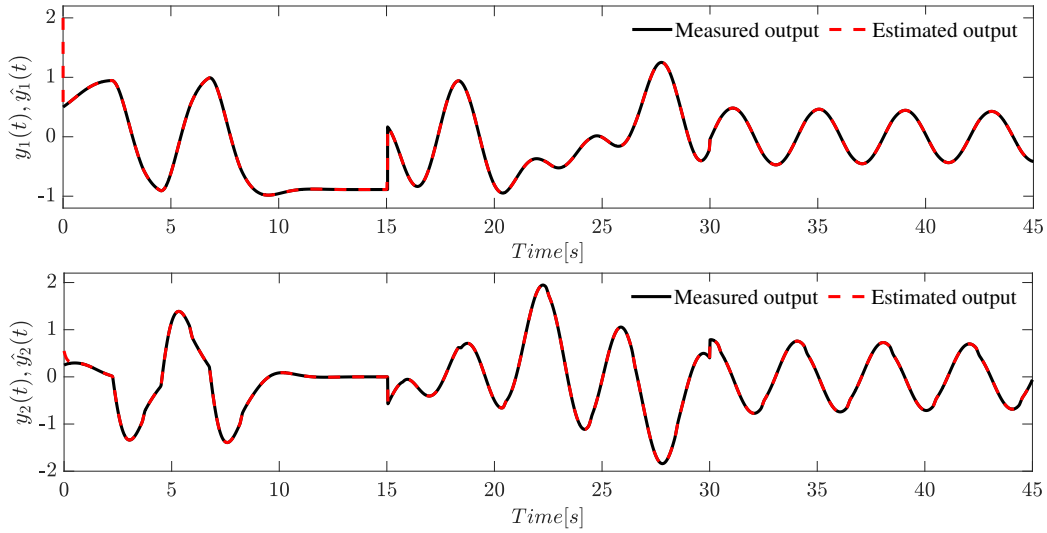

Figure 5.10: Evolution of the output estimation (illustrative example).

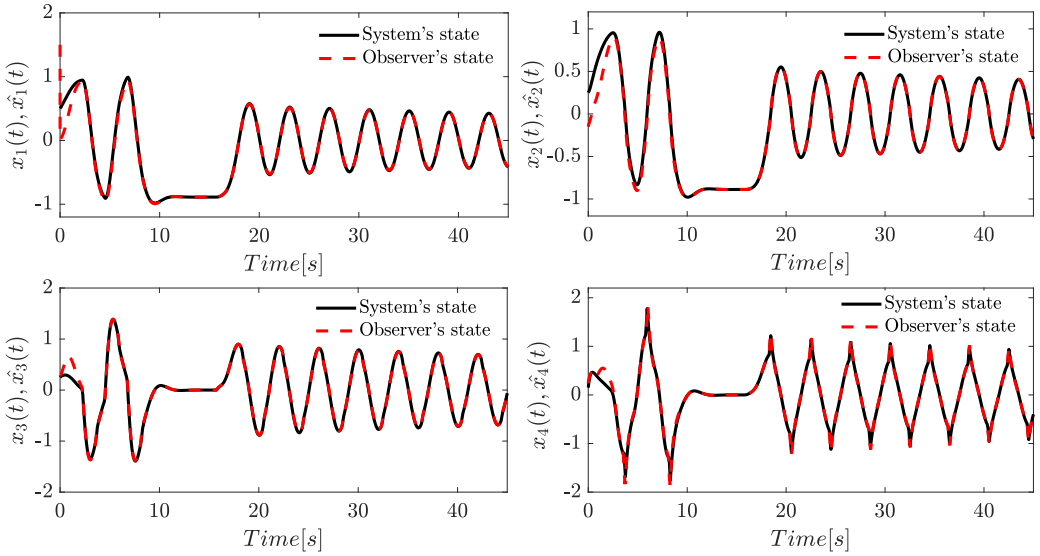

Figure 5.11: Evolution of the state vector estimation (illustrative example).

$U = \begin{bmatrix} -1 & 1 & 0 & 0 \end{bmatrix}$.

Moreover, the membership functions are:

$$h_{1_j}(x_1(t) = \frac{x_1^2(t)}{4} \text{ and } h_{2_j}(x_1(t) = \frac{4 - x_1^2(t)}{4} \text{ where } h_{1_j}(x_1(t)) + h_{2_j}(x_1(t)) = 1, \forall j \in \{1, 2\} \tag{5.78}$$

The validity domain $\mathcal{D}_x$ in (5.7) can be defined with:

$$\zeta = \begin{bmatrix} 1 & 0 & 0 & 0 \\ -1 & 0 & 0 & 0 \\ 0 & 1 & 0 & 0 \\ 0 & -1 & 0 & 0 \end{bmatrix} \text{ and } \mathcal{Q} = \begin{bmatrix} 2 \\ 2 \\ 1 \\ 1 \end{bmatrix}. \tag{5.79}$$

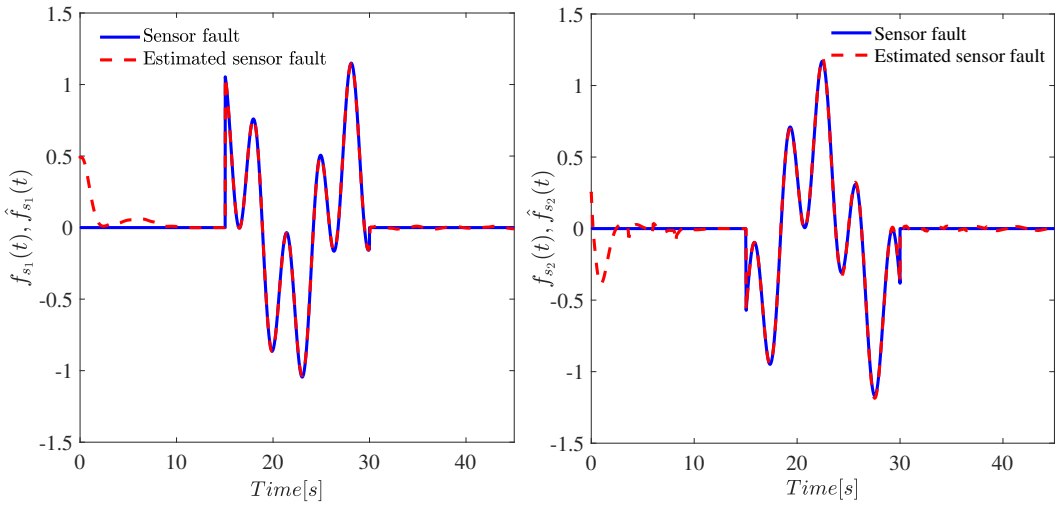

Figure 5.12: Evolution of the sensor faults estimation (illustrative example).

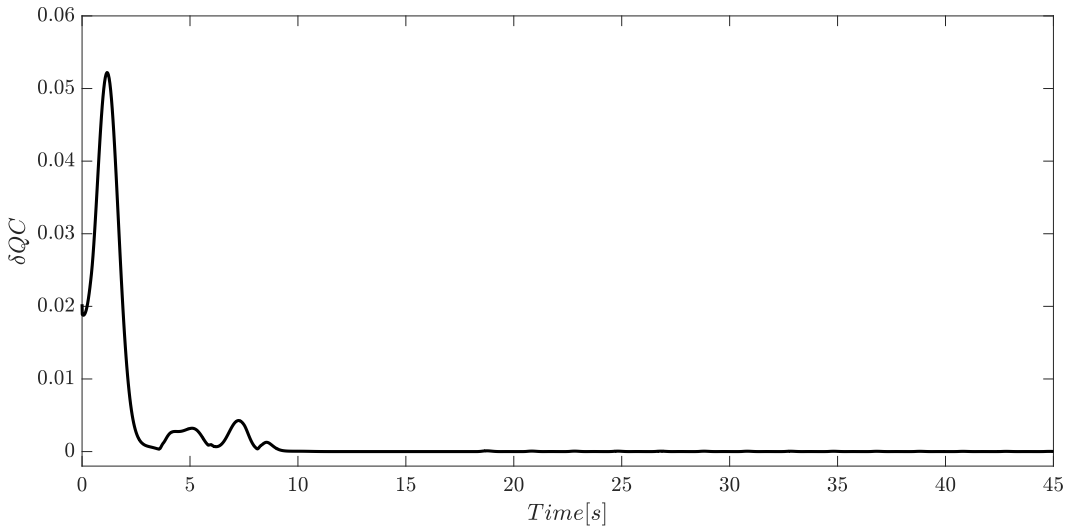

Figure 5.13: Evolution of the δQC constraint (illustrative example).

So, the validity domain $\mathcal{D}_{\bar{x}}$ of the extended switched N-TS systems defined in (5.9) with $\bar{\zeta} = \begin{bmatrix} 1 & 0 & 0 & 0 & 0 & 0 \\ -1 & 0 & 0 & 0 & 0 & 0 \\ 0 & 1 & 0 & 0 & 0 & 0 \\ 0 & -1 & 0 & 0 & 0 & 0 \end{bmatrix}$.

Following the steps 2, 3 and 4 of the Algorithm (1), let us consider the matrices $L_j^{1_2}$ (arbitrary nonsingular matrices) as follows:

$$L_j^{1_2} = \begin{bmatrix} 0.3 & 0 \\ 0 & 0.3 \end{bmatrix} \text{ with } j \in \{1, 2\} \tag{5.80}$$

So, the parameter matrices of the switched N-TS observers can be constructed as:

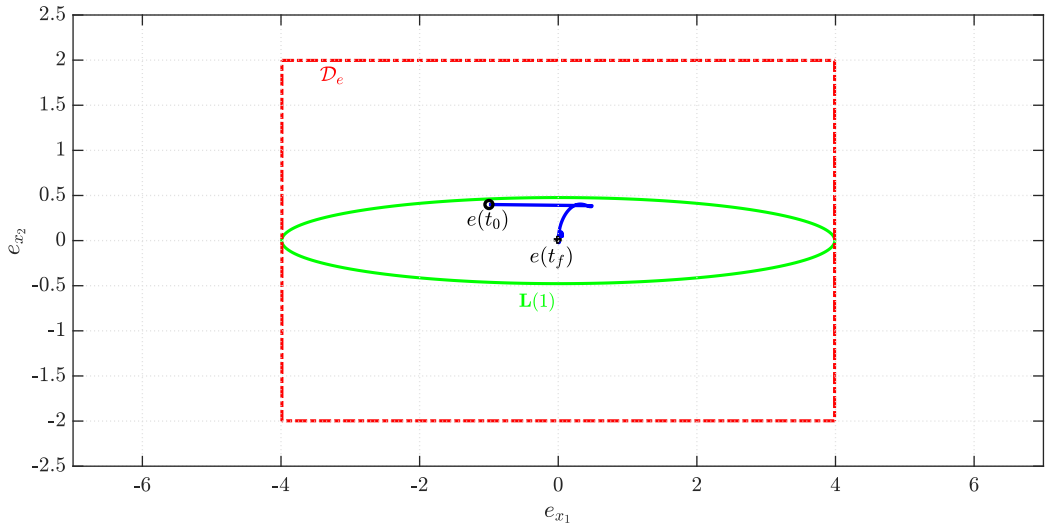

Figure 5.14: The estimate of the state error domain of attraction $\mathbf{L}(1)$ (green line), the state error domain of attraction $\mathcal{D}_e$ (red dashed-lines), state error trajectories (blue line) (illustrative example).

$$A_{2_1}^2 = \begin{bmatrix} 0 & 0 & 1 & 0 & 0 & 0 \\ 0 & 0 & 0 & 1 & 0 & 0 \\ -3.32 & 1.65 & -0.83 & 0 & 0 & 0 \\ 9.90 & -9.90 & 0 & -5 & 0 & 0 \\ -3.33 & 0 & -1 & 0 & -3.33 & 0 \\ 3.32 & -1.65 & -2.50 & 0 & 0 & -3.33 \end{bmatrix}, H_{i_1}^2 = \begin{bmatrix} 0 \\ 0 \\ 0.0167 \\ -0.1000 \\ 0 \\ -0.0167 \end{bmatrix}, H_{i_2}^2 = \begin{bmatrix} 0 \\ 0 \\ 0.1333 \\ -0.8000 \\ 0 \\ -0.1333 \end{bmatrix},$$

$$B_{i_j}^2 = \begin{bmatrix} 0 \\ 0 \\ 0.1667 \\ 0 \\ 0 \\ -0.1667 \end{bmatrix}$$

$$A_{1_1}^2 = \begin{bmatrix} 0 & 0 & 1 & 0 & 0 & 0 \\ 0 & 0 & 0 & 1 & 0 & 0 \\ -4.38 & 1.65 & -0.83 & 0 & 0 & 0 \\ 9.90 & -9.90 & 0 & -5 & 0 & 0 \\ -3.33 & 0 & -1 & 0 & -3.33 & 0 \\ 4.38 & -1.65 & -2.50 & 0 & 0 & -3.33 \end{bmatrix}$$

$$F_{s_1}^3 = F_{s_2}^3 = \begin{bmatrix} 0 & 0 \\ 0 & 0 \\ 0 & 0 \\ 0 & 0 \\ 3.3333 & 0 \\ 0 & 3.3333 \end{bmatrix}, A_{2_2}^2 = \begin{bmatrix} 0 & 0 & 1 & 0 & 0 & 0 \\ 0 & 0 & 0 & 1 & 0 & 0 \\ -4.87 & 3.20 & -0.83 & 0 & 0 & 0 \\ 19.20 & -19.20 & 0 & -5 & 0 & 0 \\ -3.33 & 0 & -1 & 0 & -3.33 & 0 \\ 4.87 & -3.20 & -2.50 & 0 & 0 & -3.33 \end{bmatrix}$$

$$A_{1_2}^2 = \begin{bmatrix} 0 & 0 & 1 & 0 & 0 & 0 \\ 0 & 0 & 0 & 1 & 0 & 0 \\ -5.93 & 3.20 & -0.83 & 0 & 0 & 0 \\ 19.20 & -19.20 & 0 & -5 & 0 & 0 \\ -3.33 & 0 & -1 & 0 & -3.33 & 0 \\ 5.93 & -3.20 & -2.50 & 0 & 0 & -3.33 \end{bmatrix}.$$

For simulation purpose, let the δQC constraints (see Assumption 5.5) be set as $\Xi_{ij}^{11} = 0.9$, $\Xi_{ij}^{22} = -1$. Using YALMIP and SeDuMi in Matlab Labit et al., 2002 to solve the optimization problem (5.29) defined in Theorem 1, we obtain a minimized H_∞ performance index of $\gamma = 9.0676$ and the switched N-TS observer gain matrices given by: $K_{1_1} = \begin{bmatrix} 9845.0 & 70.5 \\ -88.5 & -0.6 \\ 50.1 & 4.0 \\ 71.5 & 1.5 \\ 96.2 & 0.2 \\ -50.1 & 0.8 \end{bmatrix}$, $K_{1_2} = \begin{bmatrix} 9845.2 & 211.7 \\ -88.7 & -1.8 \\ 49.9 & 4.8 \\ 71.8 & 2.3 \\ 96.2 & 1.7 \\ -50.1 & 0 \end{bmatrix}$, $K_{2_1} = \begin{bmatrix} 9845.7 & 70.6 \\ -88.5 & -0.6 \\ 50.1 & 4.0 \\ 71.5 & 1.5 \\ 96.2 & 0.2 \\ -50.1 & 0.8 \end{bmatrix}$,

$$K_{2_2} = \begin{bmatrix} 9844.9 & 70.4 \\ -88.7 & -0.6 \\ 50.0 & 4.0 \\ 71.8 & 1.5 \\ 96.2 & 0.2 \\ -50.0 & 0.8 \end{bmatrix}.$$

and the Lyapunov matrices are given as:

$$P_1 = \begin{bmatrix} 0.0628 & -0.0001 & 0 & 0 & 0.0006 & 0 \\ -0.0001 & 4.3923 & 0.5608 & 0.3930 & 3.0004 & -0.6400 \\ 0 & 0.5608 & 76.7176 & 0.0352 & -0.1655 & 75.5481 \\ 0 & 0.3930 & 0.0352 & 0.2058 & 0.1680 & -0.0825 \\ 0.0006 & 3.0004 & -0.1655 & 0.1680 & 8.8234 & 0.1235 \\ 0 & -0.6400 & 75.5481 & -0.0825 & 0.1235 & 76.7278 \end{bmatrix},$$

$$P_2 = \begin{bmatrix} 0.0628 & 0 & 0 & 0 & 0.0007 & 0 \\ 0 & 4.3923 & 0.5586 & 0.3930 & 3.0005 & -0.6422 \\ 0 & 0.5586 & 76.7179 & 0.0351 & -0.1646 & 75.5472 \\ 0 & 0.3930 & 0.0351 & 0.2058 & 0.1680 & -0.0825 \\ 0.0007 & 3.0005 & -0.1646 & 0.1680 & 8.8235 & 0.1243 \\ 0 & -0.6422 & 75.5472 & -0.0825 & 0.1243 & 76.7256 \end{bmatrix}.$$

Furthermore, let us assume that the switched mass-spring system switches according to the hyper-planes (5.3) with $S_{12} = \begin{bmatrix} 1 & 0 & 0.1 & 0 \end{bmatrix}$ and $S_{21} = \begin{bmatrix} 1 & 0 & -0.1 & 0 \end{bmatrix}$. So, to shed light on the asynchronous behavior caused by mismatching switching hyper-planes, the observer switches according to different hyper-planes (5.3) with $\hat{S}_{12} = \begin{bmatrix} 2.1 & 0 & 0.35 & 0 \end{bmatrix}$ and $\hat{S}_{21} = \begin{bmatrix} 2.8 & 0 & -0.3 & 0 \end{bmatrix}$. Moreover, the case of asynchronous initialization is also considered in this example. For this purpose, the initial conditions are tuned as: $x(0) = \begin{bmatrix} 0.5 & 0.25 & 0.25 & 15 \end{bmatrix}^T$ and $z(0) = \begin{bmatrix} 1.5 & -0.15 & 0.3 & 0.25 & 0 & 0 \end{bmatrix}^T$, so that the system and the observer are respectively initialized in different modes, i.e.

$j_{t=0} = 1$ and $\hat{j}_{t=0} = 2$. To perform the simulation, assume that the input vector, the disturbance and the sensor faults are defined as:

$$\begin{cases} u(t) = 10 & 0 \leq t \leq 3.25 \text{ and } 4.5 < t \leq 6.75 \\ u(t) = -10 & 2.25 < t \leq 4.5 \text{ and } 6.75 < t \leq 15.75 \\ u(t) = -10\cos(0.5\pi t)e^{-0.01t} & 15.75 < t \leq 45 \end{cases} \tag{5.81}$$

$$\begin{cases} d(t) = 0.25 & 0 \leq t \leq 7.5 \\ d(t) = 0 & 7.5 < t \leq 45 \end{cases} \tag{5.82}$$

$$\begin{cases} f_{s_1}(t) = 0.6\sin(0.16\pi t) + 0.55\sin(0.6\pi t - 10) & 15 < t \leq 30 \\ f_{s_1}(t) = 0 & \text{otherwise} \end{cases} \tag{5.83}$$

$$\begin{cases} f_{s_2}(t) = -0.65\sin(0.16\pi t) - 0.55\sin(0.6\pi t - 10) & 15 < t \leq 30 \\ f_{s_2}(t) = 0 & \text{otherwise} \end{cases} \tag{5.84}$$

The simulation results are depicted in Figures 5.9-5.14. Figure 5.9 exhibits the progression of asynchronous switched modes of the system and the observer where the asynchronous behaviour can be clearly visualized. Figure 5.10 shows the measured outputs subject to faults and the estimated outputs. The trajectories of both states of the system and the observer are shown in Figure 5.11. The evolution of the sensor fault vector and its estimated are presented in Figure 5.12. As illustrated, the asynchronous switched N-TS observer is properly estimating the states vector and the sensor fault vector. Figure 5.13 confirms that the δQC constraints (5.44) is always fulfilled since it remains positive. The estimation of the domain of attraction $\mathcal{D}_e$ are illustrated in Figure 5.14, where it is easy to observe that the state error trajectory remain in $\mathbf{L}(1)$. Moreover, based on simulation results, for $t \in [0, t_f]$ with $t_f = 45s$, the estimation of the achieved disturbance attenuation level as:

$$\sqrt{\frac{\int_0^{t_f} e^T(t)\mathcal{W}e(t)dt}{\int_0^{t_f} \bar{d}^T(t)\Omega\bar{d}(t)dt}} = 0.0146 \tag{5.85}$$

which is lower than the obtained $\gamma = 9.0676$ obtained by solving Theorem 1.

In a nutshell, these simulations have demonstrated that the designed switched N-TS observer simultaneously estimate the sensor faults' and state's vector despite the switched asynchronous phenomena.

5.5 Conclusion

This chapter investigated the challenge of robust state and sensor fault estimation within a specific class of switched nonlinear Takagi-Sugeno (T-S) systems. These systems were characterized by inherent nonlinearities and subject to disturbances with bounded L_2 norms and mismatched switching laws.

To address this challenge, an asynchronous switched T-S fuzzy observers was proposed. These observers boast several key advantages. First, they exhibit robustness against uncontrolled switching sequences. This translates to reliable operation even when the switching between system modes is uncontrolled, follows an arbitrary pattern, or remains entirely unknown. Second, they can handle asynchronous initialization. In simpler terms, perfect synchronization between the system and observer at the outset is not required. They can begin in different modes, and the observer will still effectively estimate the state and sensor faults. Finally, these observers achieve enhanced estimation accuracy by utilizing an extended state vector and specific mathematical transformations.

The design process for these observers leveraged a candidate multiple Lyapunov function and incorporated H_∞ disturbance attenuation for enhanced robustness. This formulation translates into LMI conditions, offering significant advantages. Additionally, the approach eliminates dwell-time restrictions often present in prior works, providing greater flexibility in system design. Finally, the LMI conditions exhibit relaxed matrix rank preconditions compared to older methods, broadening the applicability of the observer design.

The effectiveness of the proposed observer design was rigorously evaluated through two comprehensive simulations. The first simulation focused on demonstrating the superiority of the proposed LMI-based conditions in reducing conservatism compared to existing methods, highlighting the efficiency of the proposed approach. The second simulation adopted a more practical approach, showcasing the observer's ability to accurately estimate state and sensor faults even in the face of external disturbances and mismatched switching sequences. This emphasizes the observer's robustness in real-world scenarios.

In conclusion, this chapter presented a novel and effective solution for robust state and sensor fault estimation in switched nonlinear T-S systems. The asynchronous switched T-S fuzzy observers offer several advantages, including the ability to handle uncontrolled switching sequences, asynchronous initialization, and external disturbances. These features make them a valuable tool for a wide range of applications.

Chapter 6

Conclusion and Future Outlook

THis dissertation investigated the design of an observer-based fault estimation scheme for a class of switched nonlinear systems. The work is presented in five chapters.

The **first chapter** provided a general introduction to the thesis, outlining its fundamental objectives, context, and significance. It also presented a summary of the key contributions made, highlighting their impact and relevance within the research domain. Additionally, this chapter offered a comprehensive overview of the thesis structure, detailing the organization of the subsequent chapters to guide the reader through the study's logical progression.

The **second chapter** established a firm foundation for the analysis and design of switched systems. It began with a comprehensive overview, introducing fundamental modeling concepts and illustrating them with well-chosen examples. Next, the chapter explored two key categorization schemes: switching mechanism (state-dependent or time-dependent) and control nature (autonomous or controlled). Following these classifications, the chapter addressed the crucial issue of stability analysis, presenting two primary approaches: arbitrary switching and constrained switching. Finally, it introduced observer design for switched systems, differentiating between synchronous and asynchronous observers relative to the system dynamics.

The **third chapter** provided a comprehensive foundation for T-S fuzzy multi-model systems. Core concepts were explored, along with various derivation methodologies, emphasizing the sector nonlinearity approach. Lyapunov function theory was employed to analyze system stability. This chapter addressed the critical challenge of state observer design for T-S systems. The impact of unmeasurable premise variables on observer design methodologies was meticulously examined, highlighting the resulting complexities. Finally, the chapter ventured into switched T-S fuzzy systems. Their structural characteristics were analyzed, and their application was demonstrated using a switched tunnel diode circuit example. The chapter concluded by emphasizing the specific challenges faced in observer design for switched T-S systems.

The **fourth chapter** embarked on a comprehensive exploration of fault diagnosis for nonlinear systems. It established a foundation with clear fault definitions and

a meticulous classification system, facilitating the development of effective diagnosis strategies. Subsequently, the chapter examined various approaches used for fault diagnosis, encompassing both model-free and model-based methods, along with their quantitative and qualitative subcategories.

The **fifth chapter** culminated in the introduction of a novel and effective solution for robust state and sensor fault estimation in switched nonlinear T-S systems. Asynchronous switched T-S fuzzy observers offer significant advantages, including the ability to handle uncontrolled switching sequences, asynchronous initialization, and external disturbances. These capabilities render them a valuable tool for a wide range of real-world applications.

The main contributions of this thesis were as follows:

- This work introduced a novel observer design approach based on H_∞ disturbance attenuation for a class of switched nonlinear systems. This approach overcame the limitations of observer matching conditions (OMCs), detectability constraints, and stringent matrix rank preconditions. Furthermore, it did not require prior knowledge of sensor fault bounds or their derivatives, making it more practical for switched systems subject to fast time-varying and unbounded faults.

- This research addressed the challenge of UPVs by proposing an alternative method to the traditional Lipschitz condition-based approach. The proposed method separated the measured and unmeasured nonlinearities of the switched system and applied Takagi-Sugeno (T-S) modeling techniques exclusively to the measured nonlinearities. This led to T-S multi-models with nonlinear consequent parts (N-TS), where the membership functions depended solely on measured premise variables. A key advantage of this approach was the reduction in the number of vertices involved in LMI-based conditions compared to classical T-S modeling methods, resulting in less conservative estimates and lower computational complexity.

- The third contribution established dwell-time-free conditions for the design of asynchronous switched observer-based fault estimation. Unlike most existing works, the proposed switched observers could handle unknown, arbitrary, or uncontrolled switching sequences while addressing the initialization problem, where the observer's switching mode might be asynchronous with that of the system.

- This work proposed an optimization procedure aimed at expanding Lyapunov level sets to estimate the domain of attraction more effectively.

- The final contribution focused on reducing the conservatism inherent in the proposed LMI conditions. By employing quadratic constraint methods to handle

nonlinear consequent parts and utilizing standard relaxation techniques, significant improvements in feasibility domains were achieved. These enhancements were compared with prior studies, demonstrating notable performance gains.

As future work, this dissertation paves the way for further exploration in several exciting directions:

- Adapting the observer design approach to address fault-tolerant control based on the reconstructed faults offers a promising avenue for future research. This would allow the system to maintain stable operation even in the presence of faults.
- Developing robust observer design methods that can handle modeling uncertainties and state/input constraints in switched nonlinear systems is crucial for practical applications. Real-world systems often experience these limitations.
- Extending the current work to deal with multiple time-varying delayed T-S fuzzy switched systems represents a significant advancement. This type of system is highly relevant for real-world applications where delays and multiple interacting subsystems are common.
- Implementing the proposed observer in a real experimental setup would provide valuable insights into its practical performance and limitations. This would bridge the gap between theoretical development and real-world application.

Bibliography

[1] Behçet Açıkmeşe and Martin Corless. Observers for systems with nonlinearities satisfying incremental quadratic constraints. *Automatica*, 47(7):1339–1348, 2011.

[2] Liron I Allerhand and Uri Shaked. Robust stability and stabilization of linear switched systems with dwell time. *IEEE Transactions on Automatic Control*, 56 (2):381–386, 2010.

[3] Sabrina Aouaouda, Mohammed Chadli, and Moussa Boukhnifer. Speed sensor fault tolerant controller design for induction motor drive in ev. *Neurocomputing*, 214:32–43, 2016.

[4] RV Beard. Fault accommodation in linear systems through self-reorganization. *Rep. Man-Vehicle Laboratory MVT-71*, 1, 1971.

[5] Djamel Eddine Chouaib Belkhiat. *Diagnostic d'une classe de systèmes linéaires à commutations: Approche à base d'observateurs robustes.* PhD thesis, 2011. Université de Reims Champagne-Ardennes, France.

[6] Djamel Eddine Chouaib Belkhiat, Dalel Jabri, Kevin Guelton, Noureddine Manamanni, and Issam Chekakta. Asynchronous switched observers design for switched takagi-sugeno systems subject to output disturbances. 2019.

[7] Stephen Boyd, Laurent El Ghaoui, Eric Feron, and Venkataramanan Balakrishnan. *Linear matrix inequalities in system and control theory.* SIAM, 1994.

[8] Michael S Branicky. Multiple lyapunov functions and other analysis tools for switched and hybrid systems. *IEEE Transactions on automatic control*, 43(4): 475–482, 1998.

[9] Issam Chekakta, Djamel EC Belkhiat, Kevin Guelton, Dalel Jabri, and Noureddine Manamanni. Asynchronous observer design for switched t-s systems with unmeasurable premises and switching mismatches. *Engineering Applications of Artificial Intelligence*, 104:104371, 2021.

[10] Issam Chekakta, Djamel EC Belkhiat, Koffi Motchon, Kevin Guelton, and Dalel Jabri. Synthèse de filtres h de type takagi-sugeno avec commutations asynchrones pour les systèmes non linéaires à commutations. In *Rencontres Francophones*

sur la Logique Floue et ses Applications (LFA 2021), pages 103–110. Cépaduès-éditions, 2021.

[11] Issam Chekakta, Djamel EC Belkhiat, Kevin Guelton, Koffi MD Motchon, and Dalel Jabri. Asynchronous switched takagi-sugeno h∞ filters design for switched nonlinear systems. *IFAC-PapersOnLine*, 55(1):351–356, 2022.

[12] Issam Chekakta, Dalel Jabri, KM Motchon, Kevin Guelton, and Djamel EC Belkhiat. Design of asynchronous switched ts model-based H_∞ filters with non-linear consequent parts for switched nonlinear systems. *International Journal of Adaptive Control and Signal Processing*, 2023.

[13] Bor-Sen Chen, Min-Yen Lee, Tzu-Han Lin, and Weihai Zhang. Robust state/fault estimation and fault-tolerant control in discrete-time t–s fuzzy systems: An embedded smoothing signal model approach. *IEEE Transactions on Cybernetics*, 52(7):6886–6900, 2021.

[14] Liheng Chen, Shasha Fu, Yuxin Zhao, Ming Liu, and Jianbin Qiu. State and fault observer design for switched systems via an adaptive fuzzy approach. *IEEE Transactions on Fuzzy Systems*, 28(9):2107–2118, 2019.

[15] Liheng Chen, Yongjie Tan, Yanzheng Zhu, and Hak-Keung Lam. Fault reconstruction for continuous-time switched nonlinear systems via adaptive fuzzy observer design. *IEEE Transactions on Fuzzy Systems*, 2023.

[16] Weitian Chen and S Mehrdad. Observer design for linear switched control systems. In *Proceedings of the 2004 American Control Conference*, volume 6, pages 5796–5801. IEEE, 2004.

[17] Xueqin Chen and Ming Liu. A two-stage extended kalman filter method for fault estimation of satellite attitude control systems. *Journal of the Franklin Institute*, 354(2):872–886, 2017.

[18] Francis H Clarke, Yu S Ledyaev, and Ronald J Stern. Asymptotic stability and smooth lyapunov functions. *Journal of differential Equations*, 149(1):69–114, 1998.

[19] Wijesuriya P Dayawansa and Clyde F Martin. A converse lyapunov theorem for a class of dynamical systems which undergo switching. *IEEE Transactions on Automatic control*, 44(4):751–760, 1999.

[20] Raymond A DeCarlo, Michael S Branicky, Stefan Pettersson, and Bengt Lennartson. Perspectives and results on the stability and stabilizability of hybrid systems. *Proceedings of the IEEE*, 88(7):1069–1082, 2000.

[21] Kürşad Derinkuyu and Mustafa Ç Pinar. On the S-procedure and some variants. *Mathematical Methods of Operations Research*, 64(1):55–77, 2006.

[22] Steven X Ding. *Advanced methods for fault diagnosis and fault-tolerant control*. Springer, 2021.

[23] Jiuxiang Dong, Youyi Wang, and Guang-Hong Yang. Control synthesis of continuous-time ts fuzzy systems with local nonlinear models. *IEEE Transactions on Systems, Man, and Cybernetics, Part B (Cybernetics)*, 39(5):1245–1258, 2009.

[24] Dongsheng Du and Vincent Cocquempot. Fault diagnosis and fault tolerant control for discrete-time linear systems with sensor fault. *IFAC-PapersOnLine*, 50(1):15754–15759, 2017.

[25] Lior Fainshil, Michael Margaliot, and Pavel Chigansky. On the stability of positive linear switched systems under arbitrary switching laws. *IEEE Transactions on Automatic Control*, 54(4):897–899, 2009.

[26] Shasha Fu, Jianbin Qiu, Liheng Chen, and Shaoshuai Mou. Adaptive fuzzy observer design for a class of switched nonlinear systems with actuator and sensor faults. *IEEE Transactions on Fuzzy Systems*, 26(6):3730–3742, 2018.

[27] Shasha Fu, Jianbin Qiu, Liheng Chen, and Mohammed Chadli. Adaptive fuzzy observer-based fault estimation for a class of nonlinear stochastic hybrid systems. *IEEE Transactions on Fuzzy Systems*, 30(1):39–51, 2020.

[28] Pascal Gahinet, Arkadii Nemirovskii, Alan J Laub, and Mahmoud Chilali. The lmi control toolbox. In *Proceedings of 1994 33rd IEEE conference on decision and control*, volume 3, pages 2038–2041. IEEE, 1994.

[29] Yosr Garbouj, Thach Ngoc Dinh, Talel Zouari, Moufida Ksouri, and Tarek Raïssi. Interval estimation of switched takagi-sugeno systems with unmeasurable premise variables. *IFAC-PapersOnLine*, 52(11):73–78, 2019.

[30] Komi Gasso, Gilles Mourot, and José Ragot. Identification of an output error takagi-sugeno model. In *Smc 2000 conference proceedings. 2000 ieee international conference on systems, man and cybernetics.'cybernetics evolving to systems, humans, organizations, and their complex interactions'(cat. no. 0*, volume 1, pages 14–19. IEEE, 2000.

[31] Kevin Guelton. *Estimation des caractéristiques du mouvement humain en station debout. Mise en œuvre d'observateurs flous sous forme descripteur*. PhD thesis, Université de Valenciennes et du Hainaut-Cambresis, 2003.

[32] Thierry Marie Guerra and Laurent Vermeiren. Lmi-based relaxed nonquadratic stabilization conditions for nonlinear systems in the takagi–sugeno's form. *Automatica*, 40(5):823–829, 2004.

[33] Hamed Habibi, Amirmehdi Yazdani, Mohamed Darouach, Hai Wang, Tyrone Fernando, and Ian Howard. Observer-based sensor fault tolerant control with prescribed tracking performance for a class of nonlinear systems. *IEEE Transactions on Automatic Control*, pages 1–8, 2023. doi: 10.1109/TAC.2023.3296494.

[34] Sigurdur Freyr Hafstein. A constructive converse lyapunov theorem on exponential stability. *Discrete and Continuous Dynamical Systems*, 10(3):657–678, 2004.

[35] Jian Han, Huaguang Zhang, Yingchun Wang, and Xiuhua Liu. Robust state/fault estimation and fault tolerant control for t–s fuzzy systems with sensor and actuator faults. *Journal of the Franklin Institute*, 353(2):615–641, 2016.

[36] Jian Han, Huaguang Zhang, Yingchun Wang, and Kun Zhang. Fault estimation and fault-tolerant control for switched fuzzy stochastic systems. *IEEE Transactions on Fuzzy Systems*, 26(5):2993–3003, 2018. doi: 10.1109/TFUZZ.2018.2799171.

[37] Jian Han, Xiuhua Liu, Xinjiang Wei, Xin Hu, and Huifeng Zhang. Reduced-order observer based fault estimation and fault-tolerant control for switched stochastic systems with actuator and sensor faults. *ISA Transactions*, 88:91–101, 2019. ISSN 0019-0578. doi: https://doi.org/10.1016/j.isatra.2018.11.045. URL https://www.sciencedirect.com/science/article/pii/S0019057818304890.

[38] Jian Han, Xiuhua Liu, Xinjiang Wei, and Xin Hu. Adaptive adjustable dimension observer based fault estimation for switched fuzzy systems with unmeasurable premise variables. *Fuzzy Sets and Systems*, 452:149–167, 2022. ISSN 0165-0114. doi: https://doi.org/10.1016/j.fss.2022.06.017. URL https://www.sciencedirect.com/science/article/pii/S0165011422002962.

[39] Jian Han, Xiuhua Liu, Xinjiang Wei, and Shaoxin Sun. A dynamic proportional-integral observer-based nonlinear fault-tolerant controller design for nonlinear system with partially unknown dynamic. *IEEE Transactions on Systems, Man, and Cybernetics: Systems*, 52(8):5092–5104, 2022. doi: 10.1109/TSMC.2021.3114326.

[40] Jian Han, Xiuhua Liu, Xiangpeng Xie, and Xinjiang Wei. Dynamic output feedback fault tolerant control for switched fuzzy systems with fast time varying and unbounded faults. *IEEE Transactions on Fuzzy Systems*, 2023.

[41] Minghao Han, Ruixian Zhang, Lixian Zhang, Ye Zhao, and Wei Pan. Asynchronous observer design for switched linear systems: A tube-based approach. *IEEE/CAA Journal of Automatica Sinica*, 7(1):70–81, 2019.

[42] FA Haouari, Mohamed Djemai, and Brahim Cherki. Sliding mode observers for ts fuzzy systems with application to sensor fault estimation. In *2015 3rd International Conference on Control, Engineering & Information Technology (CEIT)*, pages 1–5. IEEE, 2015.

[43] Yingzheng Hong, Hongbin Zhang, and Qunxian Zheng. Asynchronous H∞ Filtering for Switched T–S Fuzzy Systems and Its Application to the Continuous Stirred Tank Reactor. *International Journal of Fuzzy Systems*, 20(5):1470–1482, 2018.

[44] Jun Huang, Xiang Ma, Xudong Zhao, Haochi Che, and Liang Chen. Interval observer design method for asynchronous switched systems. *IET Control Theory & Applications*, 14(8):1082–1090, 2020.

[45] D. Ichalal, B. Marx, J. Ragot, and D. Maquin. State estimation of Takagi-Sugeno systems with unmeasurable premise variables. *IET Control Theory and Applications*, 4(5):897–908, 2010.

[46] Dalil Ichalal, Benoît Marx, José Ragot, and Didier Maquin. Advances in observer design for takagi-sugeno systems with unmeasurable premise variables. In *2012 20th Mediterranean Conference on Control & Automation (MED)*, pages 848–853. IEEE, 2012.

[47] Dalil Ichalal, Benoît Marx, José Ragot, and Didier Maquin. Fault detection, isolation and estimation for takagi–sugeno nonlinear systems. *Journal of the Franklin Institute*, 351(7):3651–3676, 2014.

[48] R Isermann and P Phalle. Applied terminology of fault detection, supervision and safety for technical processes. In *IFAC Symposium on Fault Detection Supervision and Safety for Technical Process*, volume 41, 2000.

[49] Rolf Isermann. Process fault detection based on modeling and estimation methods—a survey. *automatica*, 20(4):387–404, 1984.

[50] Rolf Isermann and Peter Balle. Trends in the application of model-based fault detection and diagnosis of technical processes. *Control engineering practice*, 5 (5):709–719, 1997.

[51] Dalel Jabri. *Contribution à la synthèse de lois de commande pour les systèmes de type Takagi-Sugeno et/ou hybrides interconnectés*. PhD thesis, 2011. URL

http://www.theses.fr/2011REIMS028/document. Université de Reims Champagne Ardenne, France.

[52] Dalel Jabri, Kevin Guelton, Djamel EC Belkhiat, and Noureddine Manamanni. Decentralized static output tracking control of interconnected and disturbed takagi–sugeno systems. *International Journal of Applied Mathematics and Computer Science*, 30(2):225–238, 2020.

[53] Ali Jadbabaie. A reduction in conservatism in stability and 52 gain analysis of takagi-sugeno fuzzy systems via linear matrix inequalities. *IFAC Proceedings Volumes*, 32(2):5451–5455, 1999.

[54] Ian T Jolliffe. *Principal component analysis for special types of data*. Springer, 2002.

[55] Elkhatib Kamal and Abdel Aitouche. Fuzzy observer-based fault tolerant control against sensor faults for proton exchange membrane fuel cells. *International Journal of Hydrogen Energy*, 45(19):11220–11232, 2020.

[56] Hassan K Khalil. *Nonlinear systems; 3rd ed.* Prentice-Hall, Upper Saddle River, NJ, 2002.

[57] Yann Labit, Dimitri Peaucelle, and Didier Henrion. Sedumi interface 1.02: a tool for solving lmi problems with sedumi. In *IEEE International Symposium on Computer Aided Control System Design*, pages 272–277. IEEE, 2002.

[58] Ayyoub Ait Ladel, Abdellah Benzaouia, Rachid Outbib, and Mustapha Ouladsine. Integrated state/fault estimation and fault-tolerant control design for switched t–s fuzzy systems with sensor and actuator faults. *IEEE Transactions on Fuzzy Systems*, 30(8):3211–3223, 2021.

[59] Zsófia Lendek, Thierry Marie Guerra, Robert Babuska, and Bart De Schutter. *Stability analysis and nonlinear observer design using Takagi-Sugeno fuzzy models*, volume 262. Springer, 2011.

[60] Rongchang Li and Ying Yang. Sliding-mode observer-based fault reconstruction for ts fuzzy descriptor systems. *IEEE Transactions on Systems, Man, and Cybernetics: Systems*, 51(8):5046–5055, 2019.

[61] Shanzhi Li, Abdel Aitouche, Haoping Wang, and Nicolai Christov. Sensor fault estimation of pem fuel cells using takagi sugeno fuzzy model. *International journal of hydrogen energy*, 45(19):11267–11275, 2020.

[62] Daniel Liberzon. *Switching in systems and control*, volume 190. Springer, 2003.

[63] Daniel Liberzon. Switched systems. In *Handbook of networked and embedded control systems*, pages 559–574. Springer, 2005.

[64] Daniel Liberzon and A Stephen Morse. Basic problems in stability and design of switched systems. *IEEE control systems magazine*, 19(5):59–70, 1999.

[65] Hai Lin and Panos J Antsaklis. Stability and stabilizability of switched linear systems: a survey of recent results. *IEEE Transactions on Automatic control*, 54 (2):308–322, 2009.

[66] Shaokun Liu, Xiaojian Li, Heng Wang, and Jingjing Yan. Adaptive fault estimation for ts fuzzy systems with unmeasurable premise variables. *Advances in Difference Equations*, 2018:1–13, 2018.

[67] Ying Liu and Youqing Wang. Actuator and sensor fault estimation for discrete-time switched t–s fuzzy systems with time delay. *Journal of the Franklin Institute*, 358(2):1619–1634, 2021.

[68] Zhou-Zhou Liu, Yong He, Li Jin, and Wen-Hu Chen. Stability analysis of delayed takagi–sugeno fuzzy systems via a membership-dependent reciprocally convex inequality. *Journal of the Franklin Institute*, 361(7):106776, 2024.

[69] J. Lofberg. YALMIP : a toolbox for modeling and optimization in MATLAB. In *2004 IEEE International Conference on Robotics and Automation (IEEE Cat. No.04CH37508)*, 2004 IEEE International Conference on Robotics and Automation (IEEE Cat. No.04CH37508), pages 284–289, 2004.

[70] David Luenberger. Observers for multivariable systems. *IEEE transactions on automatic control*, 11(2):190–197, 1966.

[71] Xiao-Jun Ma, Zeng-Qi Sun, and Yan-Yan He. Analysis and design of fuzzy controller and fuzzy observer. *IEEE Transactions on fuzzy systems*, 6(1):41–51, 1998.

[72] Teodor Marcu and Paul M Frank. Parallel evolutionary approach to system identification for process fault diagnosis. *IFAC Proceedings Volumes*, 31(10):113–118, 1998.

[73] Mohammad-Ali Massoumnia. *A geometric approach to failure detection and identification in linear systems*. PhD thesis, Massachusetts Institute of Technology, 1986.

[74] Salowa Methnani. *Diagnostic, reconstruction et identification des défauts capteurs et actionneurs: application aux station d'épurations des eaux usées*. PhD thesis, Université de Toulon; École nationale d'ingénieurs de Sfax (Tunisie), 2012.

[75] Hoda Moodi and Danyal Bustan. Unmeasurable premise avoidance in T-S fuzzy observers. 2017 5th International Conference on Control, Instrumentation, and Automation (ICCIA), pages 144–149, Nov 2018.

[76] Hoda Moodi and Mohammad Farrokhi. On observer-based controller design for Sugeno systems with unmeasurable premise variables. *ISA Transactions*, 53(2): 305–316, 2014.

[77] Yann Morère. *Mise en oeuvre de lois de commande pour les modèles flous de type Takagi-Sugeno*. PhD thesis, Université de Valenciennes et du Hainaut Cambrésis, 2001.

[78] Yunfei Mu, Huaguang Zhang, Ruipeng Xi, and Zhiyun Gao. State and fault estimations for discrete-time ts fuzzy systems with sensor and actuator faults. *IEEE Transactions on Circuits and Systems II: Express Briefs*, 68(10):3326–3330, 2021.

[79] D. Peaucelle, D. Arzelier, O. Bachelier, and J. Bernussou. A new robust script D sign-stability condition for real convex polytopic uncertainty. *Systems and Control Letters*, 40(1):21–30, 2000.

[80] Stefan Pettersson. Switched state jump observers for switched systems. *IFAC Proceedings Volumes (IFAC-PapersOnline)*, 38:127–132, 2005.

[81] Matthew Philippe, Ray Essick, Geir E Dullerud, and Raphaël M Jungers. Stability of discrete-time switching systems with constrained switching sequences. *Automatica*, 72:242–250, 2016.

[82] S. Priyanka, R. Sakthivel, S. Mohanapriya, Fanchao Kong, and S. Saat. Composite fault-tolerant and anti-disturbance control for switched fuzzy stochastic systems. *ISA Transactions*, 125:99–109, 2022. ISSN 0019-0578. doi: https://doi.org/10.1016/j.isatra.2021.06.022. URL https://www.sciencedirect.com/science/article/pii/S0019057821003384.

[83] Akhilesh Kumar Ravat, Amit Dhawan, and Manish Tiwari. Lmi and yalmip: Modeling and optimization toolbox in matlab. In *Advances in VLSI, Communication, and Signal Processing: Select Proceedings of VCAS 2019*, pages 507–515. Springer, 2021.

[84] Hangli Ren, Guangdeng Zong, and Hamid Reza Karimi. Asynchronous finite-time filtering of networked switched systems and its application: An event-driven method. *IEEE Transactions on Circuits and Systems I: Regular Papers*, 66(1): 391–402, 2018.

[85] Jorge Iván Bermúdez Rodríguez, Héctor Ricardo Hernández-De-León, Juan Anzurez Marín, Alejandro Medina Santiago, Elías Neftalí Escobar Gómez, Betty Yolanda López Zapata, and Julio Alberto Guzmán-Rabasa. Fault diagnosis for takagi-sugeno model wind turbine pitch system. *IEEE Access*, 2024.

[86] Shankar Sastry and Shankar Sastry. Lyapunov stability theory. *Nonlinear Systems: Analysis, Stability, and Control*, pages 182–234, 1999.

[87] A Schwarte and Rolf Isermann. Neural network applications for model based fault detection with parity equations. *IFAC Proceedings Volumes*, 35(1):205–210, 2002.

[88] Daniel Shevitz and Brad Paden. Lyapunov stability theory of nonsmooth systems. *IEEE Transactions on automatic control*, 39(9):1910–1914, 1994.

[89] Jiayue Sun, Huaguang Zhang, Yingchun Wang, and Shaoxin Sun. Fault-tolerant control for stochastic switched it2 fuzzy uncertain time-delayed nonlinear systems. *IEEE Transactions on Cybernetics*, 52(2):1335–1346, 2020.

[90] Shaoxin Sun, Yingchun Wang, Huaguang Zhang, and Jiayue Sun. Multiple intermittent fault estimation and tolerant control for switched ts fuzzy stochastic systems with multiple time-varying delays. *Applied Mathematics and Computation*, 377:125114, 2020.

[91] Shaoxin Sun, Huaguang Zhang, Xiaojie Su, and Jinyu Zhu. Fault estimation and tolerant control for multiple time delayed switched fuzzy stochastic systems with sensor faults and intermittent actuator faults. In *Fault-Tolerant Control for Time-Varying Delayed TS Fuzzy Systems*, pages 85–122. Springer, 2023.

[92] Ibtissam Tabbi, Dalel Jabri, Issam Chekakta, and Djamel EC Belkhiat. Robust state and sensor fault estimation for switched nonlinear systems based on asynchronous switched fuzzy observers. *International Journal of Adaptive Control and Signal Processing*, 38(1):90–120, 2024.

[93] Tomohiro Takagi and Michio Sugeno. Fuzzy identification of systems and its applications to modeling and control. *IEEE transactions on systems, man, and cybernetics*, (1):116–132, 1985.

[94] Kazuo Tanaka and Michio Sugeno. Stability analysis and design of fuzzy control systems. *Fuzzy sets and systems*, 45(2):135–156, 1992.

[95] Kazuo Tanaka and Hua O. Wang. *Fuzzy Control Systems Design and Analysis: A Linear Matrix Inequality Approach*. John Wiley & Sons, Inc., sep 2001. ISBN 0471323241.

[96] Tadanari Taniguchi, Kazuo Tanaka, and Hua O Wang. Fuzzy descriptor systems and nonlinear model following control. *IEEE transactions on Fuzzy Systems*, 8 (4):442–452, 2000.

[97] Tadanari Taniguchi, Kazuo Tanaka, Hiroshi Ohtake, and Hua O Wang. Model construction, rule reduction, and robust compensation for generalized form of takagi-sugeno fuzzy systems. *IEEE Transactions on Fuzzy Systems*, 9(4):525–538, 2001.

[98] Louise Travé-Massuyès and Robert Milne. Gas-turbine condition monitoring using qualitative model-based diagnosis. *Ieee Expert*, 12(3):22–31, 1997.

[99] H.D. Tuan, P. Apkarian, T. Narikiyo, and Y. Yamamoto. Parameterized linear matrix inequality techniques in fuzzy control system design. *IEEE Transactions on Fuzzy Systems*, 9(2):324–332, 2001. doi: 10.1109/91.919253.

[100] Hoang D. Tuan, Pierre Apkarian, and Truong Q. Nguyen. Robust and reduced-order filtering: New LMI-based characterizations and methods. *IEEE Transactions on Signal Processing*, 49(12):2975–2984, 2001.

[101] Weihua Wang, Likui Wang, Xiangpeng Xie, and Hak-Keung Lam. A switching control approach for stability analysis of constrained t–s fuzzy systems. *Nonlinear Dynamics*, pages 1–11, 2024.

[102] Zhaojing Wu, Mingyue Cui, Peng Shi, and Hamid Reza Karimi. Stability of stochastic nonlinear systems with state-dependent switching. *IEEE transactions on automatic control*, 58(8):1904–1918, 2013.

[103] Weiming Xiang, Jian Xiao, and Muhammad Naveed Iqbal. Robust observer design for nonlinear uncertain switched systems under asynchronous switching. *Nonlinear Analysis: Hybrid Systems*, 6(1):754–773, 2012.

[104] Wen-Bo Xie, He Li, Zhen-Hua Wang, and Jian Zhang. Observer-based controller design for a ts fuzzy system with unknown premise variables. *International Journal of Control, Automation and Systems*, 17(4):907–915, 2019.

[105] Yuqing Yan, Huaguang Zhang, Jiayue Sun, and Yingchun Wang. Adaptive fuzzy observer-based mismatched faults and disturbance design for singular stochastic ts fuzzy switched systems. *Journal of Vibration and Control*, page 10775463221076195, 2022.

[106] Fuyu Yang and Richard W Wilde. Observers for linear systems with unknown inputs. *IEEE transactions on automatic control*, 33(7):677–681, 1988.

[107] Junqi Yang, Yantao Chen, Fanglai Zhu, Kaijiang Yu, and Xuhui Bu. Synchronous switching observer for nonlinear switched systems with minimum dwell time constraint. *Journal of the Franklin Institute*, 352(11):4665–4681, 2015.

[108] Junqi Yang, Fanglai Zhu, Xin Wang, and Xuhui Bu. Robust sliding-mode observer-based sensor fault estimation, actuator fault detection and isolation for uncertain nonlinear systems. *International journal of control, automation and systems*, 13(5):1037–1046, 2015.

[109] Jun Yoneyama. New conditions for admissibility and control design of takagi-sugeno fuzzy descriptor systems. In *2020 IEEE 16th International Conference on Control & Automation (ICCA)*, pages 1630–1635. IEEE, 2020.

[110] Jun Yoneyama, Masahiro Nishikawa, Hitoshi Katayama, and Akira Ichikawa. Design of output feedback controllers for takagi–sugeno fuzzy systems. *Fuzzy sets and systems*, 121(1):127–148, 2001.

[111] Ping Yu, Jian Han, and Xiuhua Liu. Observer based finite-time fault-tolerant control for switched stochastic systems. In *2022 First International Conference on Cyber-Energy Systems and Intelligent Energy (ICCSIE)*, pages 1–5, 2023. doi: 10.1109/ICCSIE55183.2023.10175309.

[112] LA Zadeh. Zadeh, fzzy sets. *Fuzzy sets, fuzzy logic, and fuzzy systems*, pages 19–34, 1965.

[113] Huaguang Zhang, Jian Han, Yingchun Wang, and Xiuhua Liu. Sensor fault estimation of switched fuzzy systems with unknown input. *IEEE Transactions on Fuzzy Systems*, 26(3):1114–1124, 2018. doi: 10.1109/TFUZZ.2017.2704543.

[114] Jiancheng Zhang and Fanglai Zhu. On the observer matching condition and unknown input observer design based on the system left-invertibility concept. *Transactions of the Institute of Measurement and Control*, 40(9):2887–2900, 2018.

[115] Ke Zhang, Bin Jiang, and Peng Shi. Fast fault estimation and accommodation for dynamical systems. *IET Control Theory & Applications*, 3(2):189–199, 2009.

[116] Ke Zhang, Bin Jiang, Peng Shi, and Vincent Cocquempot. *Observer-based fault estimation techniques*, volume 127. Springer, 2018.

[117] Lixian Zhang, Songlin Zhuang, and Peng Shi. Non-weighted quasi-time-dependent h∞ filtering for switched linear systems with persistent dwell-time. *Automatica*, 54:201–209, 2015.

[118] Lixian Zhang, Yanzheng Zhu, Peng Shi, and Qiugang Lu. *Time-dependent switched discrete-time linear systems: control and filtering*, volume 53. Springer, 2016.

[119] Fanglai Zhu, Yu Shan, and Yuyan Tang. Actuator and sensor fault detection and isolation for uncertain switched nonlinear system based on sliding mode observers. *International Journal of Control, Automation and Systems*, 19(9): 3075–3086, 2021.

[120] Feng Zhu and Panos J Antsaklis. Optimal control of hybrid switched systems: A brief survey. *Discrete Event Dynamic Systems*, 25:345–364, 2015.

[121] Jun-Wei Zhu, Guang-Hong Yang, Hong Wang, and Fuli Wang. Fault estimation for a class of nonlinear systems based on intermediate estimator. *IEEE Transactions on Automatic Control*, 61(9):2518–2524, 2015.

[122] G Zwingelstein. failures diagnosis. theory and practice for industrial systems. 1995.